



저작자표시-비영리-변경금지 2.0 대한민국

이용자는 아래의 조건을 따르는 경우에 한하여 자유롭게

- 이 저작물을 복제, 배포, 전송, 전시, 공연 및 방송할 수 있습니다.

다음과 같은 조건을 따라야 합니다:



저작자표시. 귀하는 원저작자를 표시하여야 합니다.



비영리. 귀하는 이 저작물을 영리 목적으로 이용할 수 없습니다.



변경금지. 귀하는 이 저작물을 개작, 변형 또는 가공할 수 없습니다.

- 귀하는, 이 저작물의 재이용이나 배포의 경우, 이 저작물에 적용된 이용허락조건을 명확하게 나타내어야 합니다.
- 저작권자로부터 별도의 허가를 받으면 이러한 조건들은 적용되지 않습니다.

저작권법에 따른 이용자의 권리는 위의 내용에 의하여 영향을 받지 않습니다.

이것은 [이용허락규약\(Legal Code\)](#)을 이해하기 쉽게 요약한 것입니다.

[Disclaimer](#)

**Doctor of Philosophy**

**An investigation on the effects of key input  
parameters to electric bicycle for high performance**

**The Graduate School  
of the University of Ulsan**

**Department of Mechanical Engineering**

**Le Trong Hieu**

**An investigation on the effects of key input parameters  
to electric bicycle for high performance**

**Supervisor: Prof. Ocktaeck Lim**

**A Dissertation**

**Submitted to**

**the Graduate School of the University of Ulsan**

**In partial Fulfillment of the Requirements**

**for the Degree of**

**Doctor of Philosophy**

**by**

**Le Trong Hieu**

**Department of Mechanical Engineering**

**University of Ulsan, Republic of Korea**

**June 2024**

**An investigation on the effects of key input parameters to  
electric bicycle for high performance**

This certifies that the dissertation  
of Le Trong Hieu is approved.



Committee Chair

Prof. Kyu Yeol Park



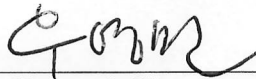
Committee Member

Assoc. Prof. Kyoungsik Chang



Committee Member

Asst. Prof. Yoon Ho Lee



Committee Member

Dr. Youngmin Woo



Committee Member

Prof. Ocktaeck Lim

**Department of Mechanical Engineering  
University of Ulsan, Republic of Korea**

**June 2024**



## **ABSTRACT**

### **An investigation on the effects of key input parameters to electric bicycle for high performance**

**Department of Mechanical Engineering  
Le Trong Hieu**

The purpose of this research is to study how the operating and structure parameter affect the dynamic, require power and electric consumption of electric bicycles (EBs). To achieve this goal, a simulation model was established through MATLAB Simulink software to investigate dynamic and electricity consumption characteristics. Based on the established mathematical models, the motion, dynamic and electric consumption of the EB are analyzed and optimized under the effects of frontal area, bicycle mass, wheel radius, and sprocket transmission ratio. On the other hand, to improve bicycle performance, the research applied an artificial neural network and genetic algorithm (ANN-GA) to forecast the bicycle performance and identify its optimal power demand. The MATLAB-Simulink model created 1000 data points, which are utilized for training, testing, verifying the ANN model. The ANN model is developed with transmission ratio, frontal area, wheel radius, bicycle velocity as an input, and power demand and battery voltage as an output parameter. After the ANN is trained, it is applied into the genetic algorithm to identify the optimal value. The study showed that the electric bicycle configuration can achieve optimal power 546.3 W at 30.7 km/h under speed level\_5, wheel radius of 0.42 m, frontal area 0.423 m<sup>2</sup>. Besides that, the experimental test was conducted on real road test at Taehwa river to verify the simulated results. The experimental and simulation results have the same trend under the same conditions.

Keywords: electric bicycle model, electric consumption, artificial neural network, genetic algorithm, effective performance area.

## ACKNOWLEDGEMENT

The first words, I would like to express my deep and sincere gratitude to my advisor Professor Ocktaeck Lim, for giving me the opportunity to come and study at The Smart Powertrain Laboratory. I have studied so much from his vision, dynamism, sincerity and motivation. It was a great honor to work and study under his guidance. I am extremely thankful for what he has supported me in the research works and thesis preparation.

I would also like to thank to all members of the Smart Powertrain Laboratory for many nice memories we have together spent and their valuable support during my research work.

I would also like to express my thanks to the Graduate School of Mechanical and Automotive Engineering, University of Ulsan for providing me the opportunity, approval, and support to pursue my PhD program.

Finally, I am thankful to my supervisory committee members for spending their time and for giving me their advice and comments to improve the quality of the PhD thesis.

This PhD thesis is written during the spring semester of 2024. This PhD thesis contains total research work conducted during the doctor's study period. All the contents of this thesis are written for partially fulfilling the degree requirement of the PhD of Science in Mechanical and Automotive Engineering at the University of Ulsan.

Le Trong Hieu

# TABLE OF CONTENTS

ABSTRACT	iii
ACKNOWLEDGEMENT	iv
TABLE OF CONTENTS	v
LIST OF FIGURES	vii
LIST OF TABLES	ix
1 INTRODUCTION	1
1.1 Background	1
1.2 Approach	3
1.3 Objective of study	4
1.4 Organization of the thesis	6
2 LITERATURE REVIEW	9
2.1 Introduction	9
2.2 Electric bicycle advantage	9
2.3 Electric bicycles classify	10
2.4 Review of previous studies on environmental benefit of electric bicycles	11
2.5 Review of previous studies relate to motor technology on electric bicycle	13
2.6 Review of previous studies relate to battery technology on electric bicycle	14
2.7 Review of previous studies on structure and operating parameters to improve electric bicycle performance	15
2.8 Summary	18
3 EXPERIMENTAL SYSTEM	19
3.1 Research electric bicycle	19
3.2 Experimental set up	19
3.3 Experimental testing condition	22
3.4 Accuracy of measurements and uncertainty	23
3.4 Summary	25
4 SIMULATION MODEL	26
4.1 Introduction	26
4.2 Governing formulas for the electric bicycle model	26

4.3	Zero-dimension model	32
4.4	Summary	36
5	AN INVESTIGATION ON THE EFFECTIVE PERFORMANCE AREA OF THE ELECTRIC BICYCLE WITH VARIABLE KEY INPUT PARAMETER	37
5.1	Comparison experiment and simulation result	37
5.2	Effects of operating parameters	40
5.3	Effects of structure parameters	47
5.4	Summary	60
6	A MACHINE LEARNING APPROACHES FOR PREDICTING POWER AND PERFORMANCE FOR ELECTRIC BICYCLE UNDER THE EFFECTS KEY PARAMETERS	62
6.1	Machine learning	62
6.2	Comparison experiment and simulation results	71
6.3	Comparison simulated and predicted results	75
6.4	Effect of key structure factor on electric bicycle performance	78
6.5	Enhancing electric bicycle performance by optimizing key structure parameters	85
6.6	Summary	89
7	CONCLUSION AND CONTRIBUTION	91
	NOMENCLATURES	95
	REFERENCES	98
	PUBLICATIONS AND CONFERENCES	109
	A. LIST OF PUBLICATIONS	109
	B. LIST OF CONFERENCES	110
	APPENDIX	111

## LIST OF FIGURES

Figure 1.1	The flowcharts of the potential strategies to enhance bicycle performance through experimental and simulation approach	6
Figure 2.1	The flowcharts of the potential strategies to enhance bicycle performance	18
Figure 3.1	The experimental system of an electric bicycle	24
Figure 4.1	The model of the electric bicycle	29
Figure 4.2	Typical discharge curve	30
Figure 4.3	The armature equivalent circuit of DC motor	30
Figure 4.4	The electrical equivalent circuit of armature	31
Figure 4.5	The calculated power flowchart of EB	32
Figure 4.6	The bicycle properties	33
Figure 4.7	The DC motor properties	34
Figure 4.5	Li-on battery properties	34
Figure 5.1	(a) Validation of bicycle velocity at speed1 and speed4 by simulation model; (b) Validation of battery voltage at speed1 and speed4 by simulation model; (c) Validation of bicycle velocity with a changed rider mass by simulation model; (b) Validation of battery voltage with a changed rider mass by simulation model	39
Figure 5.2	Impact of driver mass to (a) velocity, (b) distance, (c) and (d) battery voltage	42
Figure 5.3	Impact of slope ratio to (a) velocity, (b) distance, (c) propulsion torque and (d) battery voltage	46
Figure 5.4	Impact of EB mass to (a) velocity, (b) distance, (c) and (d) battery voltage	49
Figure 5.5	Impact of transmission ratio to (a) velocity, (b) distance, (c) and (d) battery voltage	52
Figure 5.6	Impact of wheel radius to (a) velocity, (b) distance, (c) propulsion torque and(d) battery voltage	56
Figure 5.7	Impact of frontal area to (a) velocity, (b) distance, (c) propulsion torque and (d) battery voltage	58

Figure 6.1	The artificial neural network using multi-layer feed-forward architecture	63
Figure 6.2	Variation of MSE and $R^2$ in regard to the amount of hidden neurons. (a) Mean square error, (b) Correlation coefficient	67
Figure 6.3	Recognized ANN structure of 5-12-2	68
Figure 6.4	Validation of dynamic and battery voltage electric bike with various transmission ratio and rider mass: (a), (b), (c) various speed level; (d), (e), (f) various rider mass	73
Figure 6.5	The prediction model comparison instructed with 600, 800, 100 data point using one power-velocity curve.	76
Figure 6.6	The ANN-GA approach, informed from Simulink model	77
Figure 6.7	Comparison between the simulated and ANN-GA predicted results of power demand-velocity, battery voltage-velocity curve under varying transmission ratio	79
Figure 6.8	Comparison between the simulated and ANN-GA predicted results of power demand-velocity, battery voltage-velocity curve under varying slope grade	81
Figure 6.9	Comparison between the simulated and ANN-GA predicted results of power demand-velocity, battery voltage-velocity curve under varying frontal area	79
Figure 6.10	Comparison between the simulated and ANN-GA predicted results of power demand-velocity, battery voltage-velocity curve under varying wheel radius.	83
Figure 6.11	The ANN-GA identified four input factor that yields maximum power demand and velocity, (a) five slope ratios, (b) five wheel radius, (c) five frontal area, (d) five speed level.	88

## LIST OF TABLES

Table 1.1	Thesis outline	8
Table 3.1	NI 9221 specification	20
Table 3.2	cDAQ 9171 specification	21
Table 3.3	Speed sensor specifications	21
Table 3.4	Electric bicycle specifications	22
Table 3.5	Uncertainty of measured parameters	23
Table 3.6	Experiment conditions for changing transmission ratio	24
Table 3.7	Experiment conditions for changing bicycle weight	24
Table 4.1	Description of the simulated cases regarding the various transmission ratio	34
Table 4.2	Description of the simulated cases regarding the various to bicycle weight	35
Table 4.3	Description of the simulated cases regarding the various frontal area	35
Table 4.4	Description of the simulated cases regarding the various wheel radius	36
Table 6.1	The selected ANN network was generated by the MATLAB framework	65

# 1. INTRODUCTION

The depletion of fossil fuels and the growth in environmental pollution generated by internal combustion engine cars are major global challenges that must be addressed. The use of electric vehicles is one of the most promising answers to issues of energy security and pollution. The electric bicycle is one of the most popular electric vehicles due to its numerous benefits, including zero emissions, reduced traffic congestion, excellent energy efficiency, and reduced noise pollution. This chapter introduces the research basis behind the study. Correlating relevant literature with the author's laboratory's recent progress yields an overview of the trends in electric bicycle research on dynamic and performance. The research objectives are presented at the end of this chapter, followed by the organization of the thesis

## 1.1 Background

The notion of the electric bicycle originated in the late nineteenth century, with early patents for electrically powered bicycles appearing in the 1890s. However, it took until the late twentieth and early twenty-first centuries for e-bikes to gain substantial commercial momentum [1]. The development of compact and efficient lithium-ion batteries, advances in electric motor technology, and increased environmental concerns have all contributed to the current surge in e-bike popularity. E-bikes have an electric motor and battery system that help with pedaling, making them more accessible to a larger range of users, including those with restricted physical ability or those who commute long distances [2,3]. E-bikes are now seen as both pleasure vehicles and practical options for urban commuting. The electric bicycle (e-bike) market has grown significantly over the last decade, owing to technology developments, increased environmental awareness, and changing urban mobility needs. E-bikes provide a sustainable and efficient means of transportation by combining the advantages of traditional cycling with the additional power of an electric motor [4,5]. So, studying e-bike performance is crucial for

maximizing their efficiency, durability, and user pleasure, addressing critical factors such as battery technology, motor efficiency, structural design, and environmental impact.

There are some research on battery to improve electric bicycle performance such as. Chuanxue Song et al. develop a novel Battery Monitoring System (BMS) for lithium-ion electric bicycles that uses Android and ARM microcontroller technologies. This technology intends to improve safety, lengthen battery life, and simplify battery state monitoring. Real-time monitoring of voltage, current, and temperature is one of the key aspects, as is estimating State of Charge (SOC) and State of Health (SOH). They validated the system's effectiveness in managing electric bicycle batteries [6]. Heshou Wang et al. present a unique resonator design for wireless battery charging in electric bicycles. This system supports load-independent constant current (CC) and constant voltage (CV) charging for battery loads, simplifying control algorithms and communication routes between transmitter and receiver. The study employed Maxwell software to establish continuous mutual inductance, and the experimental results showed effective regulation of output current (1.2 A) and voltage (24 V) across a range of load circumstances. Efficiency peaks at 97.17% in CC mode and 91.17% in CV mode, with consistent performance found throughout a range of distances between transmitter and receiver [7]. Yan Hong et al. present a unique charging cabinet with flood cooling capabilities, which aims to reduce thermal dangers and environmental concerns connected with lithium-ion batteries (LIBs) used in electric bikes. Flood cooling is effective at preventing thermal runaway propagation. Flood cooling produces substantially higher cooling rates than air cooling (1.80°C/s vs. 0.18°C/s). The study emphasizes the crucial roles of heat transfer power, self-heating generation, and cooling power in thermal runaway propagation suppression to improve battery thermal safety in electric bicycles [8]. Furthermore, there are some studies on motor technology to improve electric bicycle performance. Józef Gromba discusses several BLDC motor control methods, electric bike dynamics, load torque calculation approaches, and

electromagnetic torque control. Simulations and laboratory research are used in the study to validate the effectiveness of the newly created control system. The measurements included watching motor current and velocity with a constant power supply voltage, a set load torque of 20 Nm, and changing accelerometer inclination angles ( $0^\circ$  to  $3^\circ$ ). Results showed that increasing terrain slope angles increased motor current draw and electromagnetic torque, verifying the system's performance against specified assumptions [9]. Ji-Chang Son et al. presented a unique stator design for a permanent magnet-assisted synchronous reluctance motor used in electric bicycle propulsion. The proposed stator design considerably enhances the torque density, efficiency, and iron loss properties of the PMA-SynRM for electric bicycles. The use of GO on stator teeth boosted torque and efficiency by 9.89% and 1.7%, respectively, while no-load iron loss was reduced by 14.93%. This yields a smaller, more efficient motor with improved performance. Aside from that, some research have identified structure factors to increase the performance of electric bicycles. [10]. Chih-Lyang Hwan et al investigated two methods for stabilizing an electric bicycle: adjusting the center of gravity (CG) and steering handle angle. A pendulum modifies the CG, and the bicycle's lean angle also affects stability. Three parameters influence the system's dynamics: pendulum angle, lean angle, and steering angle. The study uses a variable structure under-actuated control approach to generate the torques required for handle and pendulum adjustments. The results demonstrated that a variable structure under-actuated control had improved performance and efficiency in maintaining the dynamic balance of the electric bicycle under different conditions [11]. I Ketut Adi Atmika et al studied the usage of composite materials for electric bicycle frames, which are typically made of metals and alloys for strength. The results demonstrate that the composite laminate with a woven fiber arrangement of C ( $45^\circ/45^\circ/45^\circ$ ) has the maximum strength, with a compressive stress value of 58.64 MPa in the axial plane and 1.539 MPa in the tangential plane.

This study supports the use of composite materials to construct lighter yet stronger bicycle frames [12].

In the aforementioned studies, numerous researchers worked to improve the dynamic and performance of electric bicycles by innovations in battery technology, motor improvement, and structural design, namely bicycle frame innovation. However, relatively few researchers have explored the effect of transmission ratio, frontal area, bicycle weight, and wheel size on the dynamic, voltage fluctuation during the starting phase, and performance of an electric bicycle. As a result, a thorough investigation into enhancing maximum velocity, reducing duration to reach stable velocity, and improving electric consumption based on transmission ratio, frontal area, wheel size, and bicycle weight is necessary. Finally, this work is expected to operate as a basis for visualization of critical structure parameters in enhancing maximum velocity and optimal power of an electric bicycle.

## **1.2 Approach**

In this study, an electric bicycle with a capacity of 250W weighing 21kg was used to test the maximum speed, acceleration and power consumption with variations of important structural factors such as gear ratio, bike mass, wheel size.

Firstly, the zero dimension model of electric bicycle including bicycle dynamics, lithium-ion battery model, direct current motor model were performed under mathematical equation. Among design parameters the transmission ratio wheel size, bicycle mass, bicycle weight, frontal area was chosen as the numerical and experimental parameters to investigate. To analyze the effects of these design parameters on maximum velocity acceleration, fluctuation of voltage value. The variation of wheel radius is 0.3-0.42 m, frontal area is 0.423-1.623 m<sup>2</sup>, transmission ratio is 2.18-3.43, bicycle weight 21-43 kg, while the model also considers additional parameters in the common range to analyze the above results comprehensively.

Secondary, preparing the experiment apparatus for to measure e-bike speed and acceleration and voltage value. The device to measure e-bike speed and acceleration is using a photo sensor. Which can detect wheel movement of e-bike as digital signal. The digital signal was transfer to electric control unit to calculate bicycle velocity and travel distance. Besides that, the NI-9221 was used to measure the analog signal of voltage value. All signals were collected and saved in LabVIEW program. E-bike speed and acceleration and voltage value were examined by changing transmission ratio and bicycle mass.

Next step is validating the experiment results with the numerical method. The effect of various wheel radius, frontal area, transmission ratio and bicycle weight on dynamic characteristics power, fluctuations of voltage value in starting period is necessary to investigate during bicycle operation. Therefore, the zero dimension e-bike was performed in MATLAB Simulink software to provide velocity, travel distance, battery voltage value, maximum propulsion torque characteristics.

### **1.3 Objective of study**

This thesis will mainly focus on simulation and experiment a electric bicycle to investigate the electric bicycle mass, transmission ration, wheel size, frontal area and additional parameters include wind velocity, slope ratio effect on maximum bicycle velocity, duration to reach stable velocity, fluctuation of battery in starting period. The objective of this study are given below:

- (i) Setup an experimental system for electric bicycles to provide the basic data for validation of the simulation model. The basic data are velocity curve, travel distance, duration reach stable velocity, fluctuation of battery voltage in starting period.

- (ii) Setup zero-dimension model for electric bicycle including bicycle dynamic, li-ion battery, direct current motor MATLAB-Simulink program based on mathematical equation.
- (iii) To investigate the influence of e-bike weight on maximum velocity, travel distance, and fluctuation of battery voltage.
- (iv) To investigate the effect of transmission ratio on maximum velocity, duration reach stable velocity, travel distance, and fluctuation of battery voltage.
- (v) To investigate the influence of frontal area on maximum velocity, travel distance, maximum propulsion torque, and fluctuation of battery voltage.
- (vi) To investigate the effect of wheel size on maximum velocity, travel distance, maximum propulsion torque, and fluctuation of battery voltage.
- (vii) To optimize the crucial structure parameters of frontal area, transmission ratio, wheel size on bicycle performance.

To obtain above targets, the brief explanation in the effect flowchart as seen in the Fig 1.1

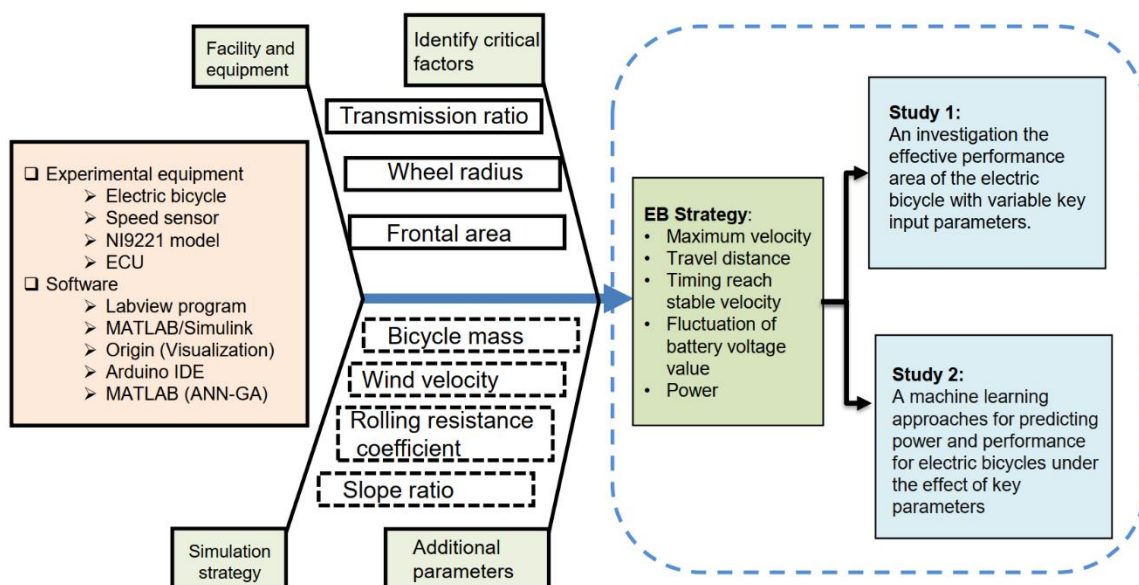


**Fig. 1.1** The flowcharts of the potential strategies to enhance bicycle performance through experimental and simulation approach

## 1.4 Organization of the thesis

The thesis comprises seven chapters which are organized into five main sections, as illustrated in Table. 1.1.

Firstly, Chapter 1 presents the scope of thesis and gives a brief explanation of the topic of e-bike research with preceding studies done on the same issue. The improvements are briefly described with the research aim and objectives. Meanwhile, in chapter 2 a review of the important findings of previous research related to objectives and present study is given. This review summary some study related to consider the crucial design parameters. Based on these reviews some issues can be inferred as a starting point for present study. Chapter 3 explained and described the experiment apparatus for e-bike the experiment test and condition were detailly introduced in this chapter. Furthermore, specification of measurement devices also detailly presented. The purpose of Chapter 4 is to provide zero-dimension model to simplified representation which easier analysis and understanding of the key dynamics of e-bike. Chapter 5 discussed and analyzed numerical and experimental results of dynamic characteristics and voltage value of e-bike for various crucial parameters, this study also considers the influence level of each parameter to dynamic and performance characteristics. Chapter 6 discusses and analyses numerical and experimental results of maximum velocity and power e-bike based on variation of crucial design parameters. And this study also utilized optimal method to improved e-bike performance. Finally, summary and conclusions of this study to understand the influence level of pivotal parameters on dynamic and battery voltage value characteristics. Based on the results obtained, this thesis provides an insight into the performance of electric bicycles.

Research objectives and literature review	<p><b>Chapter 1. INTRODUCTION</b></p> <p>Key point: background, approach, objectives</p> <p><b>Chapter 2. LITERATURE REVIEW</b></p> <p>Key point: motor control, battery technology, review on previous study</p>
Research platform	<p><b>Chapter 3: EXPERIMENTAL RESEARCH</b></p> <p>Key point: Testing condition</p> <p><b>Chapter 4: SIMULATION MODEL</b></p> <p>Key point: Zero-dimension model, boundary condition</p>
Research on dynamic and propulsion characteristics	<p><b>Chapter 5: AN INVESTIGATION ON THE EFFECTIVE PERFORMANCE AREA OF THE ELECTRIC BICYCLE WITH VARIABLE KEY INPUT PARAMETER</b></p> <p>Key points: structure factor, environment factor, maximum velocity, voltage value characteristic.</p>
Research on optimization crucial structure parameters	<p><b>Chapter 6: A MACHINE LEARNING APPROACHES FOR PREDICTING POWER AND PERFORMANCE FOR ELECTRIC BICYCLE UNDER THE EFFECTS KEY PARAMETERS</b></p> <p>Key point: ANN modeling, Genetic Algorithm optimization</p>
Research outcomes	<p><b>Chapter 7: CONCLUSION AND CONTRIBUTION</b></p> <p>Key point: summary, contribution</p>

**Table 1.1** Thesis outline

## **2. LITERATURE REVIEW**

### **2.1 Introduction**

This chapter comprehensively explains the previous research endeavors relevant to the current investigation. Additionally, a comprehensive summary of additional pertinent research studies is also included. This review is organized chronologically to provide an understanding of how previous research endeavors have established the basis for subsequent studies, including the current research effort. The initial section will explain the advantages and benefits of the electric bicycle. In this section presents previous research efforts in improving e-bike performance such as improved battery technology and methods for motor control. Finally, some. In next section, some previous studies on the effect of structural factors and external factors related to this study are specifically explained. Author will find out the drawbacks that have not been well researched or solved. This gap will be filling up by this thesis work at the end of this section.

### **2.2 Electric bicycle advantages**

Electric bicycles are referred to as green vehicles due to their low exhaust gas emissions [13]. E-bikes are a popular mode of transportation in cities, because to their fewer hazardous emissions as compared to traditional vehicles powered by internal combustion engines [14]. In some countries, such as Germany and China, electric bicycles are utilized to replace fossil-fueled mopeds and small motorcycles [15]. Electric bicycles provide numerous benefits, making them an appealing means of transportation for a diverse spectrum of consumers. E-bikes are a versatile and sustainable alternative to traditional modes of transportation, offering health and environmental benefits as well as economic savings and convenience [16]. Their

expanding popularity demonstrates their effectiveness in improving urban mobility, encouraging physical activity, and contributing to a cleaner environment [17].

### **2.3 Electric bicycle classify.**

EBs are divided into three types: pure EBs, power-assisted bicycles, and EBs with both pure and power-assisted modes. The pure EB uses an electric motor installed on the bicycle frame or wheels, with the driving force controlled via a handlebar throttle [18]. Somchaiwong and Ponglangka created a regenerative power control for a pure EB, using a permanent magnet brushless DC motor mounted inside the EB's wheel [19]. P Vishnu Sidharthan and Yashwant Kashyap completed a simulation research utilizing proportional-integral (PI) and a fuzzy controller in Matlab/Simulink to build an appropriate speed controller for a brushless direct current (BLDC) hub motor fitted on an EB's wheel [20].

A power-assisted bicycle, commonly known as a pedelec (pedal electric cycle), is a bicycle with an electric motor mounted on the bicycle frame or a wheel to assist the user in pedaling. Abagnale et al. performed a model-based control study of a power-assisted bicycle in which an electric motor was put on a motor shaft and coupled to a pedal shaft through two separate gearboxes [21]. Hung et al. investigated the impact of input settings on the dynamics and power requirements of a power-assisted bicycle (EB) with an electric motor mounted on the rear wheel. Because the electric motor is employed as a power assist, the motor power of a pedelec is usually smaller than that of a pure electric bicycle [22].

There are also differences in the maximum motor power allowed for bicycles in various countries [23]. According to McLoughlin et al., the highest motor power for electric motor assisted bicycles in the United States is 750 W, whereas 250 W is the maximum in Europe, India, and Japan [24]. Pedelects are especially good for those living in mountainous locations or riders who not only want assistance but also desire to exercise in order to improve their

health. Many research on pedelecs have been undertaken throughout the world and, which provide helpful information for planning and developing high-performance pedelecs [25,26,27,28].

The third form of EB is a hybrid of two modes, pure and power-assisted, in which the driving power of the EB can be controlled using either. In pure mode, the power from an electric motor is only regulated by a handlebar throttle. In the power-assisted mode, the driving force is a combination of rider and motor power, comparable to a pedelecs [29]. Hung et al. simulated and tested the operating performance of an EB integrated with a semi-automatic transmission, with driving power controlled by pure and power-assisted modes. Sharma et al. researched an EB with a combination of pure and power-assisted modes [30].

## **2.4 Review of previous studies on environmental benefit of electric bicycles**

There are many studies connected to the environmental benefits of electric bicycles, consequently improving people's awareness of environmental issues and encouraging people to utilize electric bicycles, especially in urban and heavily populated areas to enhance urban air quality:

Thomas Elliot et al. proposed Electric bicycles (E-bikes) could help to reduce these emissions. A life cycle review revealed that E-bikes have a lesser environmental impact than petrol or diesel vehicles, owing to New Zealand's 80% renewable electricity generation. The study assessed the environmental implications of E-bikes for various battery charging times and discovered minimal variance in performance [31]. Min Liu et al. performed a life cycle study in China, comparing the environmental and economic performance of EBs powered by four different battery types. EBs with lead-acid batteries had the worst environmental impact, while

those with lithium iron phosphate batteries did the best. Motor manufacture, which used copper, had the largest potential for metal depletion and toxicity. Promoting a circular economy may alleviate these effects. The use stage posed the most environmental pressure due to energy use, which may be lowered by 10-25% with power cleaning [32]. Dominik Bucher et al. demonstrate that substituting car commutes with e-bike excursions can cut GHG emissions by up to 10% of total emissions from diesel and gasoline cars. When combined with a more widespread deployment of electric vehicles (EVs), overall savings might reach up to 17.5%. [33]. Lorenzo Stilo et al. discovered the changing landscape of electric assisted bicycles (e-Bikes) as a sustainable means of transportation in future smart cities, with an emphasis on design difficulties and legislative implications in the UK, Europe, and the United States. As e-bike usage grows, there is an increasing need for research to inform the industry on essential cycling features that support broader and sustainable adoption [34]. Yan Chen et al. investigate the environmental benefits of bike-sharing systems in urban sustainable development, using New York City as a case study. The environmental implications of bike-sharing are assessed regionally and temporally using a quantitative analysis of substantial data from January 2014 to December 2017. During the four-year study period, bike-sharing in New York City saved approximately 13,370 tons of oil equivalent, reduced carbon emissions by 30,070 tons, and nitrogen oxide emissions by 80 tons [35]. The collective research presented provides a comprehensive overview of various aspects of sustainable transportation solutions, particularly focusing on electric bicycles (E-bikes) and bike-sharing systems, and their environmental impacts.

## **2.5 Review of previous studies on motor technology on electric bicycle**

Ivan Arango et al. presented advances in optimizing the range and energy efficiency of mid-drive motor electric bicycles (e-bikes), focusing on the use of experimental models to describe various components and their efficiencies. The study found considerable differences in efficiency across subsystems, with the Chain, Motor, and Reduction Gears (CMRGs) subsystem having the greatest influence on overall efficiency (20% to 80% variance). Other components, such as the battery and charger, influenced efficiency to a lesser amount [36]. Sheng-Peng Zhang et al. propose a method for precisely estimating the efficiency of electric bicycle powertrain systems, which include components such as electric motors, gears, sprockets, and chains. By properly estimating these losses and validating the computational method through experiments, the study provides a strong foundation for enhancing powertrain efficiency and driving the design of electric bicycles toward improved energy efficiency and performance [37]. Reza Nasiri-Zarandi et al. investigated the development and performance evaluation of an outer rotor Permanent Magnet-assisted Synchronous Reluctance Motor designed specifically for electric bike (e-bike) applications, with the goal of overcoming the limitations associated with conventional Brushless DC Motors. Simulations and actual studies show that the Permanent Magnet-assisted Synchronous Reluctance Motor increases torque density by 28% while reducing cogging torque by 50% and torque ripple by 8% when compared to a commercial 500-W Brushless DC Motor. Furthermore, permanent magnet usage and associated costs are reduced by 40% [38]. S. Farina et al. investigated the design and analysis of a Brushless DC motor with a Double Stator Slotted Rotor that was specifically designed for electric bicycle applications, with the goal of improving performance over standard Single Stator motors. The results showed that the Double Stator Slotted Rotor motor meets torque requirements for electric bicycles, with a maximum average torque of 16.2 Nm. This performance exceeds that of single-stator BLDC motors, improving total motor efficiency and power delivery [39]. These studies collectively showcase advancements in e-bike motor

technologies, emphasizing efficiency improvements, torque enhancements, and reductions in cost.

## **2.6 Review of previous studies relate to battery technology on electric bicycle**

Felipe Tobar et al. investigate improving the prediction accuracy of battery voltage in electric vehicles, notably electric bicycles, by using external variables such as altitude alongside typical battery voltage measurements. The study emphasizes the significance of incorporating external environmental parameters to improve the predictive capabilities required for maximizing electric vehicle performance and autonomy [40]. S. A. Farisi et al. analyze the environmental and energy security advantages of electric vehicles, with a special emphasis on electric bicycles (e-bikes) powered by various battery technologies. The study compares the performance of valve-regulated lead acid and lithium iron phosphate batteries in an e-bike context, demonstrating that lithium iron phosphate batteries provide better voltage stability and longer travel distances (up to 50.16 km versus 37.83 km for valve-regulated lead acid) [41]. Wayan Nata Septiadi et al. present a Battery Thermal Management System that uses (Composite Phase Change Material and heat pipes) and was specifically built and tested for e-bike battery cooling under varied discharge rates and airflow circumstances. By adding 20% Ethylene Glycol into the Phase Change Material, the Battery Thermal Management System achieves improved mass stability and a staggering 104-fold improvement in thermal conductivity. Experimental testing done at 0.5C, 1C, and 1.5C discharge rates reveal that the Battery Thermal Management System is effective at maintaining battery temperature, with findings showing a drop to 37°C at high discharge rates. Adding forced convection with airflow at 3 m/s enhances thermal performance by decreasing the battery temperature to 35.25°C and ensuring consistent temperature distribution across the battery pack [42]. Chuanxue Song et al. developed a

revolutionary battery monitoring system for electric bicycles that uses an Android client and an ARM microcontroller. The Battery Monitoring System is effective and viable for electric bicycle applications after undergoing extensive testing that includes charging/discharging cycles, estimating accuracy, and communication protocols [43]. These studies contribute significantly to the advancement of electric bicycle technology, addressing key challenges such as battery performance, thermal management, and monitoring systems. By improving efficiency, extending range.

## **2.7 Review of previous studies on structure and operating parameters to improve electric bicycle performance**

The performance of EABs is also an important aspect, there are several studies that have explored various aspects of EABs to enhance their performance and functionality. Chiharu Misaki et al. explored the use of metal hydrides (MHs) for hydrogen storage in fuel cell (FC) systems for EAB. The power demand was measured at 54 W for flat roads and 215 W for gradient roads from actual running tests—conducted on flat and gradient roads. The results showed that the FC system, combined with an auxiliary battery, provides significant benefits in terms of power capacity and weight capacity [44]. Sen-Yung Lee et al. proposed a method to enhance the fatigue safety factor of an electric assisted bicycle frame through the integration of various techniques including uniform design, entropy weighting method, grey relational analysis, and genetic algorithm. The revised design shows a maximum improvement of 19.59% in the fatigue safety factor after analyzing a fatigue finite element for each model in the uniform design table to calculate the fatigue safety factor [45]. Norihito Fukushima et al. proposed a Recursive Least Square (RLS) method for pedaling torque estimation in electric power assisted bicycles without using an expensive torque sensor. The results show that the proposed method successfully estimates the coefficients of the load torque, even on roads with upward slopes

[46]. Zhang Kai et al. conducted simulation study of control adaptive to load and road slope on speed and torque of EAB through evaluating bike body load and road slope load by handling a pedal force and bike speed signal [47]. Okan Uyar et al. presented a mini sensor system for load cells to measure a pedal force of electric bicycle by simulation and experimental research. The study results showed that when the pedal forced an oscillation appeared with high velocity and the driver torque and oscillation dropped when an electric power was assisted by DC motor [48]. Tinghua Li et al. presented a method of speed control without torque sensor for EAB. The proposed method based on the real-time of wheel angular velocity to decide assistance power instead of using torque sensors. The proposed method demonstrated that, the rapidity and stability of performance was improved [49]. C. Abagnale et al. placed the electric motor in the central position, which transmits torque to the central hub via a bevel gear and utilized a strain gauge load cell to measure instantaneous power and speed with the aim to optimize performance and environmental impact [50]. Berno J.E. Misgeld et al introduced a new method for reconstructing the physical pedaling torque based on estimating the external force acting on the bicycle due to the road slope by reconstructing the inclination angle using an orthogonal filter. To increase an accuracy in pitch angle estimation and high dynamics required to supply a good torque estimation due to fast changes in the road's slope angle [51]. In addition, there are some studies related to convenience and flexibility of EBs were conducted [52]. Qing Yu et al proposed a dynamic electric fence planning method to solve the problem of random parking. However, it may negatively impact the convenience of bike sharing. But the research indicated that the dynamic electric fence approach can save 25.31% and 27.76% of bike resources and reduce. It also improved the efficiency and organization of bicycle-sharing services while reducing energy consumption [53]. A detailed charging approaches have been studied to enhance the efficiency and convenience of bicycle use [54]. Rumeng Yin et al. advocated installing a modest off-grid solar photovoltaic system in urban public places or on

the roofs of urban facilities to encourage the use of solar energy in cities. Photovoltaic power may be stored in shared electric bike batteries for flexible use, according to the research. According to the study, the optimal sizes of one PV array unit ranged from 2 m<sup>2</sup> to 6 m<sup>2</sup> for several cities with varying climates [55]. Besides that, another research with the aim of improving the performance of electric bicycle has been also conducted [56]. Ximing Chang et al. presented a Smart Predict-then-Optimize method to balance bicycle supply and demand. The study is carried out on real-world bike-sharing data in Shenzhen, China, demonstrating reductions of 11.69% in relocation distance and 14.09% in carbon emission costs when relocating operational and unusable bicycles simultaneously [57]. Nguyen Ba Hung et al. presented the dynamic characteristics of an electric bike using a 9-speed semi-auto transmission. The study varied the parameters of gear speed level, slope ratio to control and optimize the bike velocity and power generation for electric bikes [58]. Le Trong Hieu et al. provided an experimental investigation and mathematical model simulation to increase bike performance by modifying transmission ratio, wheel radius, and slope ratio parameters. The research indicated that the bicycle velocity can significantly improve through improving the transmission ratio and wheel radius [59]. Roushan Kumar et al. provided an experimental and simulated model of a parallel hybrid electric bicycle for a mountainous location. The study examined cycle speed and power generation through changing slope gradient and wheel radius [60].

## **2.8 Summary**

This chapter gives an introduction to e-bikes and a literature review regarding motor control, battery technology and external parameters effects on maximum velocity acceleration characteristics and performance of EBs. All previous studies have focused on improving bicycle performance through innovative battery management systems and motor technology.

However, there are still many limitations in research on the influence of structure design on electric bicycle performance. Therefore, comprehensive investigations is needed to provide a best understanding of effects of crucial design parameters in bicycle performance. To fill this gap, the experiment and simulation work will be carried out to examine the influence of importance parameters to maximum velocity acceleration characteristics, and fluctuations of voltage value to improved overall performance of EBs. A brief description of how to achieve a target can be summarized in the flow chart as shown in figure 2.1. And information on the experiment set up that will be applied in this study on chapter 3.

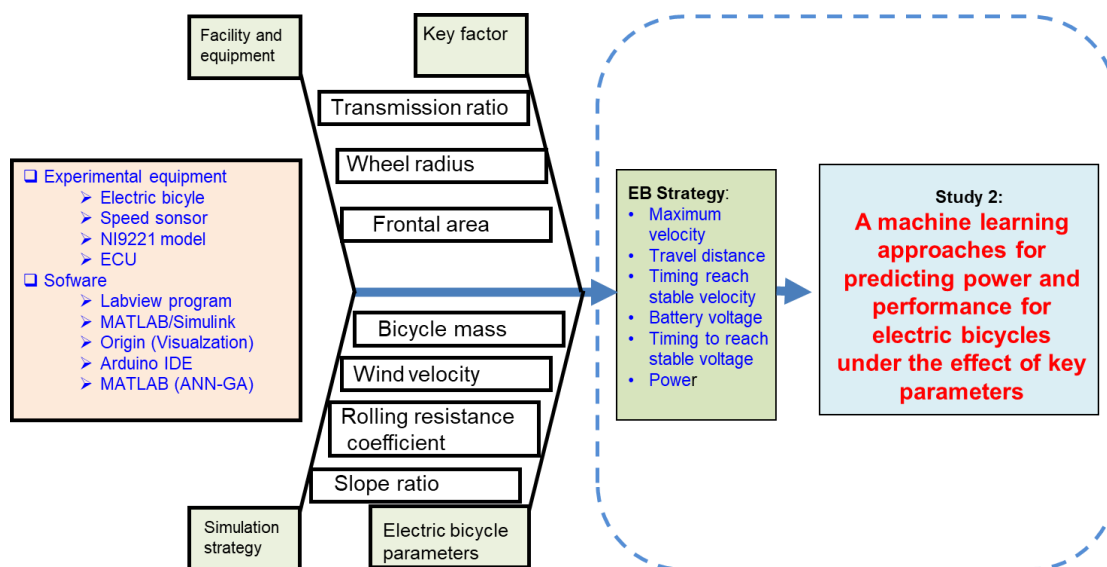


**Fig. 2.1** The flowcharts of the potential strategies to enhance bicycle performance

### **3. EXPERIMENTAL SYSTEM**

This part introduces the research electric bicycle and experimental system. Electric bicycles, commonly known as e-bikes, are bicycles equipped with an integrated electric motor used to assist propulsion. They come in a variety of styles and configurations, catering to a range of uses from commuting and recreational riding to off-road adventures. The purpose of the experimental setup is to support the basic electric behavior data such as bicycle velocity, travel distance and the fluctuation of battery voltage in starting period to valid simulation model. The details of researching bicycles and experimental system will be introduced below.

#### **3.1 Research electric bicycle**

The electric bicycle with key features including:

- **Electric Motor:** E-bikes are powered by an electric motor that assists the rider's pedaling efforts.
- **Battery:** The battery provides power to the motor. It is usually rechargeable and can be located on the down tube, rear rack, or integrated into the frame.
- **Pedal Assist and Throttle:** E-bikes often have pedal-assist systems (PAS), which engage the motor as you pedal, providing varying levels of assistance.
- **Control System:** Most e-bikes feature a control system with a display unit mounted on the handlebars. This display provides information on battery level, speed, distance traveled, and allows the rider to adjust the level of motor assistance

#### **3.2 Experimental setup**

The experimental system and research engine are introduced in this section. The experimental setup's sole goal is to provide credible simulation model support for fundamental electric

bicycle behavior data, including maximum velocity, acceleration characteristic, voltage value characteristics. Below is an introduction to the experimental system and research bicycle in detail: A 21 kg weight of bicycle, A Permanent Magnet brushed DC motor is utilized. The Li-ion battery types 18650 Lithium-ion battery cells were employed in this experiment as the intention is to reduce the overall weight of the e-bicycle. NI 9221 model is used for voltage input value with detail future mentioned in the table 3.1 Besides that, the NI 9221 is connected to cDAQ 9171, which interacts with LabView program. Compact data acquisition specification was shown in table 3.2. The speed sensor, which was used to measure bicycle velocity and travel distance with specification as mentioned in the table 3.3

**Table 3.1:** NI 9221 specification

<b>Characteristics</b>	
Number of channels	8
ADC resolution	12 bit
Maximum Sample Rate	
R Series Expansion Chassis	475 kS/s
Input range	$\pm 60$ V
Measurement voltage, channel-to-COM (V)	
Minimum	$\pm 61.4$
Typical	$\pm 62.50$
Maximum	$\pm 63.8$
Overvoltage protection, channel-to-COM	$\pm 100$ V
Input impedance	
Resistance	1 M $\Omega$
Capacitance	5 pF
Input bandwidth ( -3 dB)	950 kHz min

**Table 3.2:** cDAQ 9171 specification

<b>General-Purpose Counters/Timers</b>	
Number of counters/timers	8
Resolution	32 bits
Internal base clocks	80 MHz, 20 MHz, 100 kHz
External base clock frequency	0 MHz to 20 MHz
Output frequency	0 MHz to 20 MHz
Base clock accuracy	50 ppm
Bus Interface	
USB specification	USB 2.0 Hi-Speed
High-performance data streams	6
Data stream types available	Analog input, analog output, digital input, digital output, counter/timer input, counter/timer output

**Table 3.3:** Speed sensor specification

<b>Specification</b>	
Main chip	LM393
Detection Distance	2~30cm
Detection Angle	35 °
Working Voltage	3.3V~5V
Board Size	31 * 14mm
Board Weight	3g
supply current	20mA

**Table 3.4** Electric bicycle specifications

Parameters	Value
Mass of bicycle	21 kg
Wheel radius	0.33m
Motor power	350W
Crank length	0.17m
Battery type	Rechargeable Li-ion
Battery voltage	36 V
Battery capacity	10 Ah
Gear speed	5 level
Speed level1	3.43
Speed level2	3
Speed level3	2.66
Speed level4	2.4
Speed level5	2.18

### 3.3 Experimental testing condition

The conditions for conducting the experimental test are set as follows: an electric assisted bicycle mass of  $M_{EB} = 21$  kg, a wheel radius of  $R_w = 0.33$  m, a Rider mass of  $M_r = 75$  kg. The 60-sec experimental test was conducted on real road test at Taehwa river in South Korea with the road grade of 0% and almost wind speed of 0 km/h. Table. 3.4 shows the specification of electric assisted bicycle, which is used in the real test at Taehwa river. Fig.3.1 presents the experimental system for electric assisted bicycle including Lithium-ion battery (LIB), DC motor, NI-9221 module, photo sensor, electric control unit (ECU), a computer (PC). The lithium-ion battery (LIB) was equipped on a frame of electric assisted bicycle, a DC motor was installed in the rear wheel to create propulsion torque. In addition, the computer is equipped with a Lab-view program to collect and store experimental data transferred from

ECU module. When the EAB is operating the photo sensor will detect wheel movement by digital signal and send it to ECU module to calculate bicycle velocity. Besides that, an NI-9221 module with sample rate of 800kS/s was used to measure voltage of Lithium-ion battery in real time. Afterward, all the above signals will be transmitted to the computer through a USB cable, and they are monitored and stored by the Lab-view program [60]. Boundary condition for real road test for various transmission ratio and bicycle weight were mentioned in table.3.6 and 3.7

### 3.4 Accuracy of measurements and uncertainty

To ensure the reliability of measurement instruments, each piece of equipment was calibrated within a set amount of time. After every measurement, all electric equipment is cleaned and calibrated before the next measurement cycle. Three repeated measurements of each set of test conditions were made in order to remove reading uncertainty. To estimate the limiting inaccuracy associated with each calculated parameter, a comprehensive uncertainty analysis is performed based on the confidence of the instrument utilized and the measured rate. The uncertainty range of the measured parameters is summarized in Table 3.5.

**Table 3.5:** Uncertainty of measured parameters

Measured parameters	Uncertainty
Velocity	<2%
Travel distance	<2%
Voltage value	<2%



**Fig.3.1** Experimental system of an electric bicycle

**Table 3.6** Experiment conditions for changing transmission ratio

Transmission ratio	Bicycle weight (kg)	Rider weight (kg)	Slope ratio (%)	Wind velocity (km/h)
2.18	21	75	0	0
2.4	21	75	0	0
2.66	21	75	0	0
3	21	75	0	0
3.43	21	75	0	0

**Table 3.7** Experiment conditions for changing bicycle weight

Bicycle weight (kg)	Transmission ratio	Rider weight (kg)	Slope ratio (%)	Wind velocity (km/h)
21	3.43	75	0	0
26	3.43	75	0	0
31	3.43	75	0	0
36	3.43	75	0	0
41	3.43	75	0	0

### **3.5 Summary**

This chapter has detailly explained about the electric bicycle testing specification, experimental system setup, procedures and experimental condition. Based on this experimental system, the real road test was conducted at Taehwa river in South Korea to provide data. Which was analyzed to examine bicycle velocity, travel distance, and the fluctuation of battery in starting period under initial conditions.

## 4. SIMULATION MODEL

### 4.1 Introduction

MATLAB Simulink is a powerful tool for simulating and modeling dynamic systems, including electric bicycles (e-bikes). Simulink provides a block diagram environment where users can model complex systems using interconnected blocks that represent mathematical operations, system components, and data flows. Simulink is tightly integrated with MATLAB, allowing for seamless use of MATLAB functions and scripts within Simulink models. This integration facilitates complex computations and data analysis. Simulink includes a wide range of toolboxes and libraries tailored for specific applications, such as control systems, signal processing, and physical modeling. By using Simulink, the study can create detailed simulations of e-bike systems to analyze performance, optimize components, and test control strategies.

### 4.2 Governing formulas for the electric bicycle model

The model analyzed kinetic and dynamic inputs in motion conditions of an electric bike on the road, as shown in Fig.4.1.

Newton's second law was applied to electric bike dynamics as below:

$$F_{pf} - F_{sf} - F_{af} - F_{rf} = M \frac{d^2x}{dt^2} \quad (1)$$

The force of air resistance can be determined by:

$$F_{af} = \frac{1}{2} A_a C_a \rho (v_w + v_{EB})^2 \quad (2)$$

The force of rolling resistance can be determined by:

$$F_{rf} = gM C_{rr} \cos \alpha \quad (3)$$

The force of slope resistance can be determined by:

$$F_{sf} = Mg C_s \quad (4)$$

where  $C_s$  is the slope resistance coefficient ( $C_s = \sin(\alpha)$ ).

The propulsion force can be calculated by:

$$F_{pf} = F_{sf} + F_{af} + F_{rf} + M \frac{d^2x}{dt^2} \quad (5)$$

Therefore, the total driving torque required is:

$$T = (F_{sf} + F_{af} + F_{rf} + M \frac{d^2x}{dt^2}) R_w = F_{ch} R_{rg} = F_{pf} R_w \quad (6)$$

The electric bicycle uses a battery as the power source to supply energy for the DC motor. The battery installed on the EB is a lithium-ion battery. Fig. 4.2 shows a typical discharge curve of the battery. The model battery used on the EB is a discharge model, it is similar to the Shepherd model, which can present accurately the voltage dynamic while the current varies and considers the open circuit. A term concerning the polarization voltage is added to represent the open-circuit voltage behavior, concerning the polarization resistance was modified. The voltage of the battery is given by:

$$V_b = E_0 - \frac{KQ}{Q-i(t)} (i) - R \cdot i + A e^{(-B \cdot i(t))} - \frac{KQ}{Q-i(t)} i^* \quad (7)$$

The electric bicycle uses a direct current (DC) motor attached to the rear wheel, front-wheel, or both wheels. When the driver operates the e-bike the DC motor generates torque to assist the driver. The propulsion torque of an electric bicycle can be calculated by:

$$T = F_{pf} R_w \quad (8)$$

$$T = \gamma T_m \quad (9)$$

By combining Eqs. (8), (9). The propulsion torque of electric bicycle can be restated as follows:

$$F_{pf} R_w = \gamma T_m \quad (10)$$

Figure. 4.3 shows the continuous-time electromechanical equations of a separately excited DC motor circuit. Equation (11) is the electrical circuit equation of the armature, and Eq. (12) is the mechanical equation of the DC motor with a load [61].

$$E_c + R_a i_a(t) + L_a \frac{di_a}{dt} = U_a \quad (11)$$

$$B_1 \omega_m + j \frac{d\omega_m}{dt} = T_e - T_m = T_a \quad (12)$$

The electrical equivalent circuit of the armature, related to Eq. (12) is given in Fig. 4.4. The back emf is modeled by a dependent voltage source whose value is controlled by speed, a mechanical variable [62].

The electric variable of the DC motor is armature current, and the mechanical variable is speed. In Eqs. (11) and (12), back EMF ( $E_c$ ) is proportional to speed, while produced torque ( $T_e$ ) is proportional to armature current, as shown in Eqs. (13) and (14).

$$E_c = K_b \omega_m \quad (13)$$

$$T_e = K_b i_a \quad (14)$$

where  $K_b$  is the torque constant or back EMF constant in separately excited DC motors.

Combining Eqs. (11), (12), (13), and (14) present the dynamic of the DC motor as Eqs. (15) and (16):

$$L_a \frac{di_a}{dt} + i_a(t)R_a + K_b w_m = U_a \quad (15)$$

$$J \frac{dw_m}{dt} + B_1 w_m + T_m = K_b i_a(t) \quad (16)$$

By combining Eqs (10), (15), (16). The propulsion torque of electric bicycle can be re-written as follows:

$$F_{pff} = \frac{1}{R_w} \left[ \frac{K_b K_a}{R_a} u - \frac{K_b L_a}{R_a} \frac{di_a}{dt} - J \frac{dw_m}{dt} - \left( B_1 + \frac{K_a K_b}{R_m} \right) w_m \right] \quad (17)$$

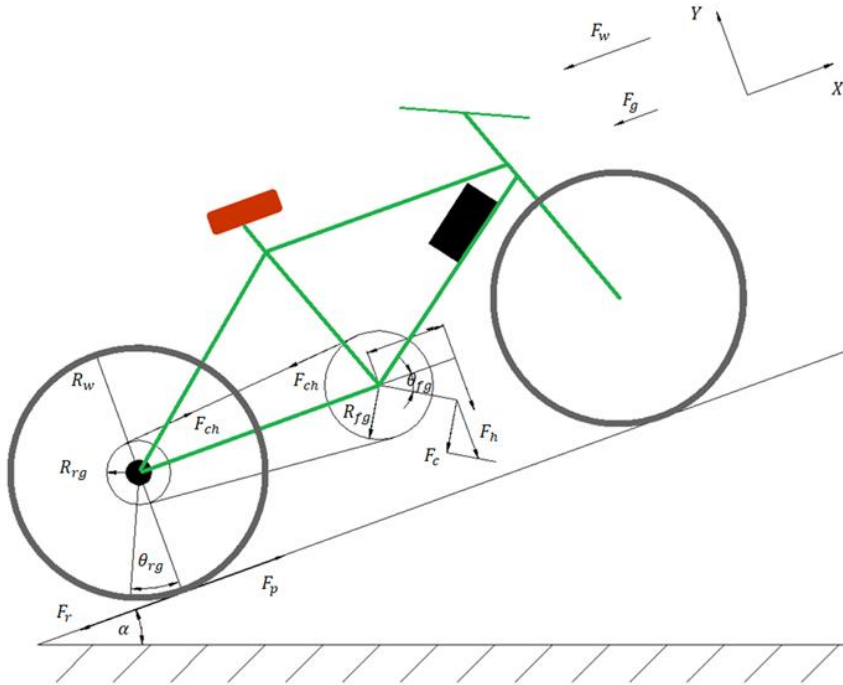


**Fig 4.1.** The model of the electric bicycle

## Nominal Current Discharge Characteristic

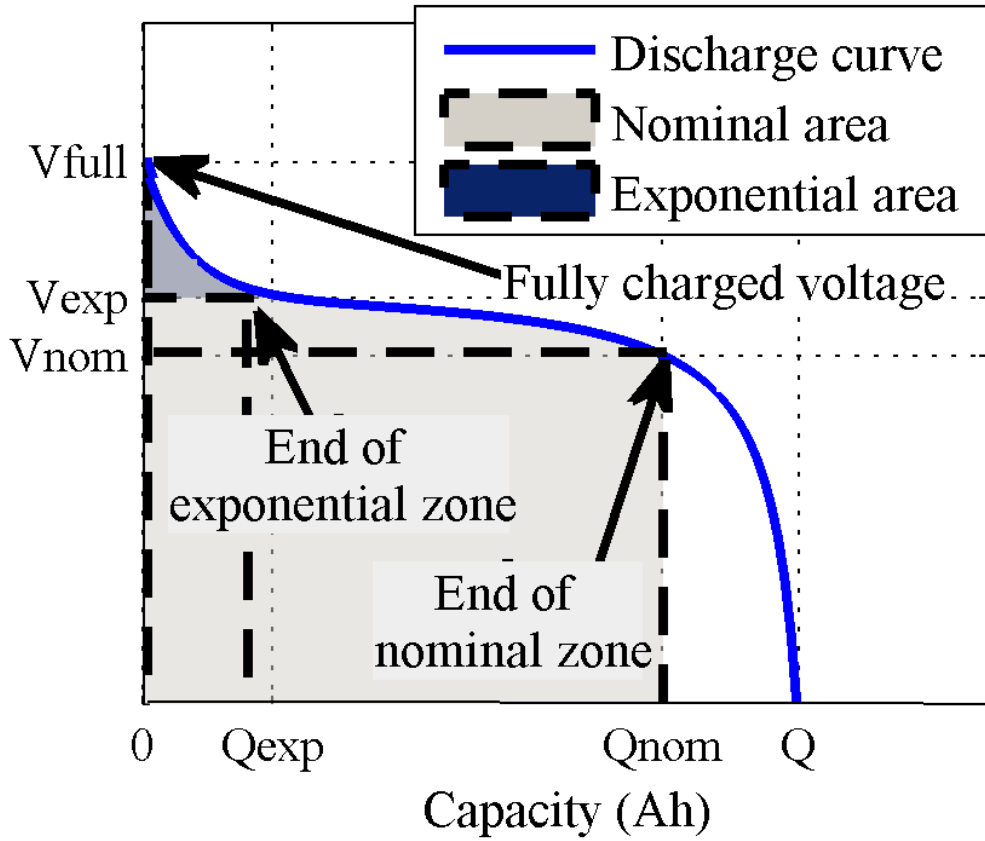


Fig. 4.2 Typical discharge cure

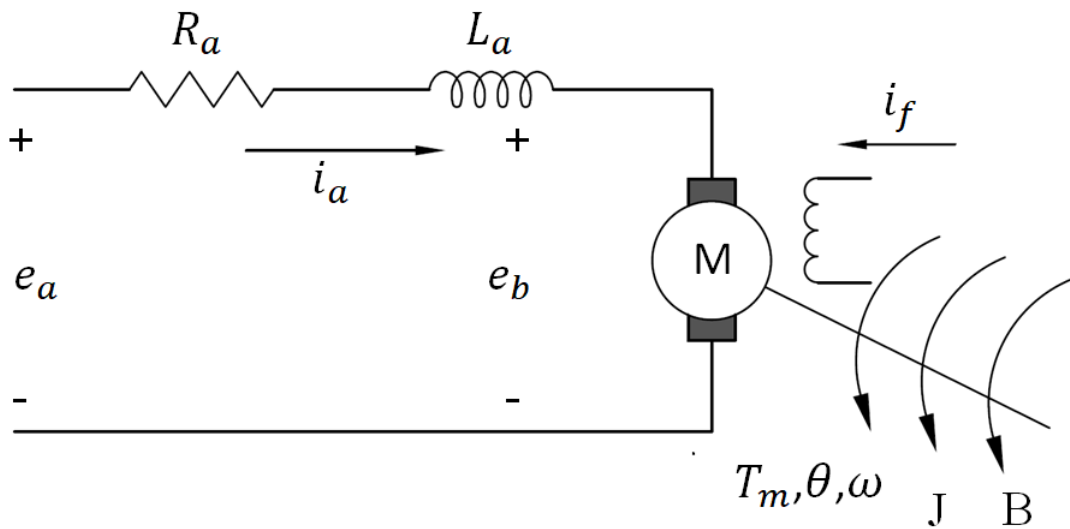
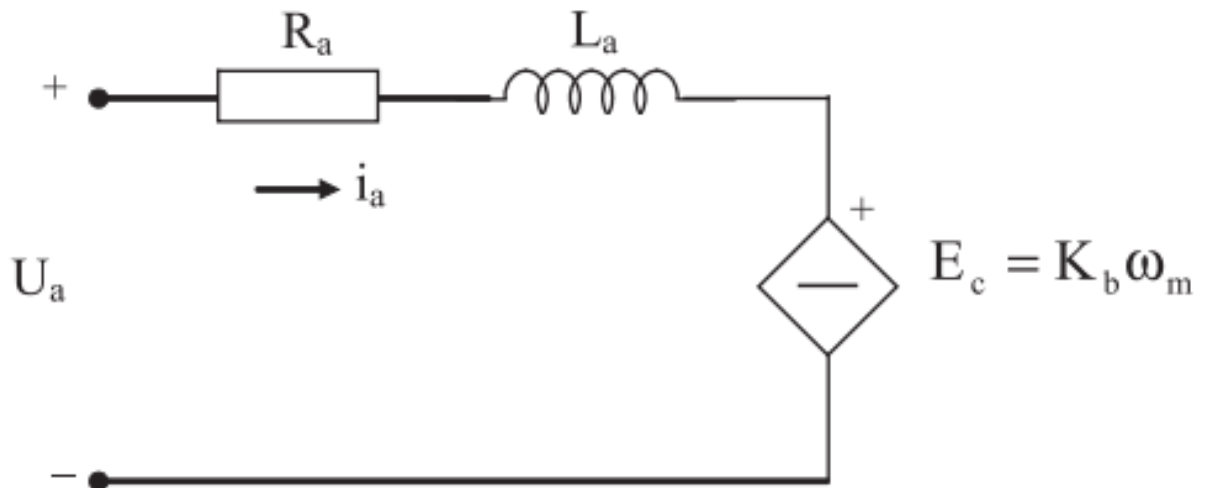


Fig. 4.3. The armature equivalent circuit of DC motor



**Fig. 4.4.** The electrical equivalent circuit of armature

The total power utilized to propel an electric bicycle and driver using to overcome friction, slope, and air resistance is given by equation.

$$P_{total} = P_{friction} + P_{slope} + P_{air} \quad (18)$$

$$P_{air} = \frac{1}{2} A_a C_a \rho (v_w + v_{EA})^2 v_{EA} \quad (19)$$

$$P_{slope} = M g C_s v_{EA} \quad (20)$$

$$P_{friction} = g M C_{rr} \cos \alpha v_{EA} \quad (21)$$

The selection of the electric motor power ( $P_m$ ) for assisting the rider during pedaling is determined based on the consumed power ( $P_{total}$ ). The calculation process for determining the required power ( $P_{rq}$ ) of the electric bike is outlined in the flowchart depicted in Fig. 4.5. The input parameters include the gear speed ( $\gamma(i)$ ), frontal area ( $A(i)$ ), and slope grade ( $G(i)$ ), with the index 'i' representing each specific input factor

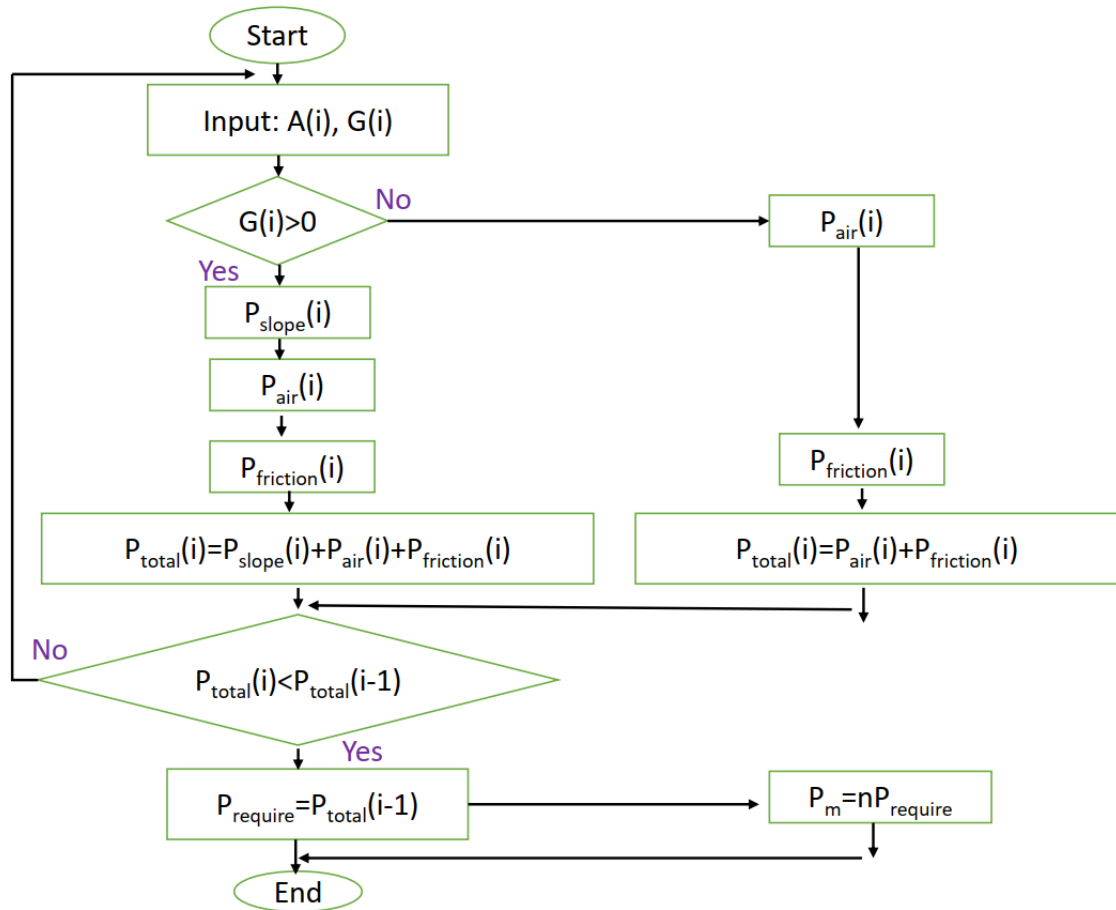


**Fig.4.5** The calculated power flowchart of EB

### 4.3 Zero-dimension model

MATLAB Simulink 2021a was used to generate the simulation. The main component of electric bicycle was defined under mathematical equation including bicycle dynamic, electric direct current motor, lithium battery. Utilizing information from experimental observations, main variable wheel size, battery capacity, acceleration due to gravity, air density were determined. A Windows PC with an Intel® Core i7™ 77003 60 GHz processor and 32 GB of RAM was used for this experiment. Additionally, this section describes the basic calculation process and covers the material properties treatment, beginning and boundary requirements, computer network computation, and post-treatment of the preprocessor.

The DC motor block was connected to DC Voltage Source, and then connected to the mechanical components representing the bicycle's inertia. The PID controller was connected to DC motor to control the motor's speed. The PS-Simulink Converter and Simulink-PS Converter blocks were used to interface between Simulink and Simscape blocks. Finally, the sensor was connected to measured output data. Set the parameters according to specification of bicycle including battery voltage in DC Voltage Source, motor parameters such as resistance, inductance, and back EMF constant in the DC motor block. Fig. 4.6, Fig4.7 and Fig 4.8 show the main component properties of an electric bicycle model. The boundary conditions for each simulation case were shown in table below:

Main	Drag	Pitch	Variables
Mass:	21	kg	▼
Number of wheels per axle:	1		
Horizontal distance from CG to front axle:	0.6	m	▼
Horizontal distance from CG to rear axle:	0.4	m	▼
CG height above ground:	0.8	m	▼
Externally-defined additional mass:	Off		▼
Gravitational acceleration:	9.81	m/s <sup>2</sup>	▼
Negative normal force warning:	Off		▼
Frontal area:	0.423	m <sup>2</sup>	▼
Drag coefficient:	1.1		
Air density:	1.225	kg/m <sup>3</sup>	▼

Fig 4.6: The bicycle properties

Electrical Torque   Mechanical   **Faults**

Field type: Permanent magnet

Model parameterization: By rated load and speed

Armature inductance: 12e-6 H

No-load speed: 350 rpm

Rated speed (at rated load): 70 rpm

Rated load (mechanical power): 250 W

Rated DC supply voltage: 36 V

Rotor damping parameterization: By damping value

**Fig 4.7:** The DC motor properties

Main   **Electrical (per cell)**   Thermal (per cell)   Table Breakpoints

Number of series-connected cells 10

Number of parallel sets of series-connected cells 5

Initial cell charge deficit (A\*hr) Qe\_init

Initial cell temperature (K) T\_init

**Fig 4.8:** Li-on battery properties

**Table 4.1** Description of the simulated cases regarding the various transmission ratio

Transmission ratio	Bicycle weight (kg)	Rider weight (kg)	Slope ratio (%)	Wind velocity (km/h)	Frontal area (m <sup>2</sup> )
2.18	21	75	0	0	0.423
2.4	21	75	0	0	0.423
2.66	21	75	0	0	0.423
3	21	75	0	0	0.423
3.43	21	75	0	0	0.423
2.18	21	75	0	0	0.423
2.4	21	75	0	1	0.423
2.66	21	75	0	2	0.423
3	21	75	0	3	0.423
3.43	21	75	0	4	0.423
2.18	21	75	0	0	0.423
2.4	21	75	0.36	0	0.423

2.66	21	75	0.48	0	0.423
3	21	75	0.65	0	0.423
3.43	21	75	0.85	0	0.423

**Table 4.2.** Description of the simulated cases regarding the various to bicycle weight

Bicycle weight (kg)	Transmission ratio	Rider weight (kg)	Slope ratio (%)	Wind velocity (km/h)	Frontal area (m <sup>2</sup> )
11	3.43	75	0	0	0.423
16	3.43	75	0	0	0.423
21	3.43	75	0	0	0.423
26	3.43	75	0	0	0.423
31	3.43	75	0	0	0.423
11	3.43	75	0	0	0.423
16	3.43	75	0	1	0.423
21	3.43	75	0	2	0.423
26	3.43	75	0	3	0.423
31	3.43	75	0	4	0.423
11	3.43	75	0	0	0.423
16	3.43	75	0.36	0	0.423
21	3.43	75	0.48	0	0.423
26	3.43	75	0.65	0	0.423
31	3.43	75	0.85	0	0.423

**Table 4.3.** Description of the simulated cases regarding the various frontal area

Frontal area (m <sup>2</sup> )	Bicycle weight (kg)	Rider weight (kg)	Slope ratio (%)	Wind velocity (km/h)	Transmission ratio
0.423	21	75	0	0	3.43
0.723	21	75	0	0	3.43
1.023	21	75	0	0	3.43
1.323	21	75	0	0	3.43
1.623	21	75	0	0	3.43
0.423	21	75	0	0	3.43
0.723	21	75	0	1	3.43
1.023	21	75	0	2	3.43
1.323	21	75	0	3	3.43
1.623	21	75	0	4	3.43

0.423	21	75	0	0	3.43
0.723	21	75	0.36	0	3.43
1.023	21	75	0.48	0	3.43
1.323	21	75	0.65	0	3.43
1.623	21	75	0.85	0	3.43

**Table 4.4.** Description of the simulated cases regarding the various wheel radius

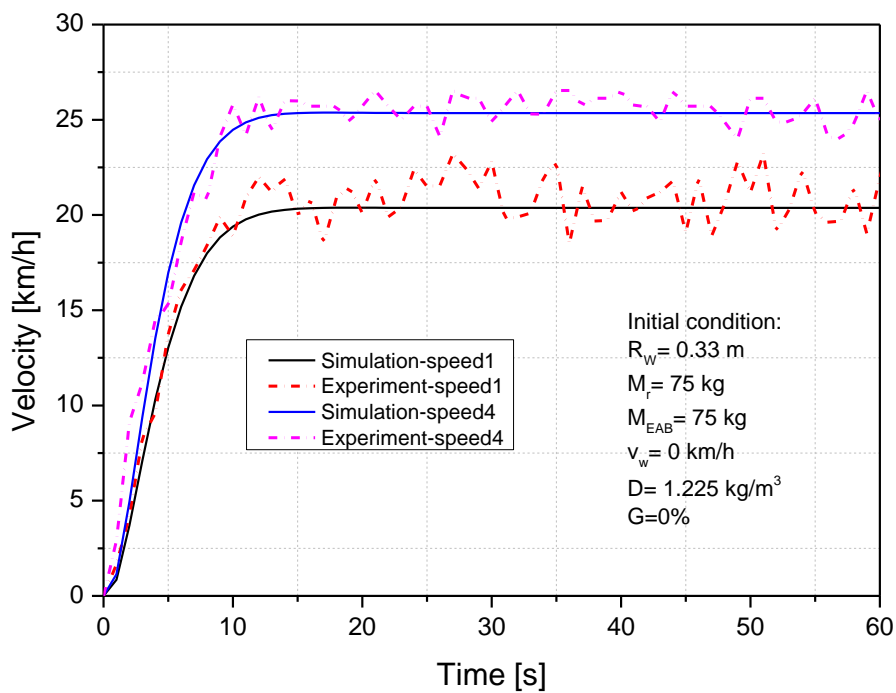
Wheel radius (m)	Bicycle weight (kg)	Rider weight (kg)	Slope ratio (%)	Wind velocity (km/h)	Frontal area (m <sup>2</sup> )
0.3	21	75	0	0	0.423
0.33	21	75	0	0	0.423
0.36	21	75	0	0	0.423
0.39	21	75	0	0	0.423
0.42	21	75	0	0	0.423
0.3	21	75	0	0	0.423
0.33	21	75	0	1	0.423
0.36	21	75	0	2	0.423
0.39	21	75	0	3	0.423
0.42	21	75	0	4	0.423
0.3	21	75	0	0	0.423
0.33	21	75	0.36	0	0.423
0.36	21	75	0.48	0	0.423
0.39	21	75	0.65	0	0.423
0.42	21	75	0.85	0	0.423

## 4.4 Summary

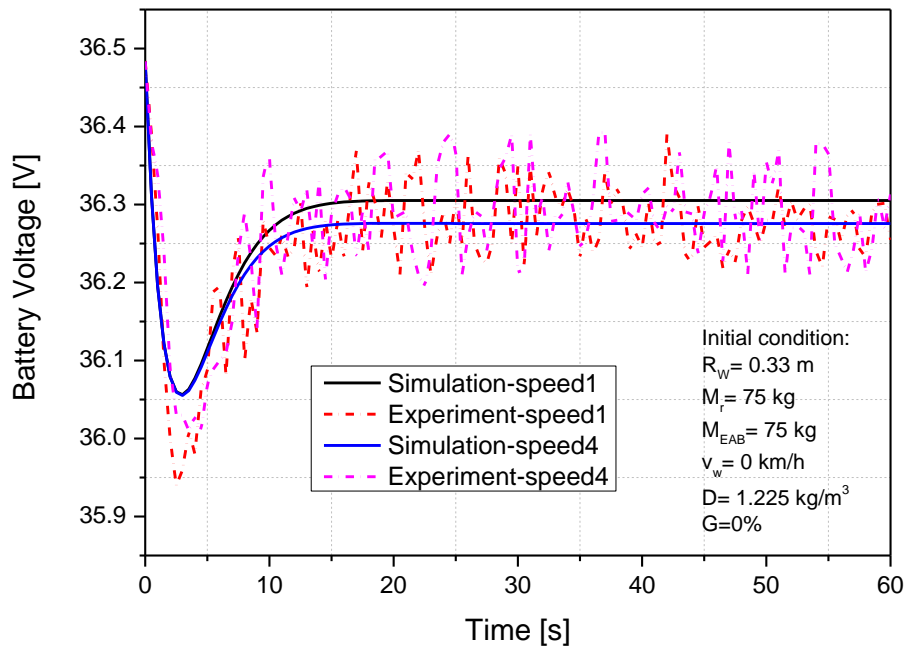
This chapter has explained the simulation modeling in MATLAB-Simulink software with version 2021. By utilizing MATLAB Simulink, this study can gain deep insights into the performance and optimization of electric bicycles, facilitating efficient and effective development processes. To ensure the accuracy of simulation model, the outcomes will be validated with experimental results.

# 5. AN INVESTIGATION ON THE EFFECTIVE PERFORMANCE AREA OF THE ELECTRIC BICYCLE WITH VARIABLE KEY INPUT PARAMETER

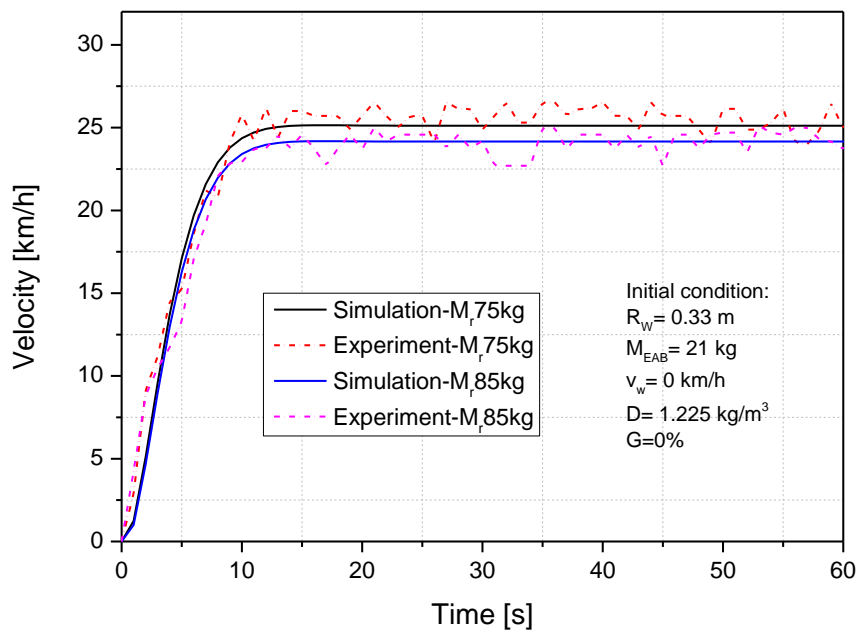
## 5.1 Comparison experiment and simulation results



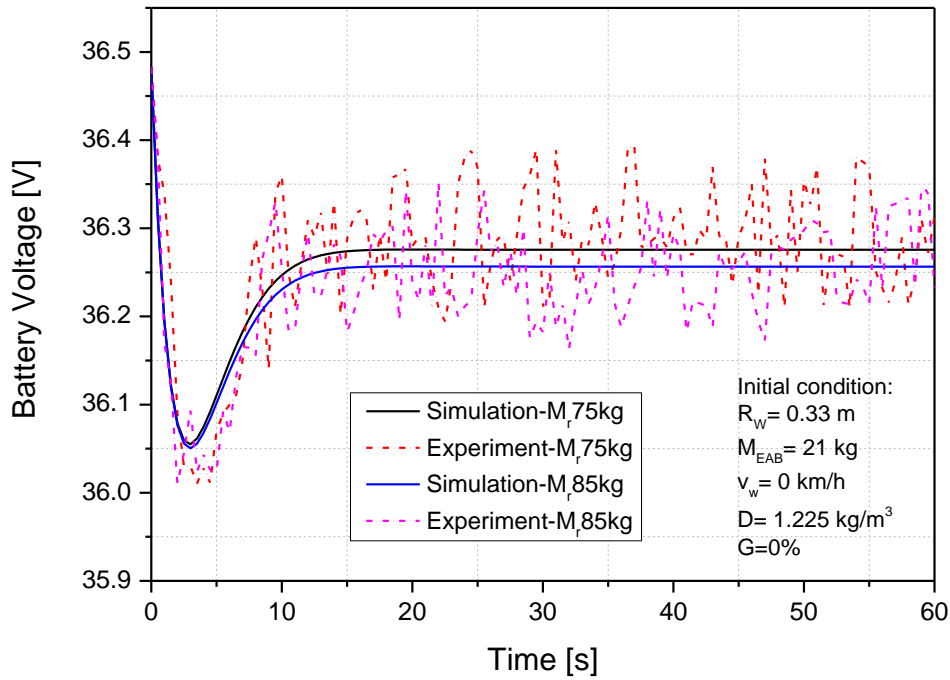
(a)



(b)



©



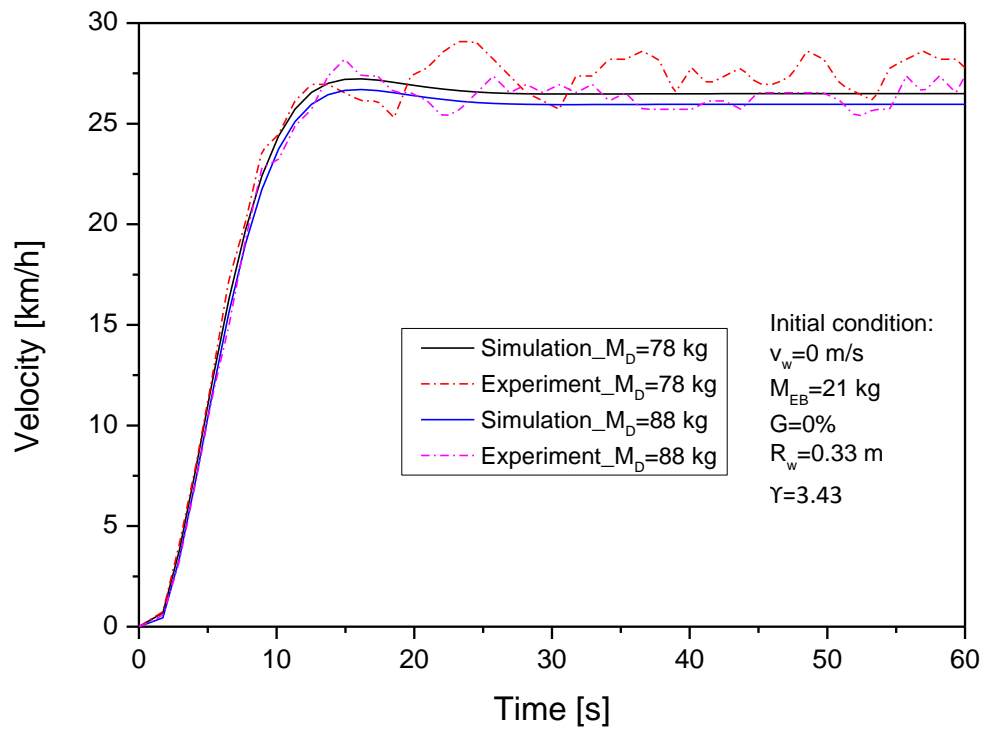
(d)

**Fig. 5.1.** (a) Validation of bicycle velocity at speed1 and speed4 by simulation model; (b) Validation of battery voltage at speed1 and speed4 by simulation model; (c) Validation of bicycle velocity with a changed rider mass by simulation model; (b) Validation of battery voltage with a changed rider mass by simulation model.

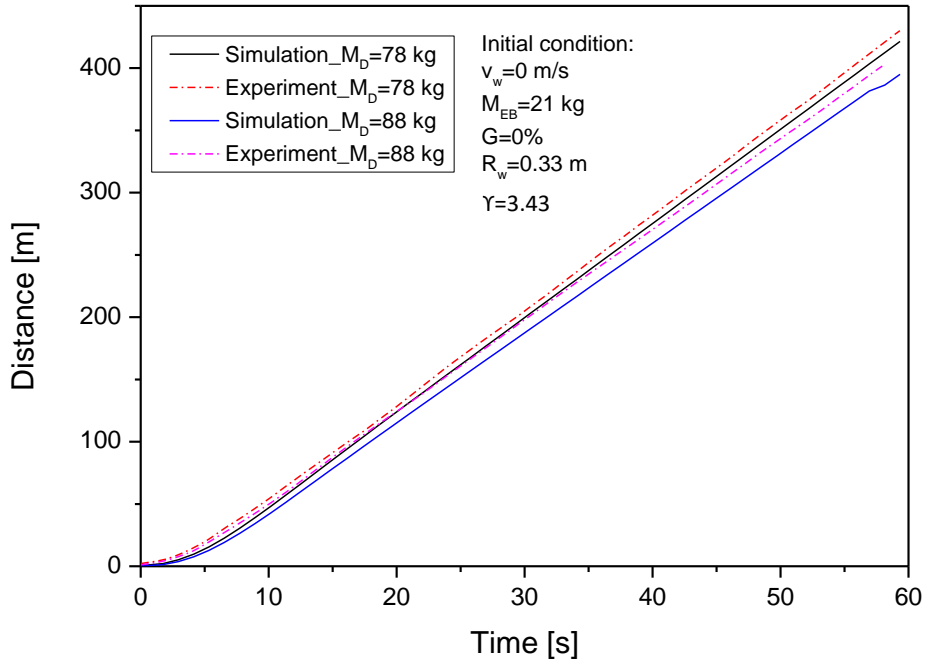
Fig.5.1 shows the validation of bicycle velocity and battery voltage between the simulation and experiment results by variable the transmission ratio and rider mass. The experimental test was conducted within 60 second under initial condition including bicycle mass of 21 kg, wind speed of 0km/h, slope grade of 0%, wheel radius of 0.33m while the rider mass and gear speed was changed from 75kg to 85kg and from speed level 1 to speed level 4. It can be seen that, the simulation results have shown good agreement with experimental results under identical condition, demonstrating the accuracy of the simulation model. The maximum difference was

notified 0.6% at 36.7 seconds with rider mass was 75 kg. This can be acceptable because the experimental result values are considered as an average value during the experiment test.

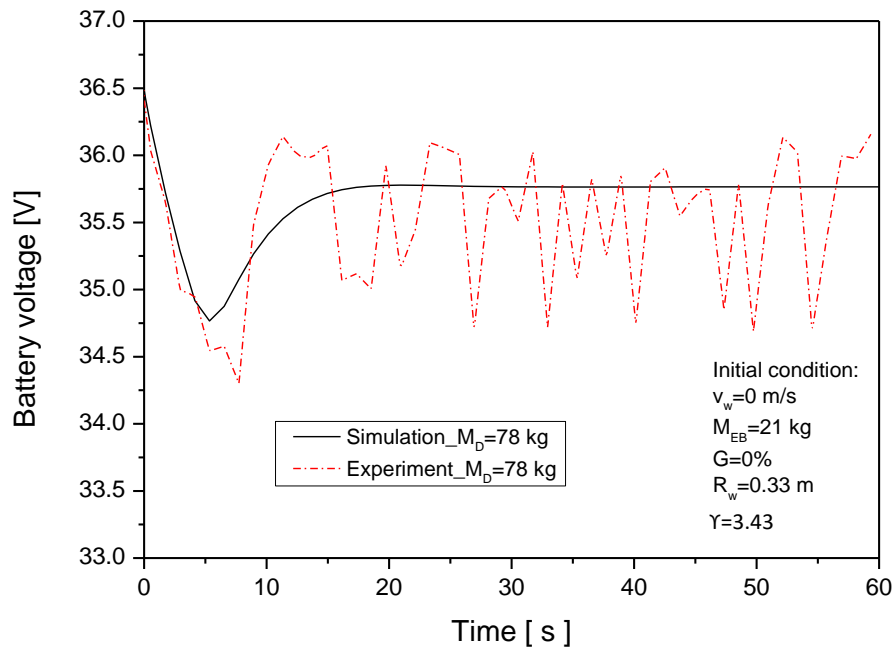
## 5.2 Effect of operating parameters



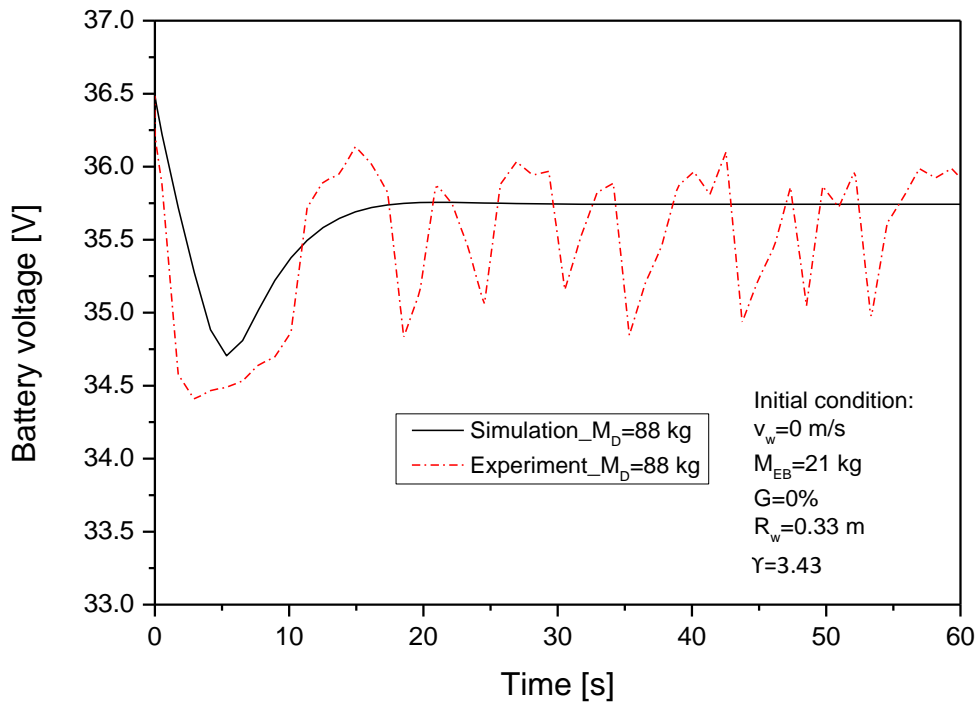
(a)



(b)



©

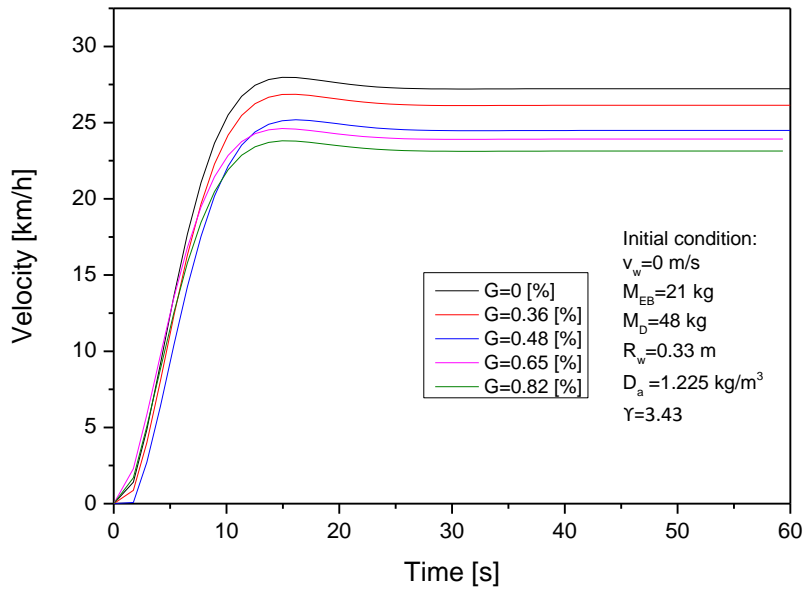


(d)

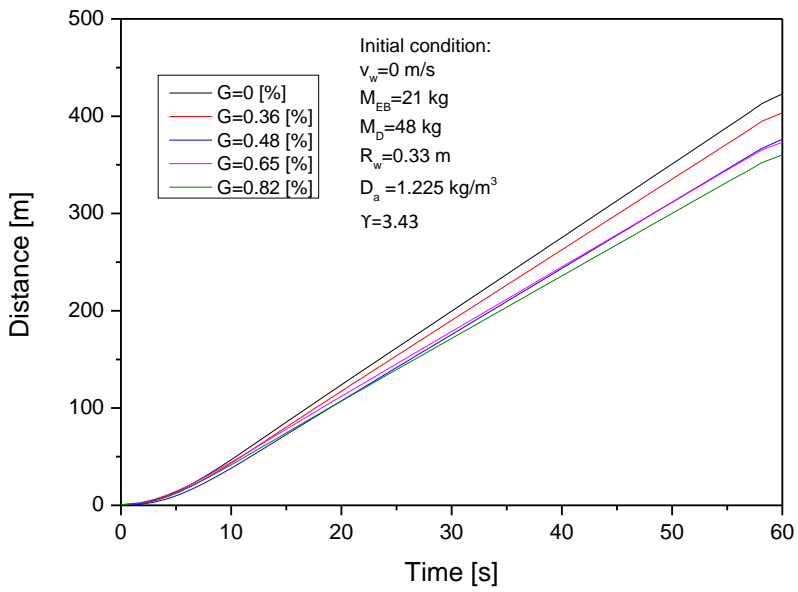
**Fig. 5.2.** Impact of driver mass to (a) velocity, (b) distance, (c) and (d) battery voltage

Driver mass directly affects EB motion through inertial force. The simulation and experimental trials were conducted under the same initial conditions of 21 kg bicycle mass, 0.33 m wheel radius, 3.43 transmission ratio, 0% slope ratio, and 0 km/h wind speed, while driver mass varied from 78 kg to 88 kg. Following the simulation results, Figures (5.2a) and (5.2b) shown that the EBs reach maximum velocity at 27.21 Km/h and 26.29 km/h when the driver mass is 78 kg and 88 kg within 14.93 seconds and 16.13 seconds. Besides that, the velocity and moving distance are slightly decreased by 2% and 6.17% when driver mass increases from 78 kg to 88 kg, respectively. The decreasing of velocity and moving distance with increasing of driver mass can be explained as follow: The increasing of driver mass led to increasing in the friction force and slope resistance force, therefore the resistance force total was increased, while the initial

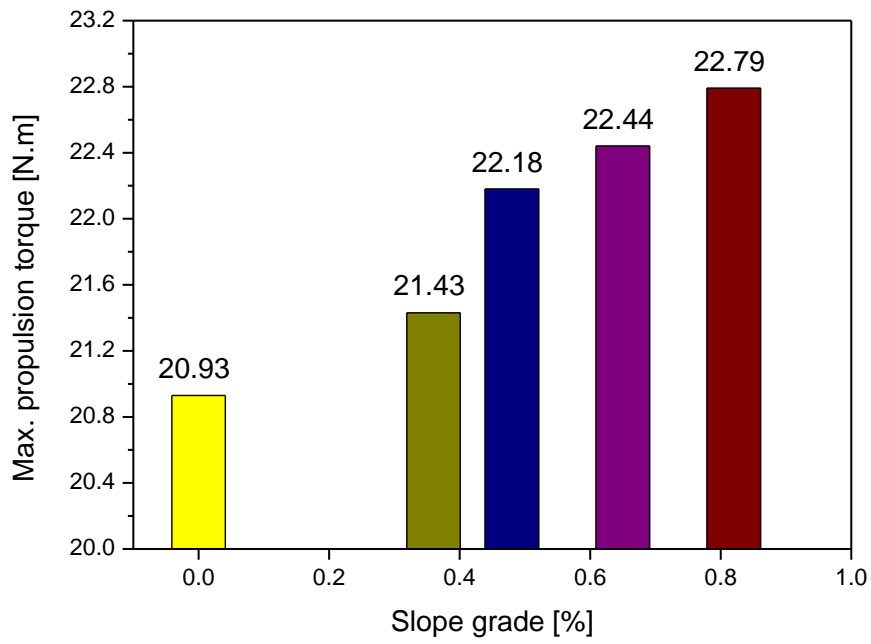
experimental condition is the same. So, the velocity and moving distance of EB were decreased. Moreover, the required time is 16.1 seconds and 17.3 seconds to reach a stable velocity it implies that, the velocity and time to reach a stable velocity of EBs can be optimized with decreasing driver mass. Figures (5.2a) and (5.2b) shown that, the experimental and simulation data have the same trend. The maximum difference of velocity was 8.47% and 5.81% at 24.5 seconds and 14.9 seconds when the driver mass was 78 kg and 88 kg, similar to the maximum difference of moving distance of 2.04% and 4.3%, respectively. This maximum scale is acceptable because the velocity value flow average value during the experiment. A sudden wind can lead to such error. The electric consumption was known as an important indicator of effective performance area during operating behavior of EBs, which was shown in Figures (5.2c) and (5.2d). With increased driver mass from 78 kg to 88 kg, electric consumption slightly increased by 0.05%. This can be explained by the increased driver mass led to increase the resistance force total, therefore the load to motor was increased, so the energy demand for motor was increased. Furthermore, the required time to reach a stable battery voltage was 18.5 and 19.7 seconds at driver mass 78 kg and 88 kg, which implies that electricity consumption and duration of fluctuating voltage during acceleration can be optimized by reducing EB mass. Figures (5.2c) and (5.2d) compare the simulated and experimental battery voltages. The maximum difference of battery voltage during operating behavior with driver mass of 78 kg and 88 kg was 3.02% and 2.55% at 54.5 seconds and 35.3 seconds, respectively. Battery voltage is an average of the experimental values and is acceptable. To reduce the error of battery voltage between simulation and experimental results, in addition to correct input parameters, sudden wind and device error should be minimized.



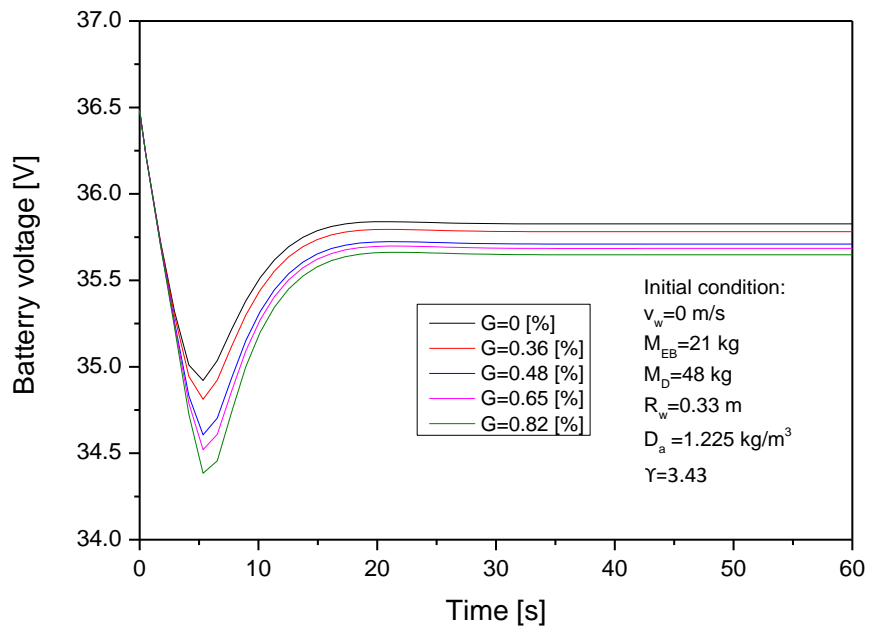
(a)



(b)



(c)



(d)

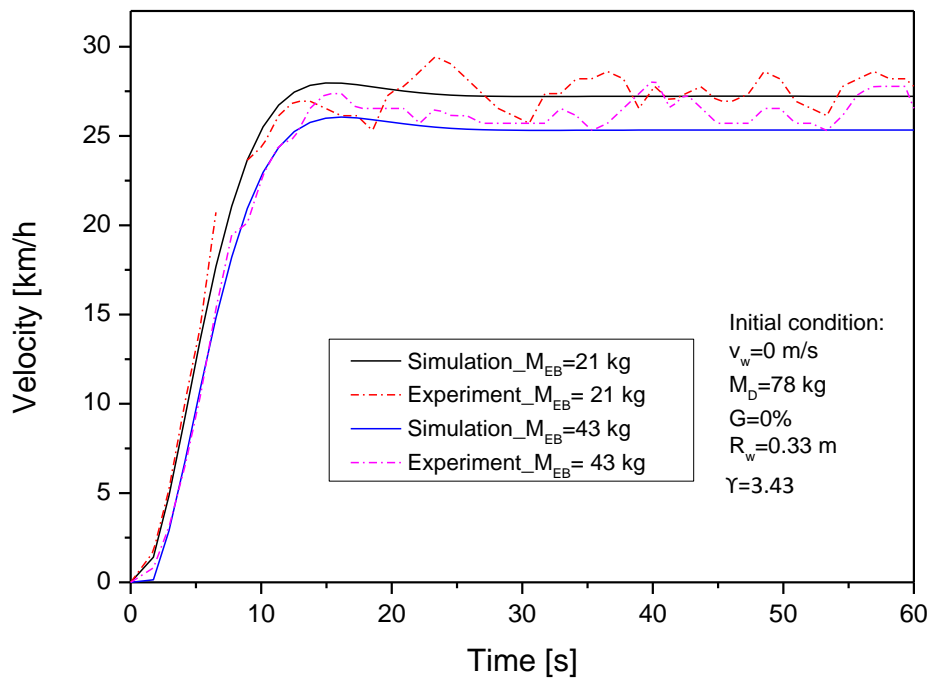
**Fig. 5.3** Impact of slope ratio to (a) velocity, (b) distance, (c) propulsion torque and (d) battery voltage

The effects of slope ratio on the operating characteristics of the EB are presented in Eqs. (3) and (4). The simulation was conducted with initial conditions of 21 kg electric bicycle mass, 48 kg driver mass, 0.33 m wheel radius, 0 km/h wind speed, 3.43 transmission ratio, and 1.225 air density while the slope ratio is varied at 0%, 0.36%, 0.48%, 0.65%, and 0.82%. Figures (5.3a) and (5.3b) present the effects of slope ratio on velocity as well as moving distance. The EB's velocity and moving distance significantly decrease by 15.02% and 15.38%, the EB reaches maximum velocity at 27.95 km/h and 23.78 km/h when slope ratio is 0% and 0.82%, respectively. Moreover, the required time to reach a stable velocity is 14.9 seconds and 16.1 seconds at 0% and 0.82%. The decreasing of velocity and moving distance can be explained as follow: The increased slope ratio led to a significant increase in slope resistance force and slight decrease of rolling resistance force, therefore the resistance force total was increased. So, the load on the motor was increased. This is why the time to reach a stable velocity is longer.

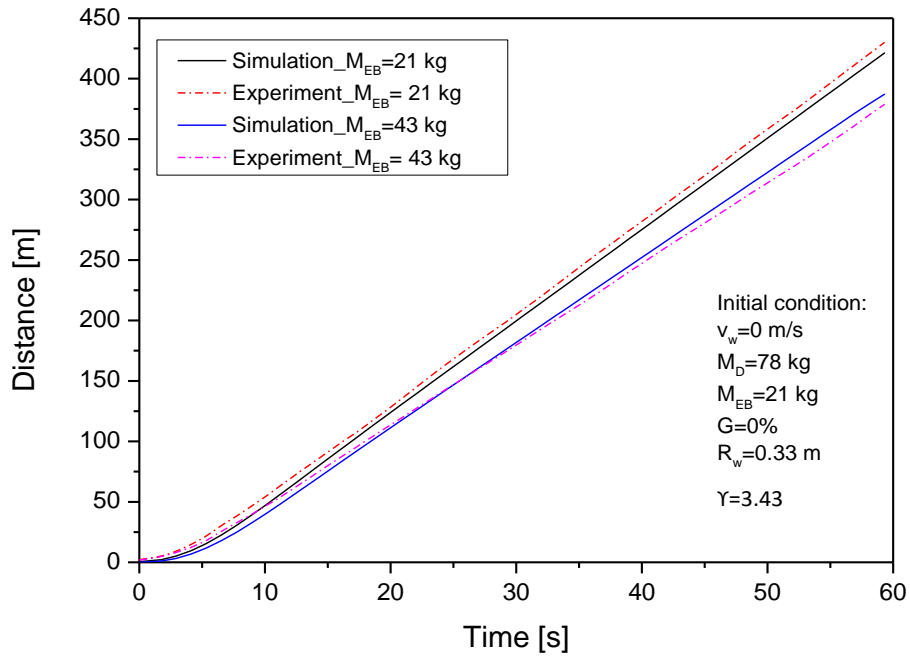
In addition, propulsion torque increases when slope ratio increases from 0 % to 0.84%, as presented in Fig. (5.4c). This could be interpreted by the increased load generated by the DC motor to produce the higher propulsion torque was required to overcome the resistive load. Figure (5.4d) shows the electricity consumption under the effect of slope ratio. The electric consumption slightly increases by about 0.08%. when the slope ratio increases from 0% to 0.84%. the increasing of electric consumption can be explained by: the increasing of slope ratio led to increasing resistance force total, therefore the load on motor was increased, while the initial condition is same, so the energy demand supplies for DC motor was increased to adapt for DC motor overcome the increase of load. Besides that, the time to stable voltage is 18.5

seconds and 19.7 seconds at slope ratio is 0% and 0.82%, respectively. It implies that the electric consumption and time required for the battery to reach a stable voltage can be optimized by reducing slope ratio. Based on the observed results, Slope ratio 0% is the optimal parameter for future investigation.

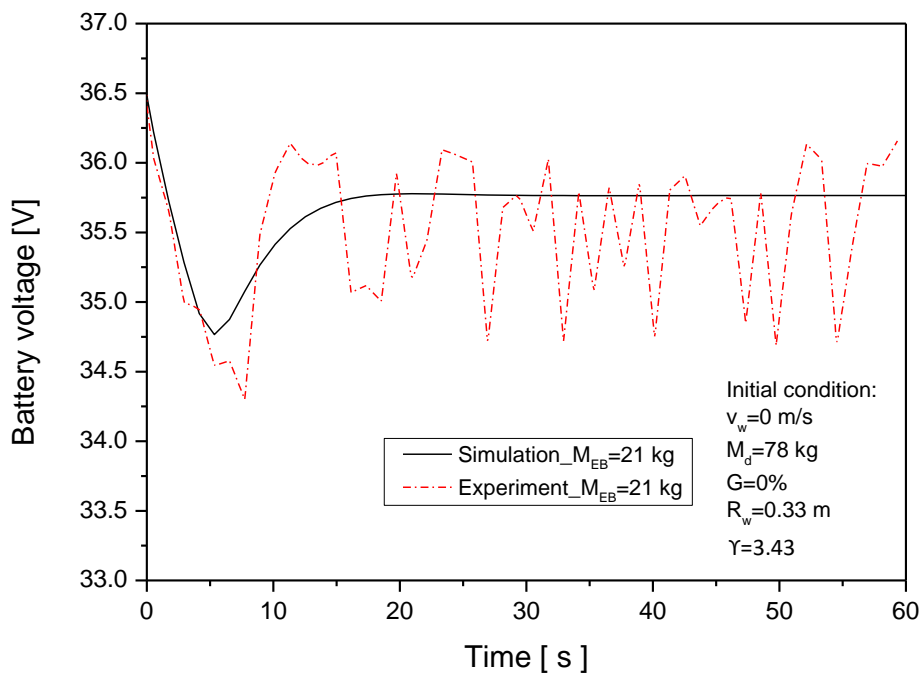
### 5.3 Effect of structure parameters



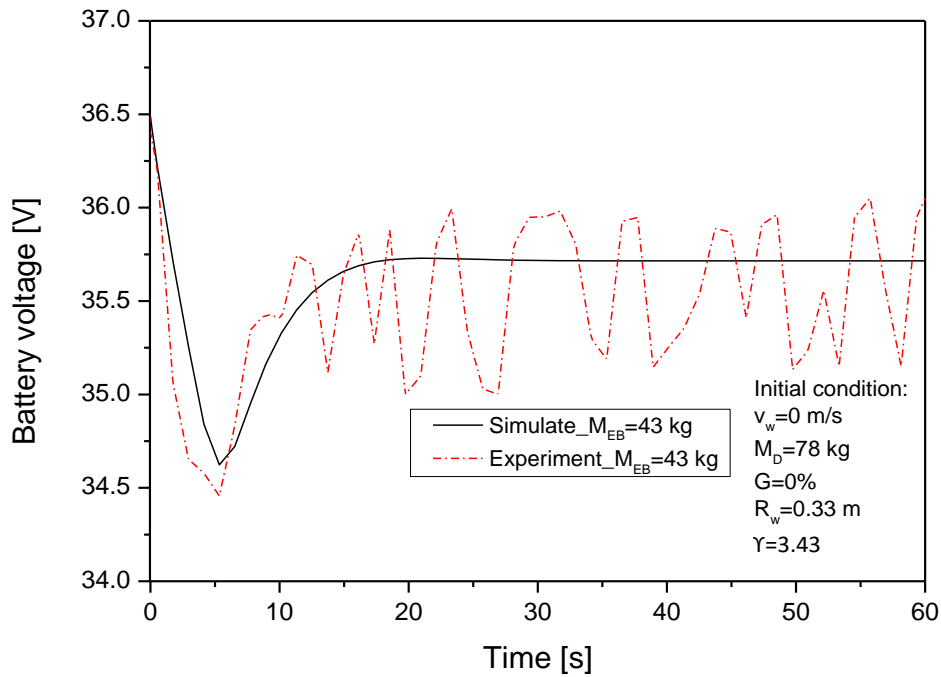
(a)



(b)



©



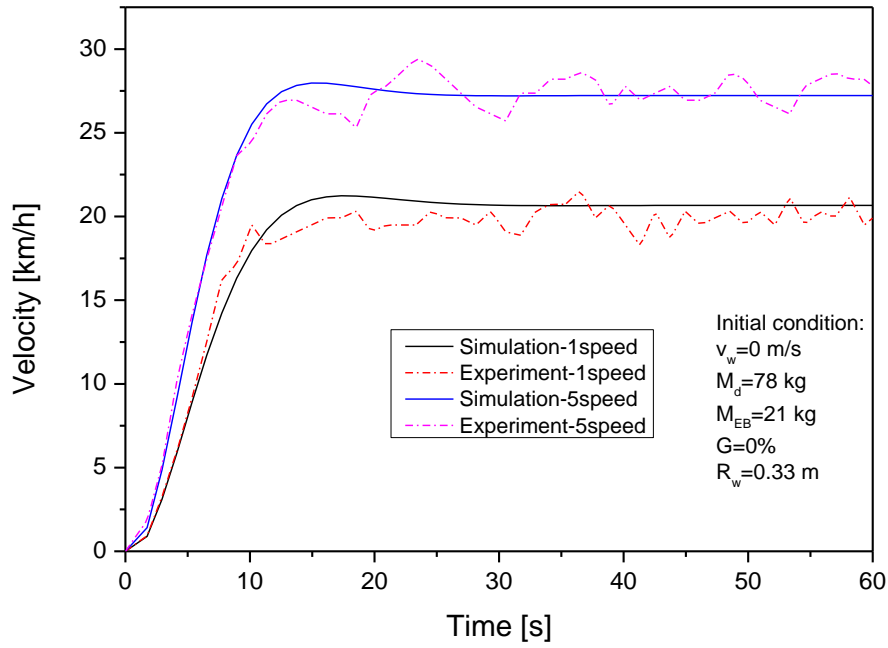
(d)

**Fig. 5.4.** Impact of EB mass to (a) velocity, (b) distance, (c) and (d) battery voltage

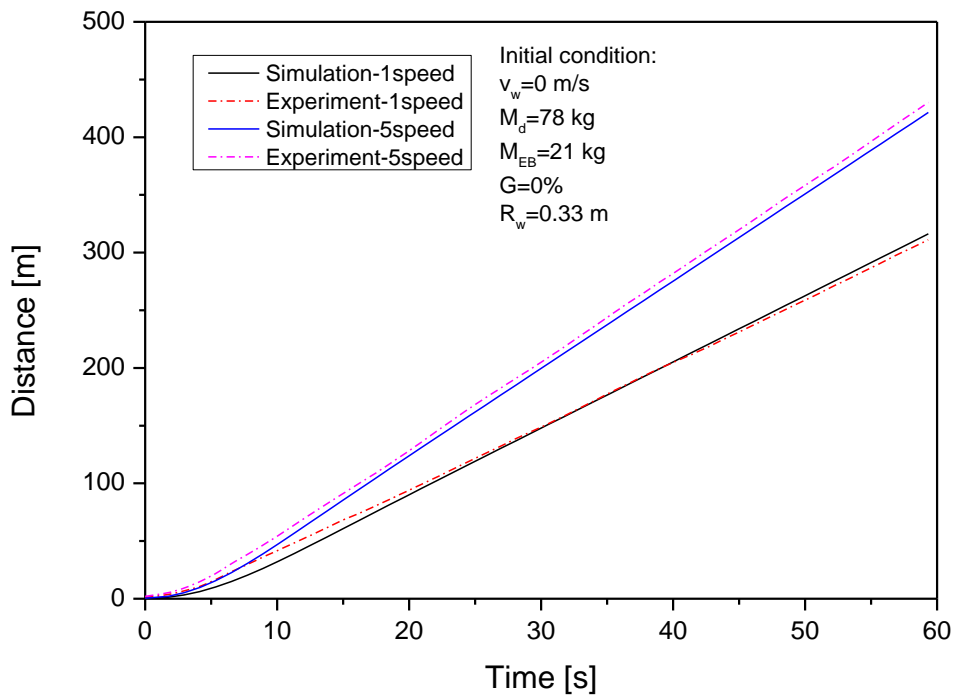
The mass of the electric bicycle ( $M_{EB}$ ) is one of the factors that directly influences the operating behavior of electric bikes because it has a relationship with rolling resistance force and slope resistance force, which is shown in Eqs. (3) and (4). According to the simulation results, we can observe Fig. (5.4a) and (5.4b), the EB reaches maximum velocity at 27.95 km/h and 25.98 km/h when EB mass is 21 kg and 43 kg within 14.9 seconds and 16.1 seconds, respectively. The EB's velocity and moving distance decreased 5.7% and 6.2% when EB mass increases from 21 kg to 43 kg. The decreasing of velocity and moving distance can be explained as follow: The increasing of EB mass led to increasing friction resistance force and slope resistance force, therefore the resistance force total was increased while the initial condition is same, so the velocity and moving distance have a decreasing trend. Furthermore,

the 23.3 seconds and 24.53 seconds are the required time to reach a stable velocity with the EB mass are 21 kg and 43 kg, which implies that the timing to reach stable operating behavior of EB is increased by increasing of EB mass. Figure. (5.4a) and 5.4b) show that the velocity and moving distance from simulation results have the same trend as experimental results. The maximum difference of velocity at EB mass 21 kg and 43 kg are 8.82% and 8.92%, similar to the maximum difference of moving distance of 2.1% and 2.3%, respectively. This maximum scale is acceptable because the velocity value flows average value during the experiment. To reduce the error of velocity and moving distance between simulated and experimental results, besides input correct input parameters, the sudden appearance of wind should be controlled.

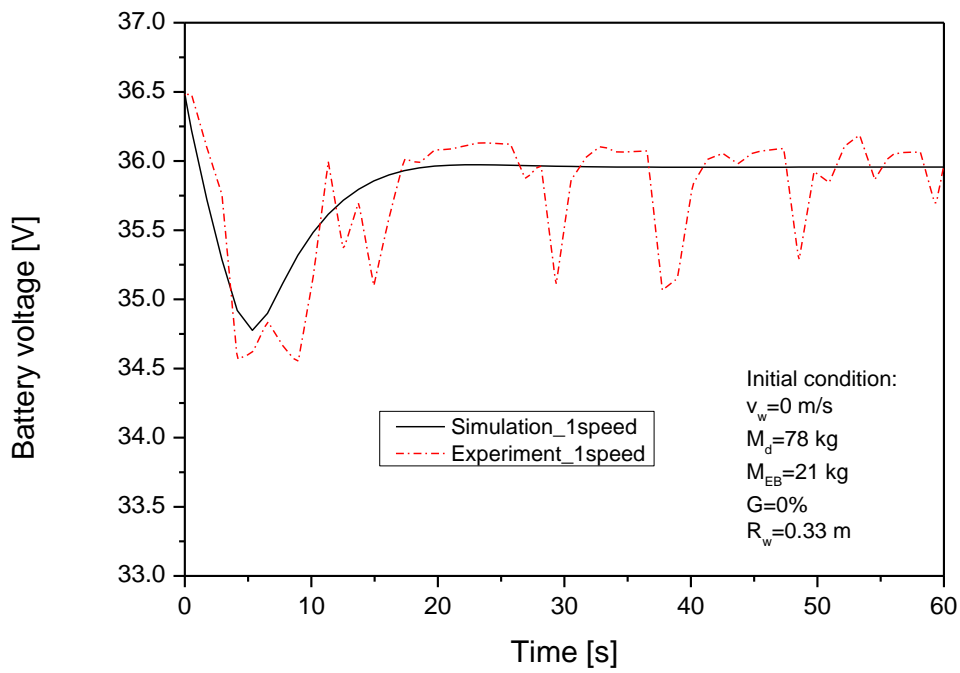
Figures (5.4c) and (5.4d) show that electric consumption increases by 0.53% when EB mass increases from 21 kg to 43 kg. This can be explained by increasing the resistance force total led to increasing the load to motor, so the energy demand for the motor was increased. Further, the time required for the battery to achieve a stable voltage status is 18.53 seconds and 14.93 seconds at EB mass 43 kg and 21 kg, which implies that electricity consumption and duration of fluctuating voltage during acceleration can be optimized by reducing EB mass. Based on the achieved results, electric bicycle mas  $M_{EB}= 21$  kg is chosen as input parameter of future investigation. Figures (5.5c) and (5.5d) compare the simulation and experimental results of battery voltage. The Maximum difference of 3.02% and 2.1% was observed at 54.5 seconds and 27 seconds when EB mass was 21 kg and 43 kg, respectively. It is acceptable because the battery voltage value flows average value during the experiment. The error can be caused by device noise as well as sudden wind.



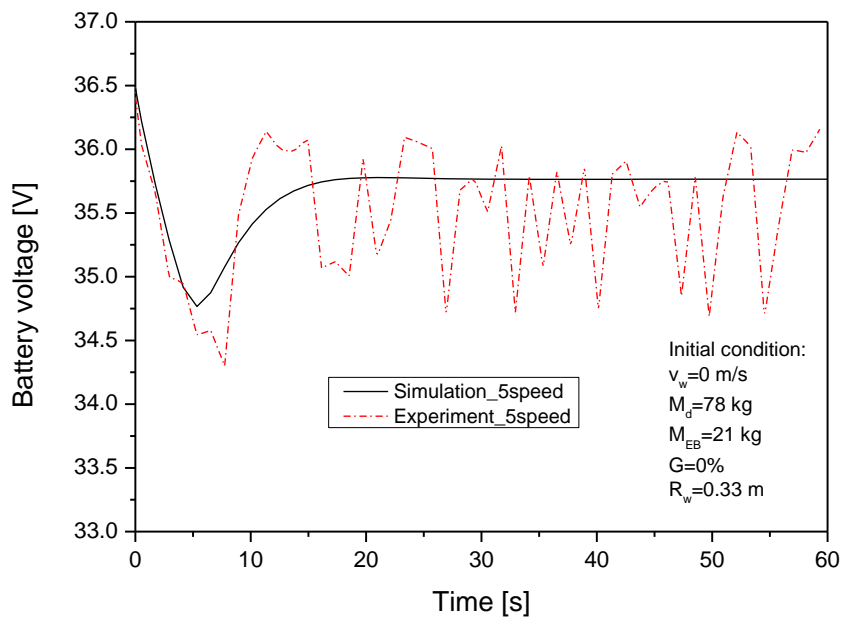
(a)



(b)



©

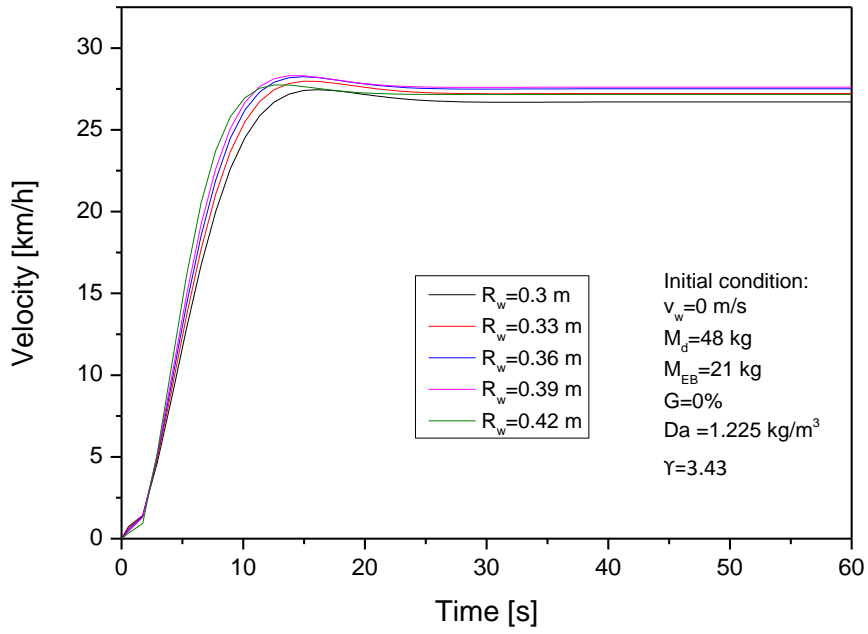


(d)

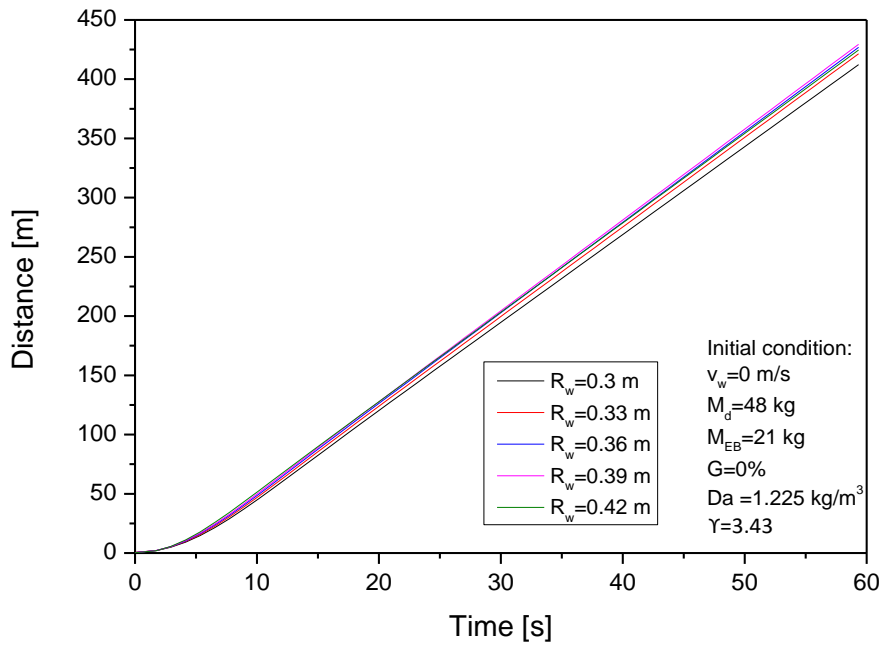
**Fig. 5.5.** Impact of transmission ratio to (a) velocity, (b) distance, (c) and (d) battery voltage

The experiment and simulation were conducted with initial conditions of 76 kg driver mass, 21 kg EB mass, 0 km/h wind speed, 0% slope ratio, and 0.33 m wheel radius with transmission ratios varying at 2.18 and 3.43 (Table 1). Figures (5.5a) and (5.5b) show the effect of transmission ratio on velocity as well as the distance of the EB. Following the change in gear speed, the velocity and moving distance of the EB significantly increased with 31.76% and 32.18% when gear speed is increased from 1-speed to 5-speed. Moving distance increases from 316.2 to 421.4 m when gear speed changes from 1-speed to 5-speed, respectively. Further, the required time to achieve stable velocity is 16.13 and 13.73 seconds with 1-speed and 5-speed, respectively. As shown in Fig. (5.5a), the experimental velocity slightly differs from the simulation velocity, with a maximum difference of velocity when 1-speed and 5-speed were notified 8.5 % and 7.1 % at 31.73 seconds and 23.3 seconds. This velocity is an average of the experimental values and is acceptable. The sudden appearance of wind can cause the error.

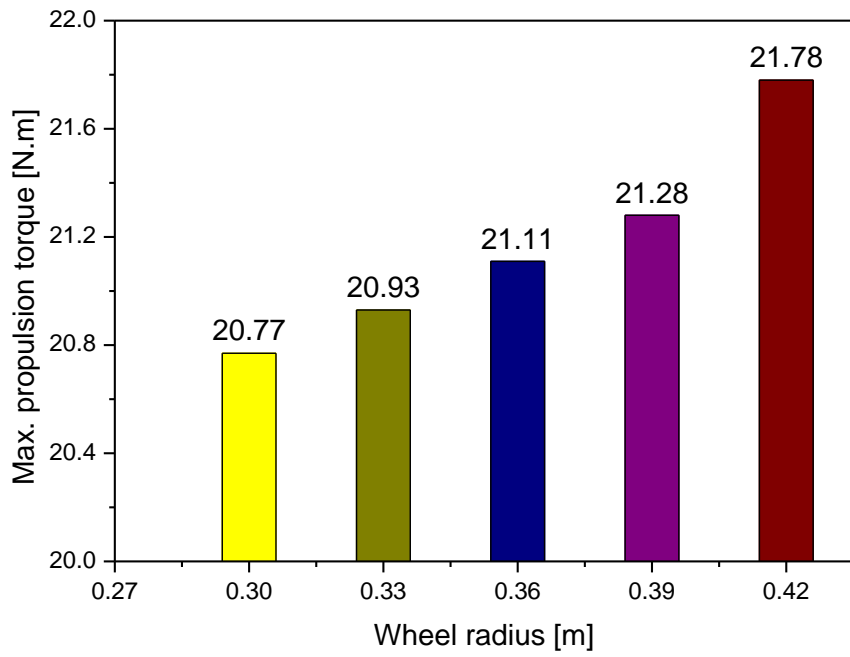
Figures (5.5c) and (5.5d) show the simulated and experimental battery voltage. The maximum voltage difference of 1-speed and 5-speed was 2.41% and 3.02% at 29.3 seconds and 54.5 seconds, respectively. Electric consumption slightly increased 0.54% by increasing the transmission ratio from 2.18 to 3.43. The increase in electric consumption can be explained as follows: The wheel revolutions are high to adapt higher velocity for EB, therefore the propulsion torque from the motor was increased. This is the reason why the energy demand for motors was increased. Besides that, the required time to achieve a stable battery voltage is 14.9 seconds and 17.3 seconds when 5-speed and 1-speed respectively. This implies that the required time to reach a stable battery voltage and electricity consumption can be optimized by transmission ratio change. Through the results obtained, the transmission ratio 3.43 is selected as one for key input parameter for future investigation.



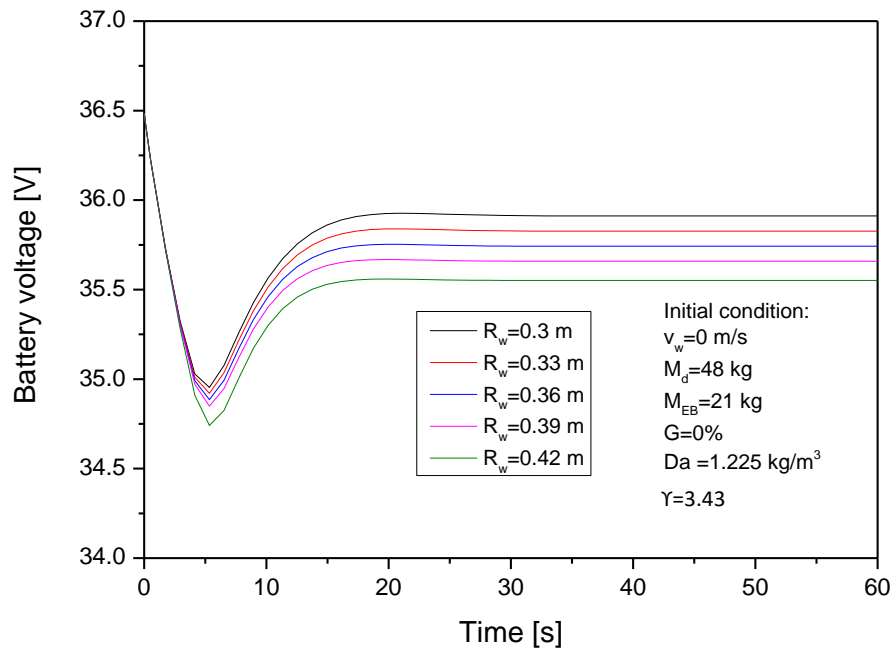
(a)



(b)



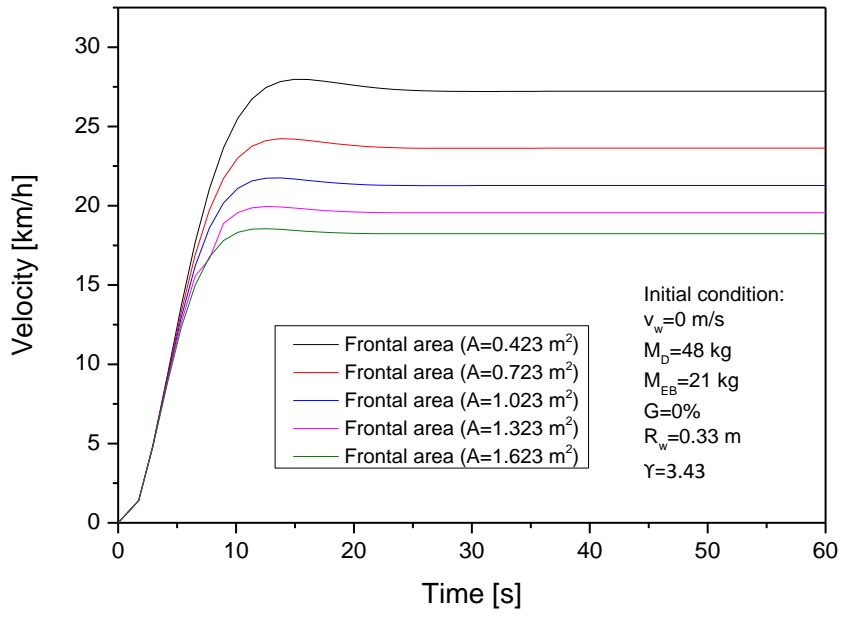
©



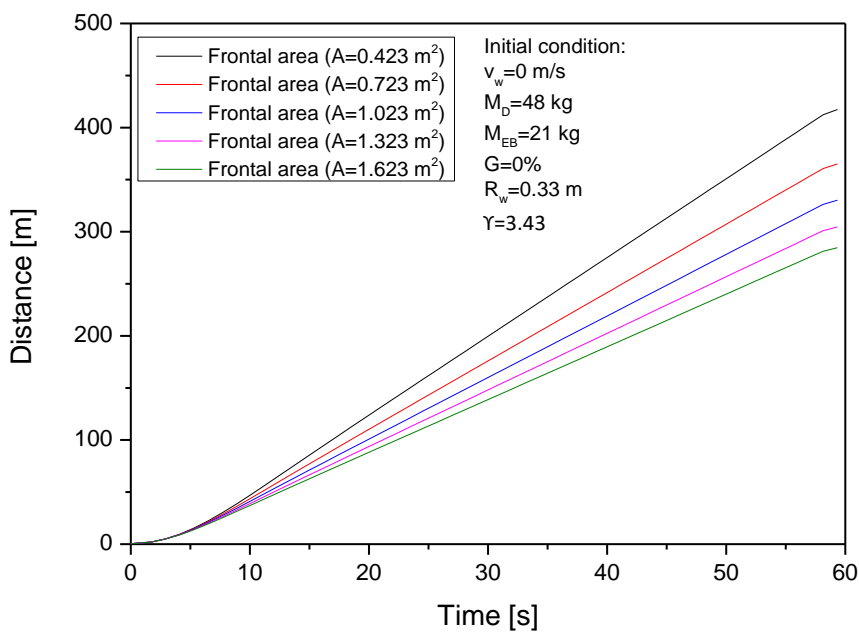
(d)

**Fig. 5.6.** Impact of wheel radius to (a) velocity, (b) distance, (c) propulsion torque and (d) battery voltage

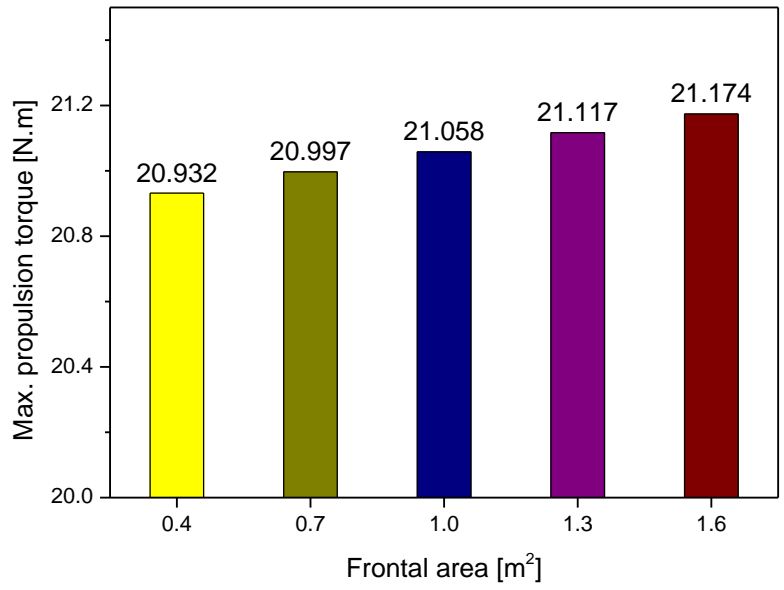
Wheel radius directly affects EB motion through the revolution of the wheel. Figures (5.6a) and (5.6b) show that the velocity as well as moving distance of the EB slightly increase with the increase of wheel radius from 0.3 m to 0.39 m but slightly decrease with the increase of wheel radius from 0.39 m to 0.42 m, respectively. The maximum velocity and moving distances are 28.31 km/h and 429.43 m at wheel radius  $R_w = 0.39$  m while the maximum velocity and moving distance are 27.5 km/h and 424.66 m at wheel radius  $R_w = 0.42$  m. Furthermore, the time to reach a stable velocity is 16.1 seconds and 17.5 seconds when the wheel radius increases from 0.3 m to 0.42 m. This result can be explained by the larger wheel radius leading to increased revolutionary inertia while the initial energy is constant. Furthermore, the increased wheel radius leads to an increase of propulsion torque, because the larger wheel radius leads to increased rotational inertia, so higher energy is needed to reach a certain velocity, but the initial energy is constant because the initial condition is the same as driver mass, EB mass, transmission ratio, slope ratio, wind speed. This explains why the increase of propulsion torque when the wheel radius is increased, as shown in Fig. (5.6c). Figure. (5.6d) shows the effect of wheel radius on electricity consumption. When the wheel radius decreases from 0.42 m to 0.3 m, the electricity consumption decreases by 0.13%, and the time required for stable voltage increases 16.1 seconds and 18.5 seconds, respectively. This could be explained by the decreasing rotational inertia leading to a decrease in load torque on the motor and extension of the time to reach a stable velocity. This implies that electricity consumption can be optimized when the wheel radius is decreased from 0.42 m to 0.3 m. Based on the observed result, wheel radius  $R_w = 0.3$  m is chosen for future investigation.



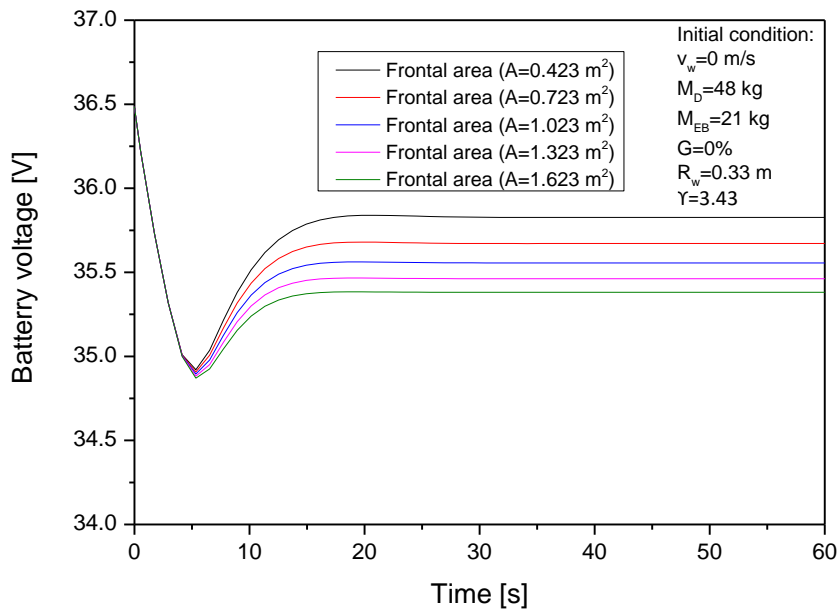
(a)



(b)



©



(d)

**Fig. 5.7** Impact of frontal area to (a) velocity, (b) distance, (c) propulsion torque and (d) battery voltage

Front area ( $A$ ) is selected for further investigation because it influences wind resistance force. The velocity and moving distance of the EB significantly increase from 18.23 km/h to 27.22 km/h and from 284.71 m to 417.413 m, respectively, when front area decreases from 1.623 m<sup>2</sup> to 0.423 m<sup>2</sup>. Moreover, the respective time required to reach a stable velocity was 12.5 seconds and 14.9 seconds, as shown in Fig. (5.7a) and (5.7b). The increase of velocity and moving distance can be explained as follow: The decreasing of the frontal area led to decrease the wind resistance force during operating behavior, therefore the resistance force total was decreased while the initial experimental condition is same. So, the velocity and moving distance was increased.

Furthermore, when the front area is increased from 0.423 m<sup>2</sup> to 1.623 m<sup>2</sup>, propulsion torque is increased by about 1.156%, as presented in Fig. (5.7c). This could be interpreted by the increasing of frontal area led to decrease the resistance force total, therefore the load placed on the DC motor was decreased. Figure (5.7d) presents the influence of front area on electricity consumption. The electric consumption decreased by 0.14% when front area decreased from 1.623 m<sup>2</sup> to 0.423 m<sup>2</sup>, and the time required for a battery to reach a stable voltage was 14.9 seconds and 17.3 seconds at frontal area 1.623 m<sup>2</sup> and 0.423 m<sup>2</sup>, respectively. This is because the decreasing of front area led to decrease the load torque on the motor, so the energy demand was decreased besides that the time to reach a stable velocity was extended. Through the research results, the effective performance area can be optimized when front area is decreased. Based on the observed results, front area  $A= 0.423 \text{ m}^2$  is the optimal parameter for future investigation.

## 5.4 Summary

The section presents a method of modeling an EB to investigate effective performance areas through analysis of the electric bicycle dynamic, DC motor model, and battery models by the MATLAB-Simulink. In addition, to validate the results from simulation, the experimental system was installed on the bicycle frame and the experiment was conducted on the real road to exam dynamic characteristics and electric consumption during operating behavior.

The importance results was summarized:

- The e-bike weight has a minor impact on e-bike dynamic. The maximum velocity increased from 25.9 km/h to 27.95 km/h and the travel distance increased 6.2 %, duration to reached stable velocity reduced from 24.5 to 23.3 seconds with reducing bicycle mass from 43 to 21 kg.
- The transmission ratio significantly influenced e-bike performance. The maximum velocity increased 31%, the travel distance increased 32%, duration to reach stable velocity extended 13.7 – 16.1 seconds with increased gear speed level from level 1 to level 5.
- The wheel size has significantly impacted on e-bike dynamic. The maximum velocity increased from 21 to 28 km/h, duration to reach stable velocity extended 16.1 – 17.5 seconds, timing to reach stable voltage extended 16.1 – 18.5 seconds with increased wheel radius 0.3 – 0.42 m.
- The frontal area has significantly influenced e-bike performance. The maximum velocity increased 18.2 – 27.2 km/h, duration to reach stable velocity reduced 14.9 – 12.5 seconds, propulsion torque reduced 1.6% duration to reach stable voltage reduced 17.3 – 14.9 seconds with decreasing frontal area 1.623 – 0.423 m<sup>2</sup>.

The contributions of this paper are as follow: By combining the results from experimental and simulation study, not only the timing to reach velocity and battery voltage stable status are completely investigated with the key input parameters effect of transmission ratio, bicycle mass, wheel radius, frontal area, slope ratio and driver mass of e-bike but also the electric consumption during operating behavior of electric bicycle is comprehensively evaluated. Through the timing to battery voltage reach stable period can be optimized to reduce aging and extend long life of battery by suitable key parameters adjustment. Furthermore, the performance efficiency of electric bicycles can be easily improved by suitable adjustment of input parameters.

# **6. A MACHINE LEARNING APPROACHES FOR PREDICTING POWER AND PERFORMANCE FOR ELECTRIC BICYCLE UNDER THE EFFECTS KEY PARAMETERS**

## **6.1 Machine learning**

### **Artificial neural networks**

#### *ANN architecture*

An Artificial Neural Network (ANN) is a computational model inspired by the human brain's biological neural networks. ANNs are widely applied for tasks such as pattern recognition, image and speech recognition, natural language processing, regression analysis, and decision-making. They excel at handling complex and nonlinear problems and are a crucial component of deep learning, a subset of machine learning that utilizes neural networks with multiple hidden layers. The standard feed-forward neural network structure, along with the widely employed backpropagation algorithm and the effective Levenberg-Marquardt training function, are commonly used in most applications. This choice is motivated by the well-established theoretical foundation and the neural network's robust ability for nonlinear mapping [63]. In the present study, the paper also employed the backpropagation neural network with the Levenberg-Marquardt training function, forming the basis for all developed ANN models.

A neural network including multiple layers: the output, hidden, input layer. Each layer contains a specific number of neurons. Neurons perform two main functions: the summation function, which calculates weighted inputs, and the activation function, which processes this sum to generate the neuron's output. Information flows unidirectionally through the network, moving from the input layer to the output layer. Each layer receives signals from the previous layer's neurons and passes its own output to the next layer. In backpropagation (BP) neural networks, the cumulative error between the final network output and the actual value, often obtained from experimental data, is propagated backward through the network [64]. This backward propagation enables the adjustment of weight values throughout the entire network mechanism. Refer to Fig. 6.1 for a visual representation of this process.

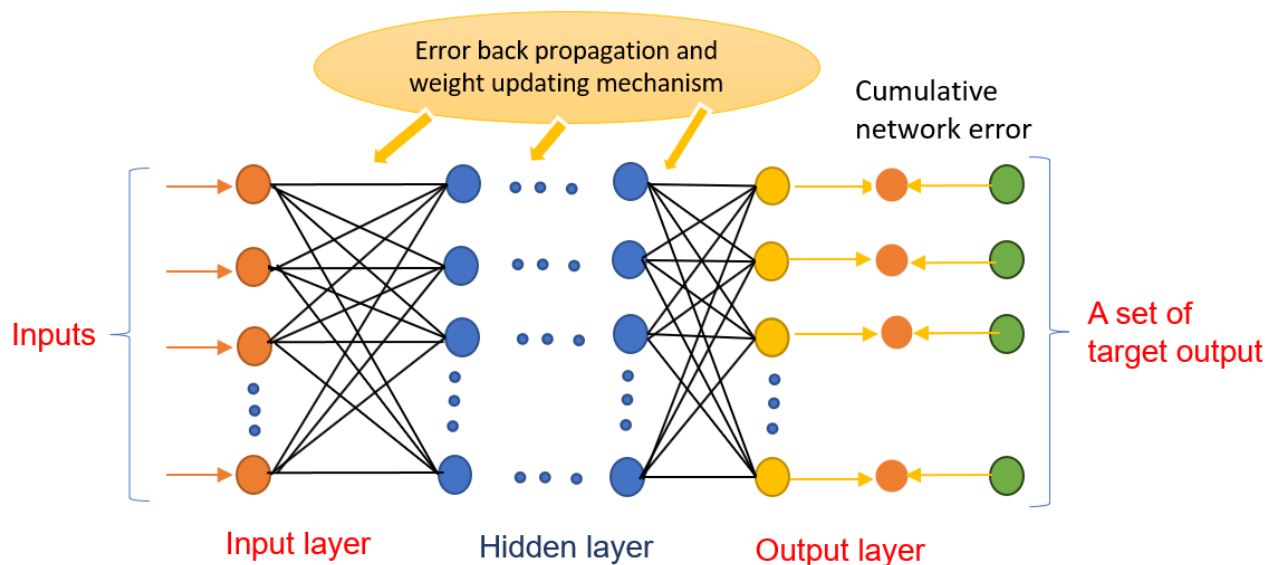


**Fig. 6.1** The artificial neural network using multi-layer feed-forward architecture.

Artificial Neural Networks (ANNs) provide faster predictions than conventional simulation programs. Neurons, which are interconnected processing nodes in ANNs, accept input from outside sources, aggregate it, perform a nonlinear operation on it, and then produce an output. The feedforward network, which has an input layer, an output layer, and numerous hidden layers, is a well-known ANN model. Each neuron in the network has weighted inputs and

outputs, allowing for flexible information processing [65]. The process of adjusting these weights between network layers to achieve the desired outcome is known as "training" the network. The output equation can be presented by following.

$$y = \sum_{i=1}^p w_i x_i + b$$

In evaluating and optimizing Artificial Neural Network (ANN) models, three main criteria are commonly used. Firstly, the primary criterion is the least Mean Square Error (MSE) during the validation phase. Secondly, the correlation coefficient ( $R^2$ ) is analyzed to assess the regression between the network outputs and the corresponding targets. Finally, the Mean Absolute Percentage Error is used in a model performance evaluation index. The correlation coefficient ranges from 0 to +1, with values closer to +1 indicating a strong positive linear correlation, and values closer to 0 indicating a weak correlation. Choosing the network configuration with the least MSE during validation is given priority when determining the hidden neuron number [66]. However, the other two criteria are also important for a comprehensive evaluation.

$$MSE = \frac{1}{N} \sum_{i=1}^N (t_i - o_i)^2$$

$$R^2 = 1 - \left( \frac{\sum_{i=1}^n (t_i - o_i)^2}{\sum_i^n (o_i)^2} \right)$$

$$MAPE = \frac{1}{N} \sum_{i=1}^N \left| \frac{t_i - o_i}{t_i} \right|$$

where t is actual, o is predicted.

**Table 6.1.** The selected ANN network was generated by the MATLAB framework.

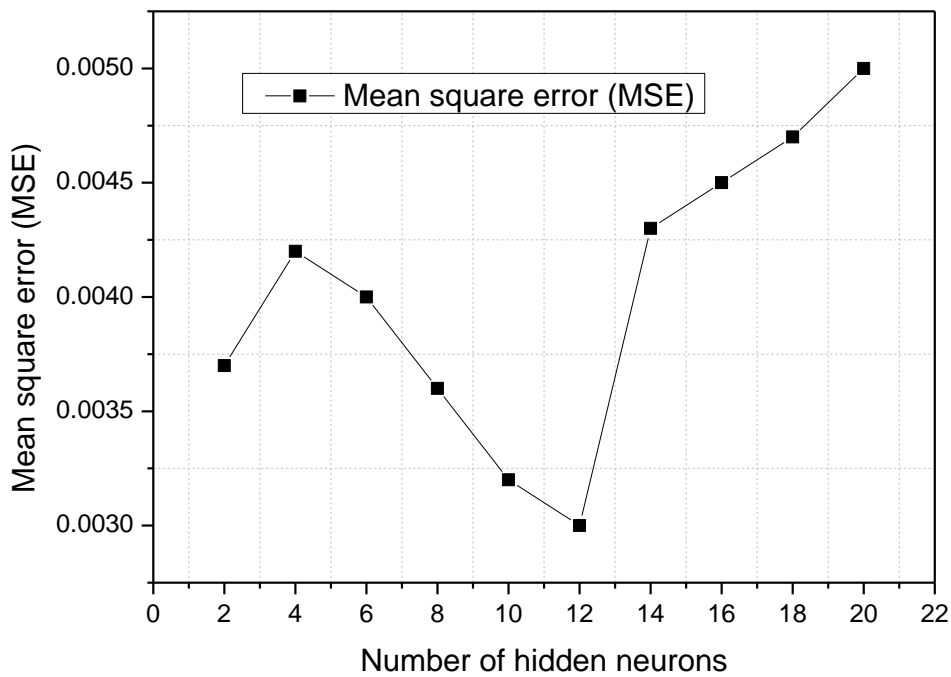
Type of network	Feed-forward back propagation
Function for training	Levenberg-Marquardt
Function for learning	LEARNDGM
Transfer function	Mean squared error (MSE)
Performance function	Tan sigmoid
Data selection	Training data set: 70% Training (randomly selected) Validation data set: 15% validation (randomly selected) Test data set: 15% test (randomly selected)
Input parameters	wheel radius, bike velocity, mass, slope ratio, transmission ratio.
Output parameters	Power demand, battery voltage

*Input and output parameter choice*

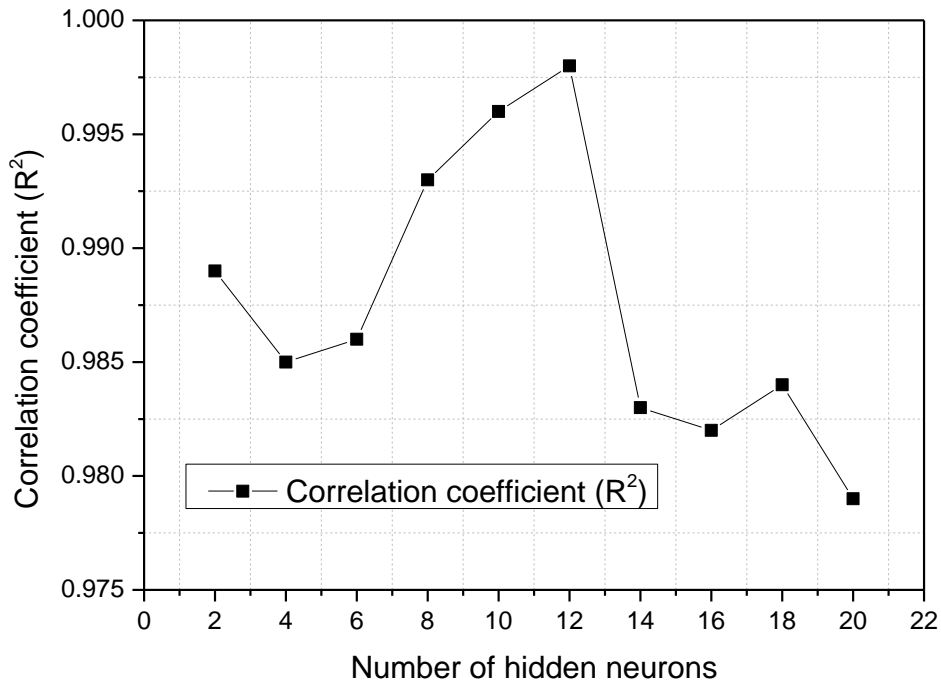
The choice of input and output variables plays a crucial role in determining the system's process proceeds. It is essential to choose variables that have a significant influence on the system, as selecting the wrong variables with less impact can prevent the attainment of the desired output. Therefore, careful consideration is given to the selection of input variables based on their influence over the process, prioritizing those that can be measured and adjusted [67]. In the current study, numerous parameters affect the performance and the EB. However, to examine the outcomes, the input variables are carefully chosen by focusing on the major influential parameters and those that are deliberately varied. This selection ensures that the most relevant and impactful factors are included as input variables in the analysis. The five

input variables are speed levels (from speed level\_1 to speed\_5), wheel radius (0.3, 0.33, 0.36, 0.39, 0.42 m), frontal area (0.423, 0.723, 1.023, 1.323, 1.623 m<sup>2</sup>), slope ratio (0, 0.36, 0.48, 0.65, 0.85%). Meanwhile, the power demand and battery voltage are chosen as output parameters for the performance model. The relationship between the input and output factors are expressed by the following equation, which captures their inclusive correlation:

$$j = F(R_w, v, A_a, G, \gamma)$$



(a)



(b)

**Fig. 6.2** Variation of MSE and  $R^2$  in regard to the amount of hidden neurons.

(a) Mean square error, (b) Correlation coefficient

### *Development of ANN structure*

The neural network architecture encompasses various components that are crucial for training, testing, validating, and predicting data. These components include the network type, training function, transfer function, performance function, learning function, number of neurons, number of hidden layers, number of input parameters, number of output parameters, and the interlinking between each layer [68]. In this study, the network parameters utilized are provided in Table 6.1. The input layer consists of 5 neurons, the output layer consists of 2 neurons, and the number of neurons in the hidden layer needs to be optimized. To determine

the ideal number of hidden neurons, a sensitivity analysis was conducted to examine the relationship between mean squared error (MSE) and R-squared ( $R^2$ ) values and the number of hidden neurons. Fig. 6.2 illustrates the fluctuation of MSE with respect to the number of hidden neurons using the trained network model. The largest correlation coefficient ( $R^2$ ) between the actual and predicted value during validation phase is 0.998 with 12 hidden neurons. The MSE was minimized (0.003) at 12 hidden neurons. The architecture of the ANN model used in this analysis was configured as 5-12-2, indicating five input neurons, 12 hidden neurons, and two output neurons, as shown Fig. 6.3

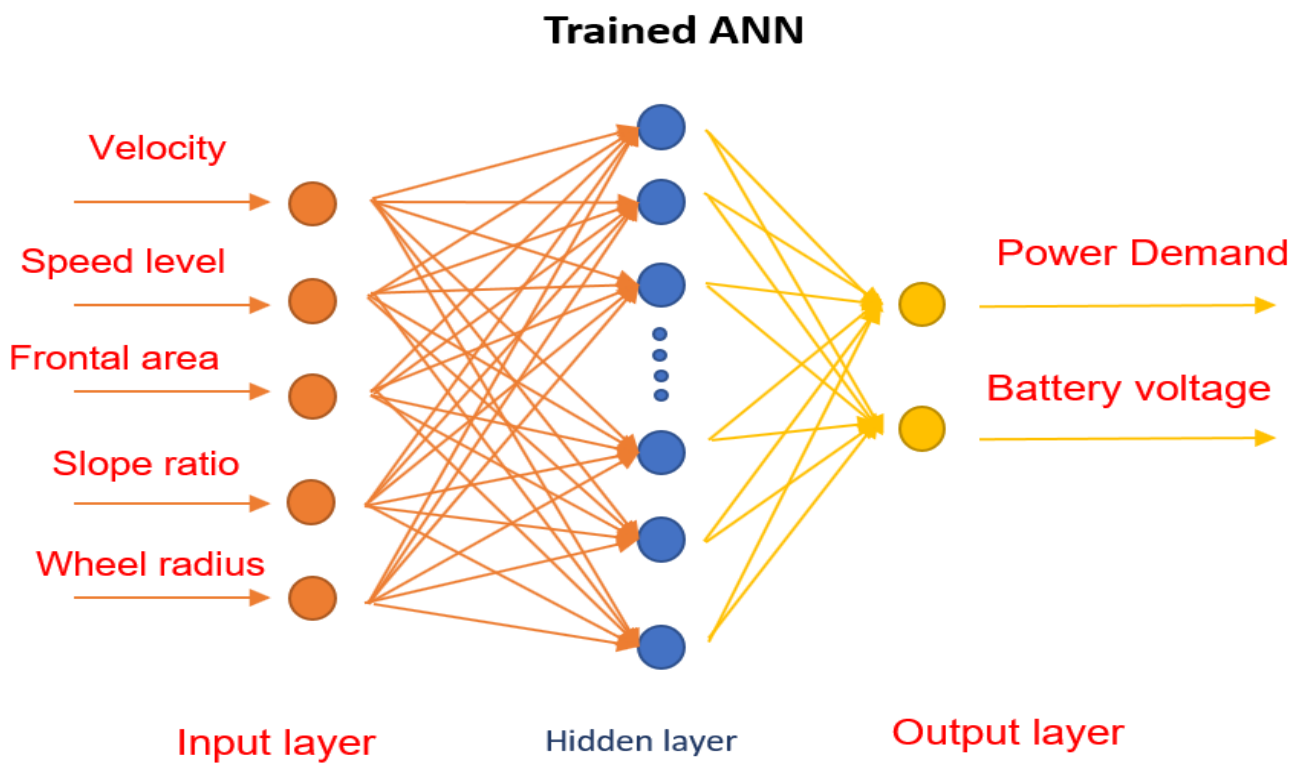


**Fig. 6.3** Recognized ANN structure of 5-12-2

## Genetic algorithm

A genetic algorithm (GA) is a metaheuristic optimization algorithm inspired by the process of natural selection and genetic evolution. It is commonly used to solve complex optimization

problems where traditional methods may be inefficient or infeasible. The common component of genetic algorithm including:

- Population: A set of potential solutions to the given problem. Each individual in the population is called a chromosome.
- Chromosomes: Representations of solutions encoded in a way that can be manipulated by the algorithm, often as strings of bits (0s and 1s), but they can also be more complex structures.
- Genes: Parts of a chromosome that encode specific traits of the solution, typically represented by bits, numbers, or symbols.
- Fitness Function: A function that evaluates how close a given solution is to the optimal solution of the problem. It assigns a fitness score to each chromosome.
- Selection: The process of choosing the fittest individuals from the population to reproduce. Common methods include roulette wheel selection, tournament selection, and rank selection.
- Crossover (Recombination): A genetic operator used to combine the genetic information of two parents to generate new offspring. Common techniques include single-point crossover, multi-point crossover, and uniform crossover.
- Mutation: A genetic operator used to maintain genetic diversity within the population by randomly altering the genes of individual chromosomes. This helps prevent premature convergence to suboptimal solutions.
- Generation: A single iteration of the algorithm where a new population of solutions is created through selection, crossover, and mutation

Genetic algorithms are powerful and flexible tools for solving optimization problems where traditional methods may fall short. Their ability to mimic natural evolutionary processes makes them particularly useful for complex and high-dimensional search spaces.

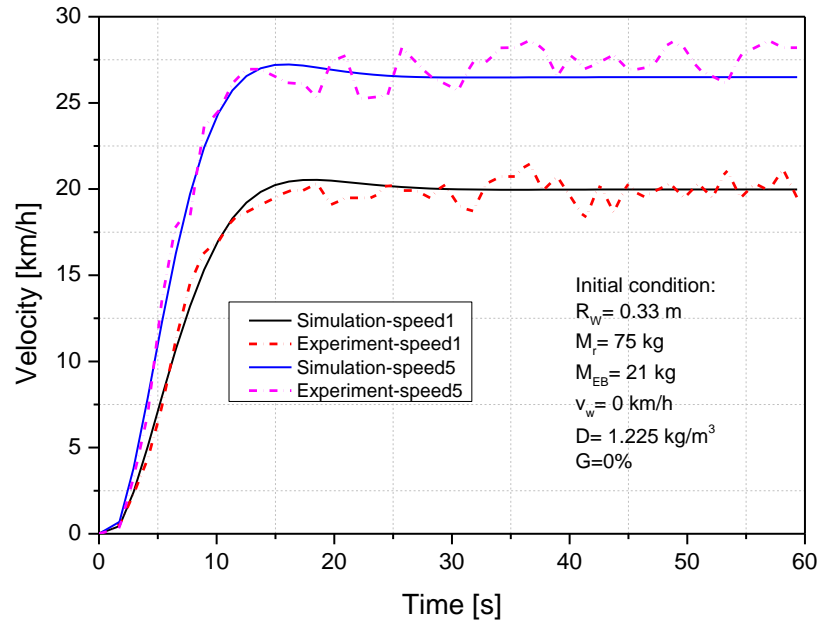
An n-dimensional chromosome is a structure of data that provides a prospective answer to an issue in the context of an genetic algorithm. It consists of n genes, where each gene represents a choice varying in the solution space. In this case, the chromosome could be expressed using the following equation [69]:

$$Chromosome = [c_1, c_2, \dots, c_n]$$

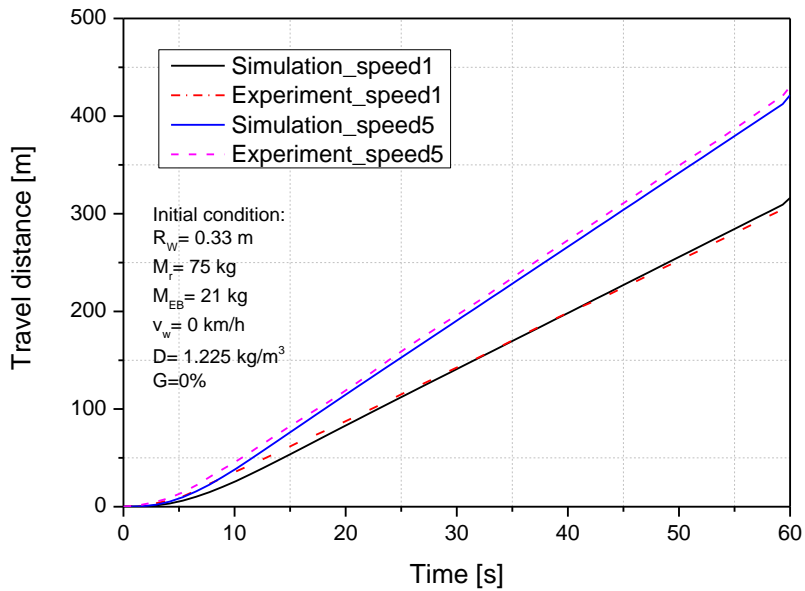
where  $c_i$  is the i-th value of parameters, n is the number of genes. This research incorporates five parameter values, namely wheel radius ( $R_w$ ), bike velocity ( $v$ ), frontal area ( $A_a$ ), slope ratio ( $G$ ), and speed level ( $\gamma$ ). To reach an optimization target, it is chosen as a suggested element in the ANN-GA approach, with the following details: the power demand and voltage. In order to solve optimization problems, the fitness function is utilized to assess each chromosome's quality, and genetic operators like crossover and mutation are used to create new offspring chromosomes. In this instance, the chromosomal possibility yielding's optimal necessary power can be expressed as follows [70]:

$$C(v_{jmax}, A_{a,jmax}, G_{jmax}, R_{w,jmax}, \gamma_{jmax}) = \frac{j(v_{jmax}, A_{a,jmax}, G_{jmax}, R_{w,jmax}, \gamma_{jmax})}{\sum_1^N j(v_{jmax}, A_{a,jmax}, G_{jmax}, R_{w,jmax}, \gamma_{jmax})}$$

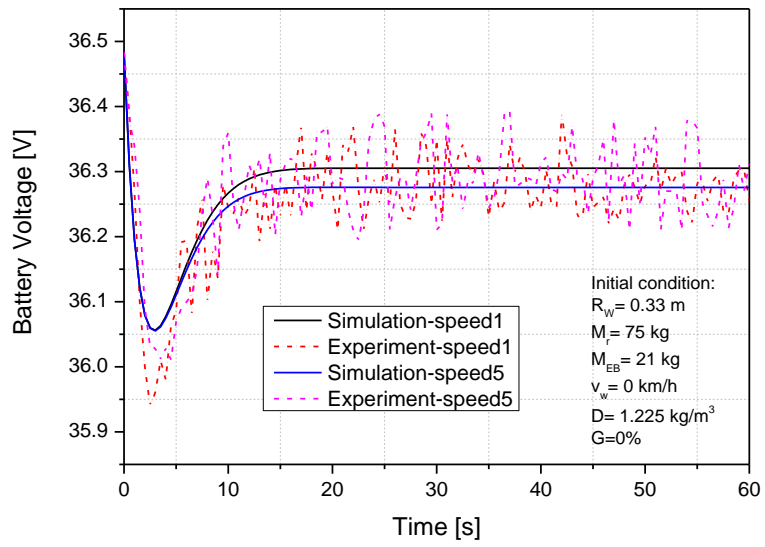
## 6.2 Comparison experiment and simulation results



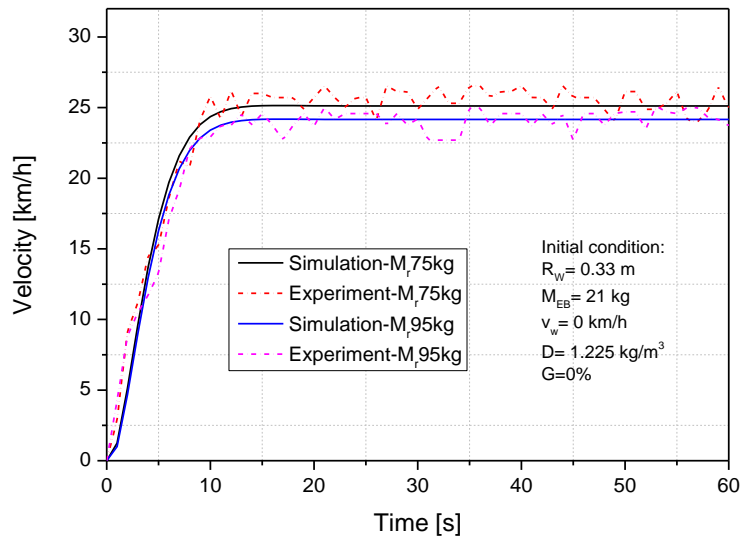
(a)



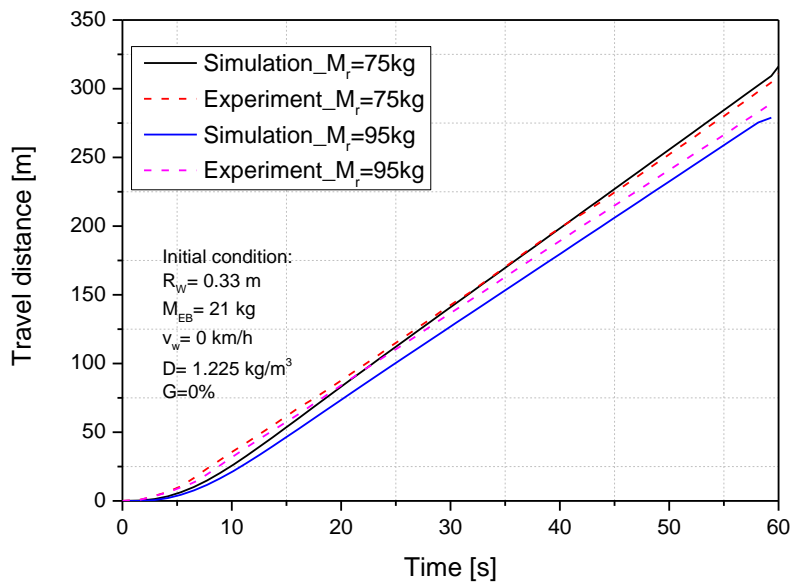
(b)



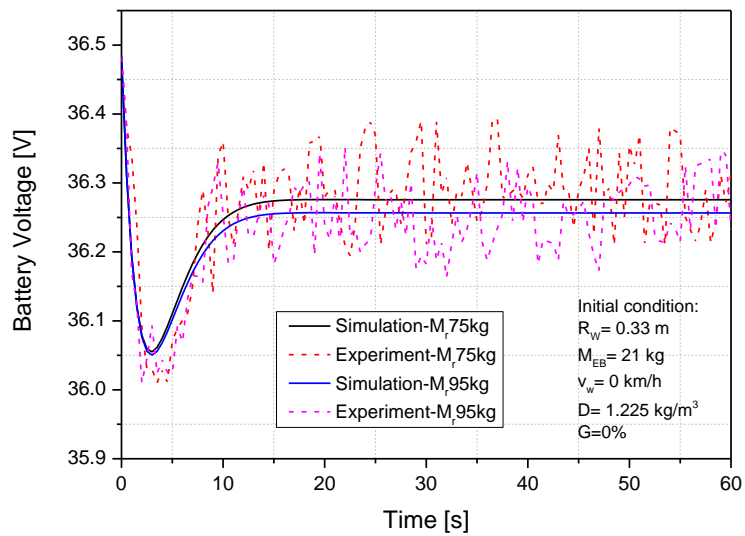
©



(d)



(e)



(f)

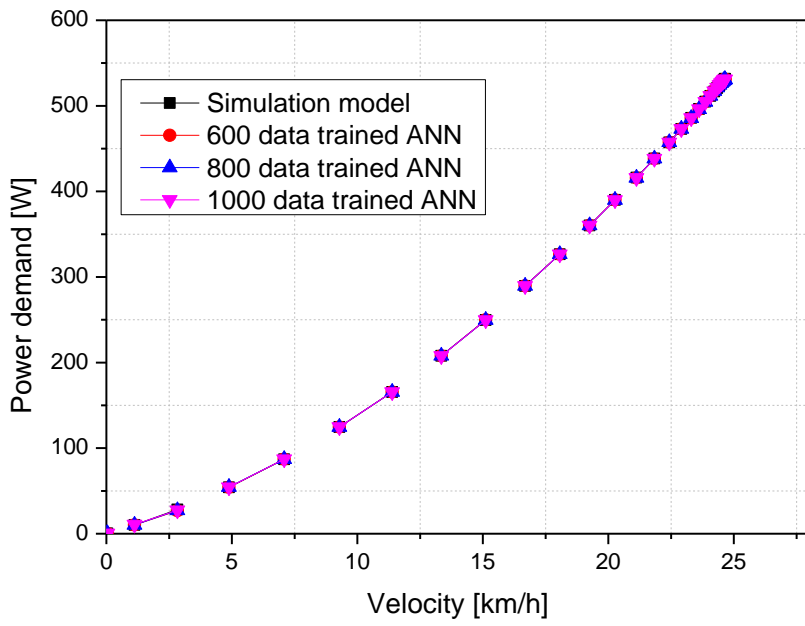
**Fig. 6.4.** Validation of dynamic and battery voltage electric bike with various transmission ratio and rider mass: (a), (b), (c) various speed level; (d), (e), (f) various rider mass

The experiments were carried out to provide basic EB performance data which was validated with the simulation study. Fig. 6.4 presents the validation between the experimental and simulation output data. The straight lines describe the simulated results while the segmented line describes the experimental results. The speed level was adjusted from speed\_level1 to speed\_level5 to evaluate the dynamic and electric consumption of EB during moving condition. Fig. 6.4 (a) shows the highest difference in bike speed is 8.25% at 37 seconds. The bike velocity is an experimental average value and is thus acceptable. When the wind speed, slope grade, wheel radius and ES mass are kept at a constant, the bicycle velocity increases with the increase in speed level. Fig. 6.4 (b), (c) show the validated moving distance and battery voltage. The same trend could be seen in the simulation and experimental data values. The highest difference in the moving distance and battery voltage are 3.53% at 56 second and 0.4% at 3 seconds, respectively.

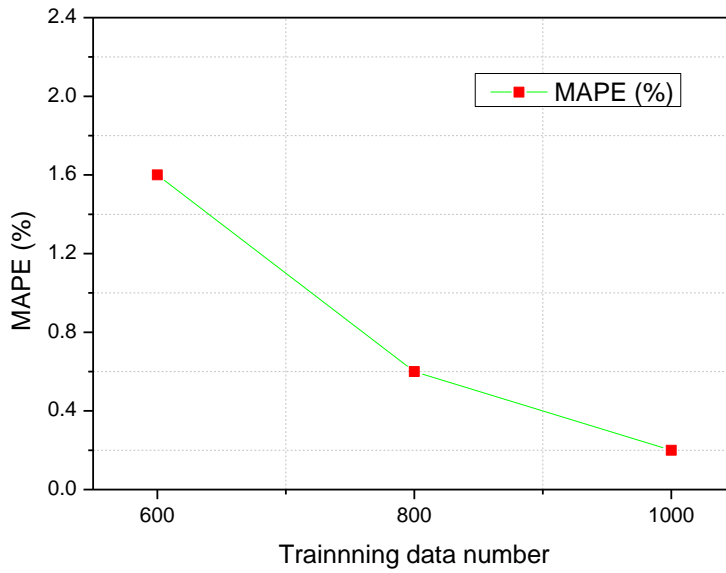
Fig. 6.4 (d), (e), (f) validate the simulation results and experiment results when the rider mass was varied. Rider mass was an important factor impacting EB characteristics. It was selected as an input factor in validating the dynamic characteristics and battery voltage of EB. With increased rider mass, the velocity decreased from 25.3 to 24.1 km/h and the maximum difference was 9.42% at 32 seconds. Fig. 6.4 (e), (f) showed that the moving distance decreased and the electric consumption increased following the rider mass. The moving distance and battery voltage were well correlated with simulated and experimental time. The highest difference of moving distance and battery voltage were 3.38% at 54 second and 0.47% at 27 second.

### 6.3 Comparison simulated and predicted results

After being correctly trained under 75% data points for training, 15% validation, and 15% testing, the ANN model with 5 and 2 input and output parameters and 12 hidden neurons serves as the fitness function for the Genetic Algorithm optimization process. Furthermore, to increase the accuracy of prediction model, the mean absolute percentage error is used in ANN model. Fig. (6.5) showed a comparison of prediction accuracy with using 600, 800, 1000 data points. The results showed that the 1000 data point-based ANN offers the best prediction accuracy with a MAPE of 0.2% during the training process. By feeding input data to the trained ANN and receiving power demand and electric consumption forecasts, the GA optimization makes use of the trained ANN to establish the operating state. Initially, a set of random chromosomes is generated, and although the GA predictions may contain random errors, this study addresses this issue by utilizing a large number of initial chromosomes (around 5000). To ensure computational efficiency, the total number of evolutionary generations is set to 200. The flowchart depicted in Fig. 6.6 illustrates the training and prediction process of the ANN-GA method. Once the ANN is effectively trained, each GA optimization, involving the determination of maximum power demand and its corresponding operating condition, can be completed within a fraction of a second on a single node. This efficiency allows for the rapid control of electric bikes in real-world applications.



(a)



(b)

**Fig. 6.5** The prediction model comparison instructed with 600, 800, 100 data point using one power-velocity curve.

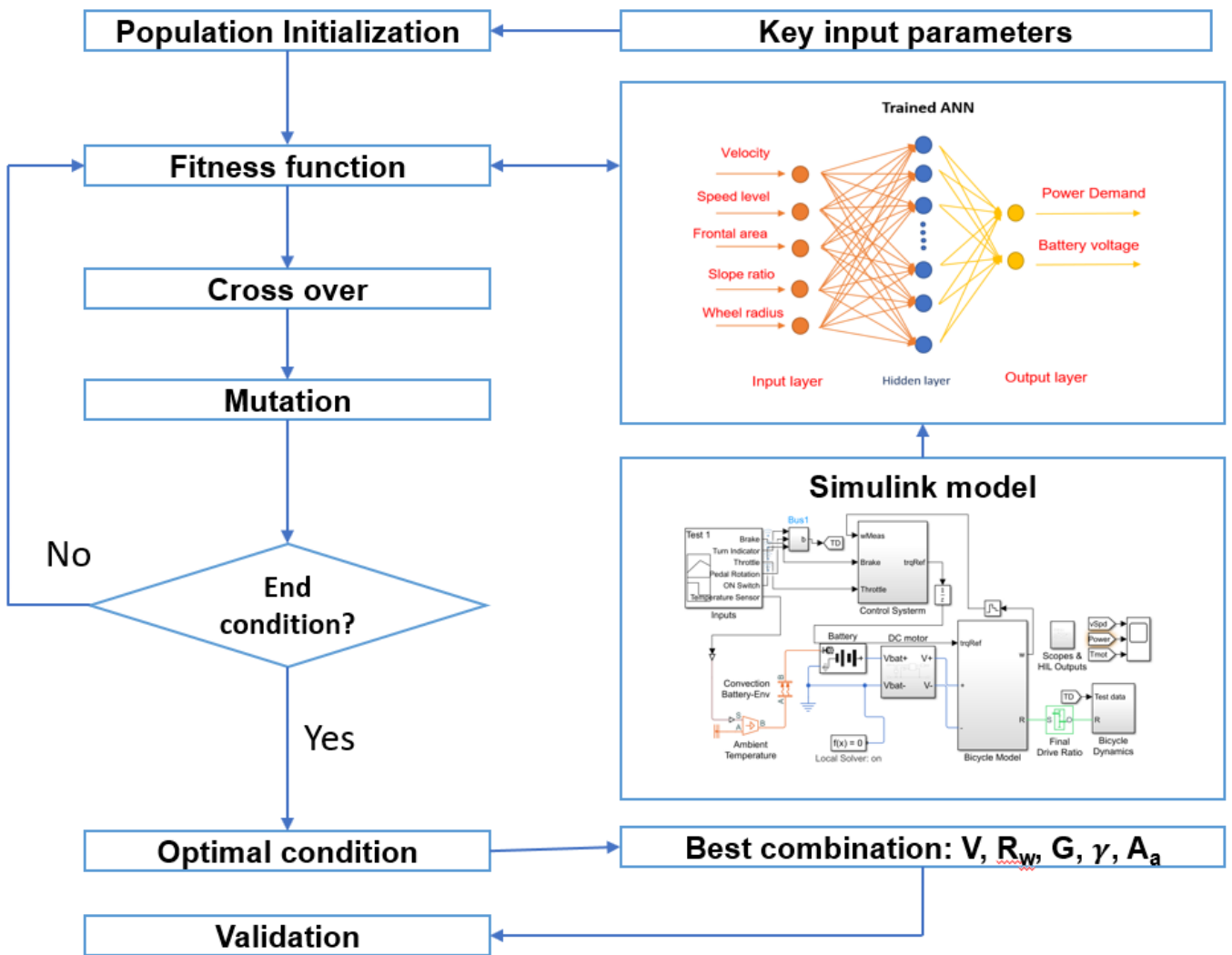
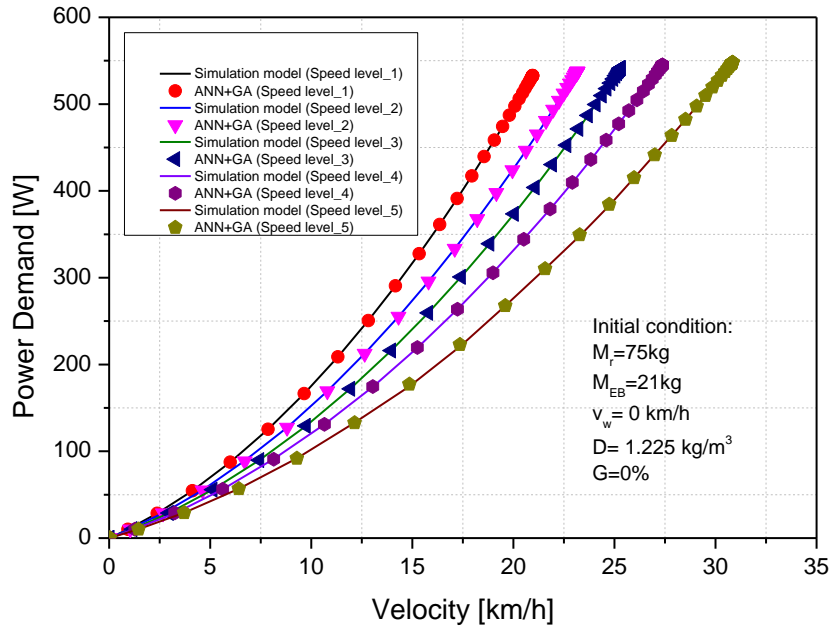
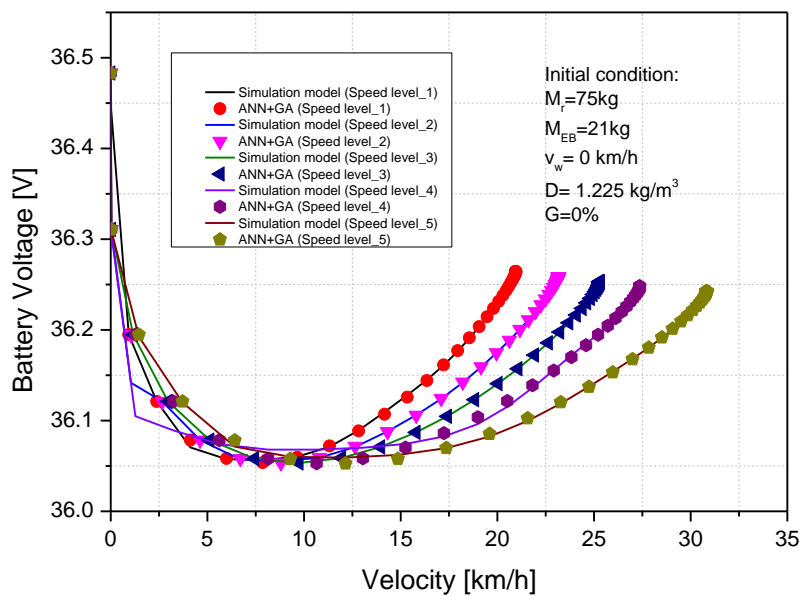


Fig. 6.6 The ANN-GA approach, informed from Simulink model.

## 6.4 Effect of key structure factor on electric bicycle performance



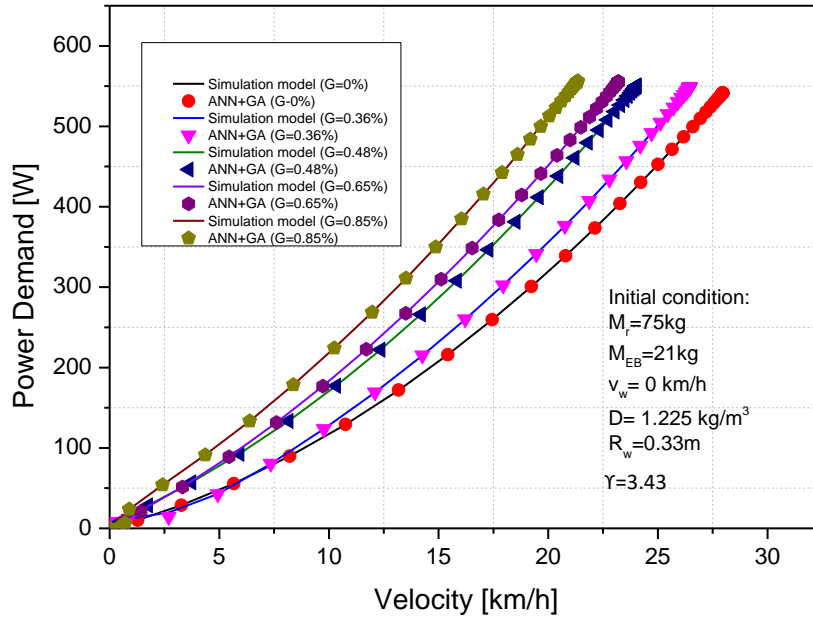
(a)



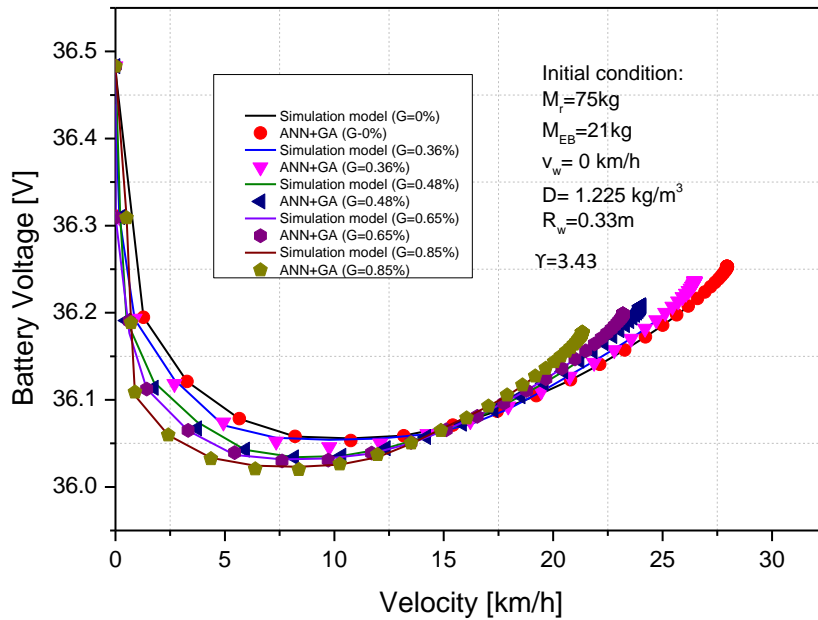
(b)

**Fig. 6.7** Comparison between the simulated and ANN-GA predicted results of power demand-velocity, battery voltage-velocity curve under varying transmission ratio.

The paper thoroughly summarizes and discusses the key parameters affected to dynamic and consumed energy of EB during operation conditions. Which hasn't been shown elsewhere in the literature. Therefore, the ANN model with 1 hidden layer including 12 neurons was incorporated with a GA optimization to predict and enhance power demand and voltage of battery using wheel radius, slope ratio, bike velocity, transmission ratio, frontal area as input parameter. The 1000 data point from simulation study was applied into ANN training. Fig. 6.7 presents the power demand and consumed energy versus the bike velocity under speed level changing. In using electric bicycles, the transmission ratio is one of the important operating factors, which has significantly effect on the power demand and consumed energy. To examine the transmission ratio dependence on the optimized power demand and consumed energy, the combined ANN-GA method was applied under five typical speed levels. As shown in Fig. 6.7 (a), when the speed level 1 to level 5, the power demand showed an uptrend as well as the bicycle velocity uptrend, specifically increasing 531 to 546 W and from 20.9 to 30.7 km/h. The maximum differences in the power demand between predicted and simulated results were 3.4% at 4.27 km/h with speed level\_3 case, respectively. A larger wheel revolution to adapt the higher bike speed while the other parameters were kept at constant, therefore the power demand will be greater to accommodate the increase in bike velocity. Fig. 6.7 (b) presents the effect of speed level on battery voltage. Here, the speed level changed from level\_1 to level\_5; the battery voltage during stable bike velocity showed a downtrend. This is compatible with the physical mechanism of EB operation that, when the bicycle kinetic is faster and the energy demand is greater because of the larger bike velocity. This is why the voltage fell when the speed level was changed from level\_1 to level\_5.



(a)

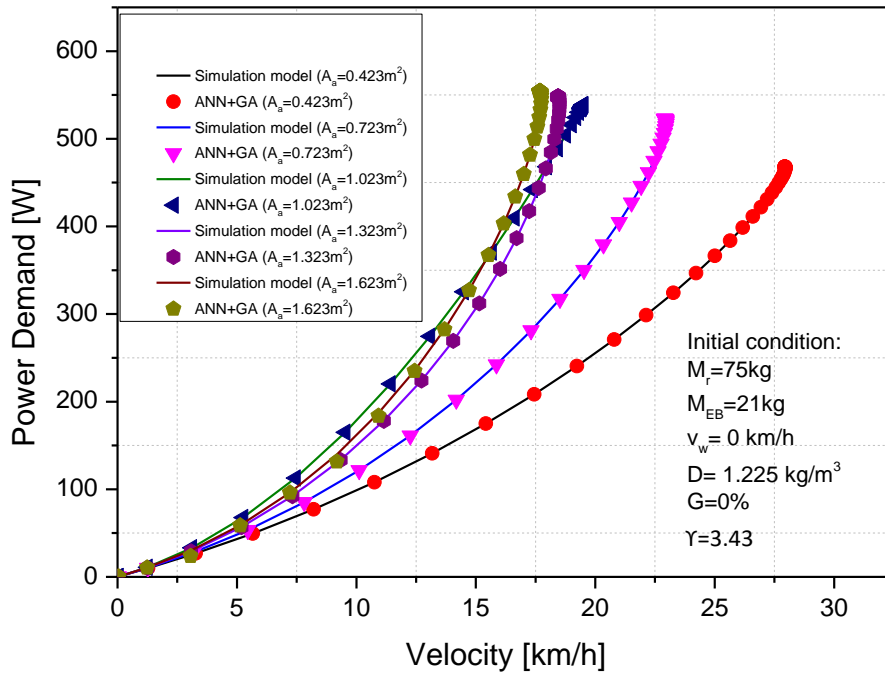


(b)

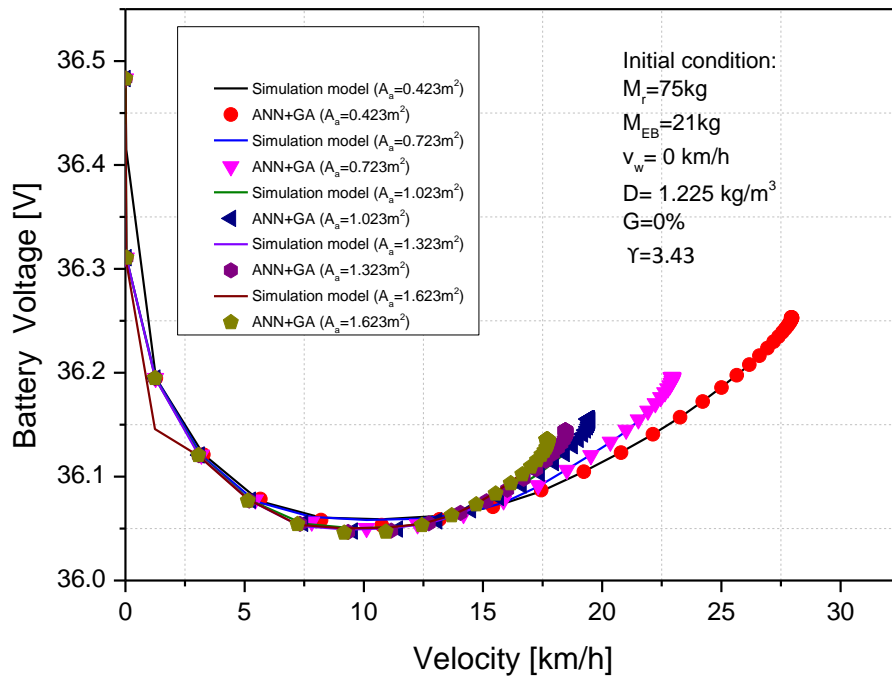
**Fig. 6.8** Comparison between the simulated and ANN-GA predicted results of power demand-velocity, battery voltage-velocity curve under varying slope grade

The slope grade has a sensitive effect to power demand and battery voltage of EB during operation. As shown in Fig. 6.8 (a), the power demand increased when the slope grade increased. This is because the increase in power demand was due to an increased slope resistance force, that will make a larger total resistance force. Therefore, the power to bicycle overcome will be greater. As a result, when the slope grade rose from 0% to 0.85%, the demanded power rose from 540.3 to 554.4 W and the maximum velocity decreased from 27.9 to 21.3 km/h, besides that, the highest difference between simulated and predicted results was 5.2% at 0.89 km/h with slope grade of 0.85%.

Fig. 6.8 (b) presents the effect of slope grade on battery voltage. It could be observed that the voltage dropped as the slope grade increased. This is also congruent with the physical mechanism of bicycle operation: when the slope ratio increases, the resistance force increases and the energy demand increases. This explains why the battery voltage decreased 0.08% when slope grade rose from 0% to 0.85%.



(a)

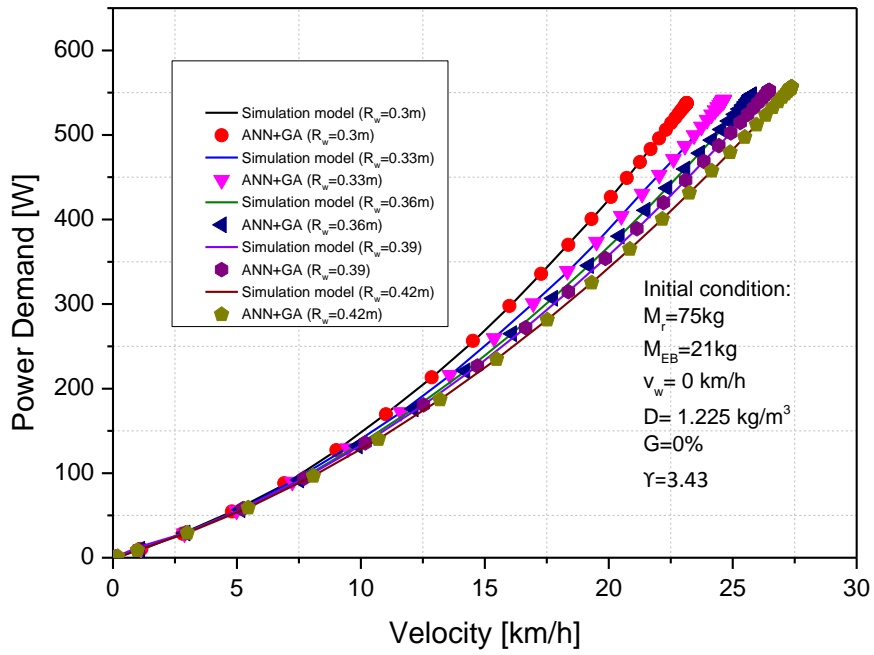


(b)

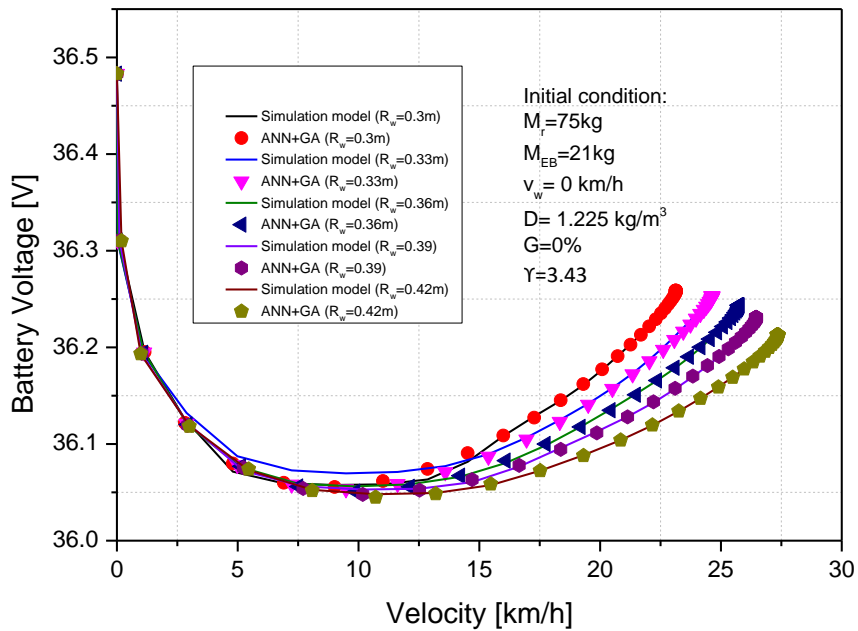
**Fig. 6.9** Comparison between the simulated and ANN-GA predicted results of power demand-velocity, battery voltage-velocity curve under varying frontal area

During using bicycle, frontal area is a design factor that has a significant effect on bicycle dynamic because the frontal area changing will directly affect to total resistance force of electric bike during operation process. Here, the effect of frontal area on the power demand is presented. As shown in Fig. 6.9 (a), when frontal area increases, the bike velocity shows a downtrend and the power demand shows an uptrend. The power demand increases from 486 to 553.6 W when the frontal area increases from 0.423 to 1.623 m<sup>2</sup>. The highest difference between simulated as predicted results is 4.6% at 3.2 km/h with frontal area case of 1.023 m<sup>2</sup>. A larger frontal area will raise air resistance force while the other parameters were kept constant; it will make a larger power demand to bike overcome resistance force. This explains why the power demand for bike increases with rise in wind speed.

The battery voltage decreases 0.3% when the frontal area increases from 0.423 to 1.623 m<sup>2</sup>, as shown Fig. 6.9 (b). This could be linked to the fact that increased frontal area led to increased air resistance force, resulting in a higher energy demand to adjust to a bigger total resistance force. This is why, when the wind speed increased, the battery voltage decreased.



(a)



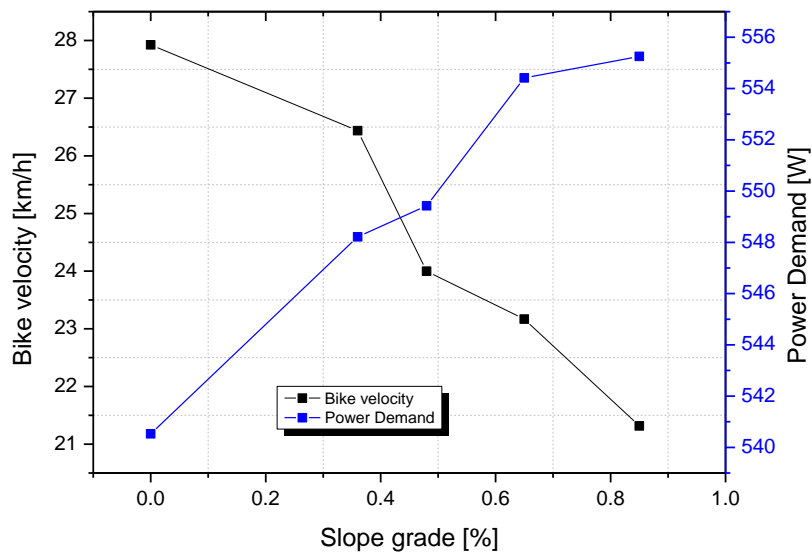
(b)

**Fig. 6.10** Comparison between the simulated and ANN-GA predicted results of power demand-velocity, battery voltage-velocity curve under varying wheel radius.

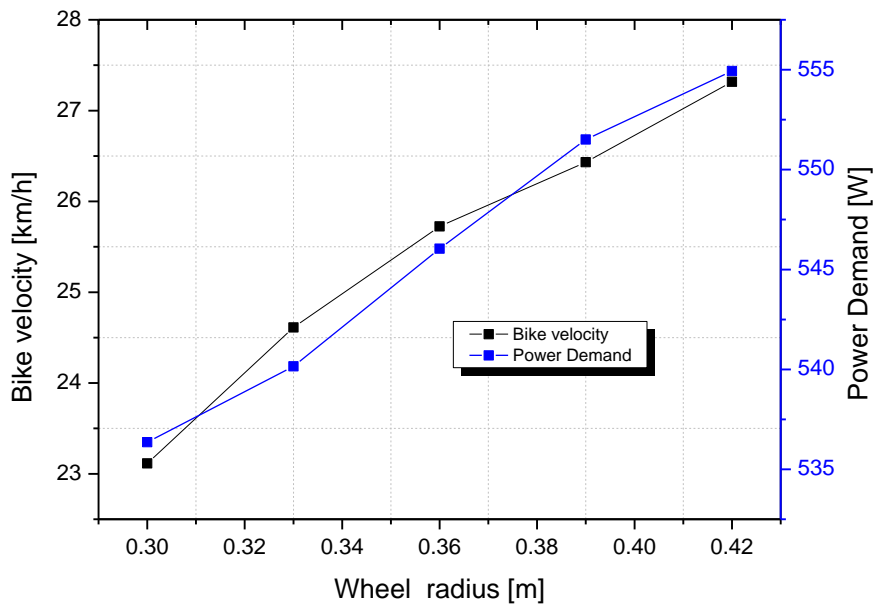
Fig. 6.10 shows the power demand and battery voltage versus bicycle speed under wheel radius changing. During EB's operating conditions, the wheel radius has a sensitive effect on the bike performance. The ANN-GA approach was used in this work to forecast the optimal necessary power and voltage output under five typical wheel radiuses including 0.3, 0.33, 0.36, 0.39 and 0.42 m. When the wheel radius increased from 0.3 to 0.42 m, the power demand increased from 536.4 to 554.9 W, as shown in Fig. 6.10 (a). The highest difference between forecasted and simulated results is 4.5% at 1.03km/h with  $R_w$  of 0.39m, respectively. This is explained by the fact that increasing the wheel radius causes an increase in the bike's speed and inertia, therefore the power demand is raised to overcome a greater inertial force and reach a specific speed.

Fig. 6.10 (b) shows the battery voltage versus bike velocity under five typical wheel radius. The wheel radius has a significant effect on battery voltage status during scooter operation; the voltage reduced from 34.26V to 34.21V during stable velocity behavior when the wheel radius increased from 0.3 to 0.42m. This is explained by the fact that raised inertial force and speed result in increased energy demand. When the wheel radius grows, the battery voltage falls to accommodate the increased energy requirement.

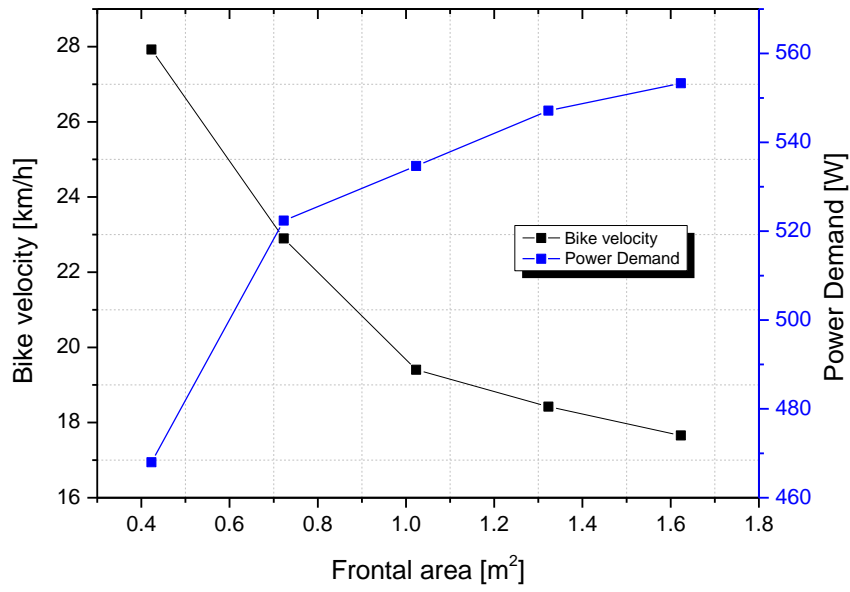
## **6.5 Enhancing electric bicycle performance by optimizing key structure parameters.**



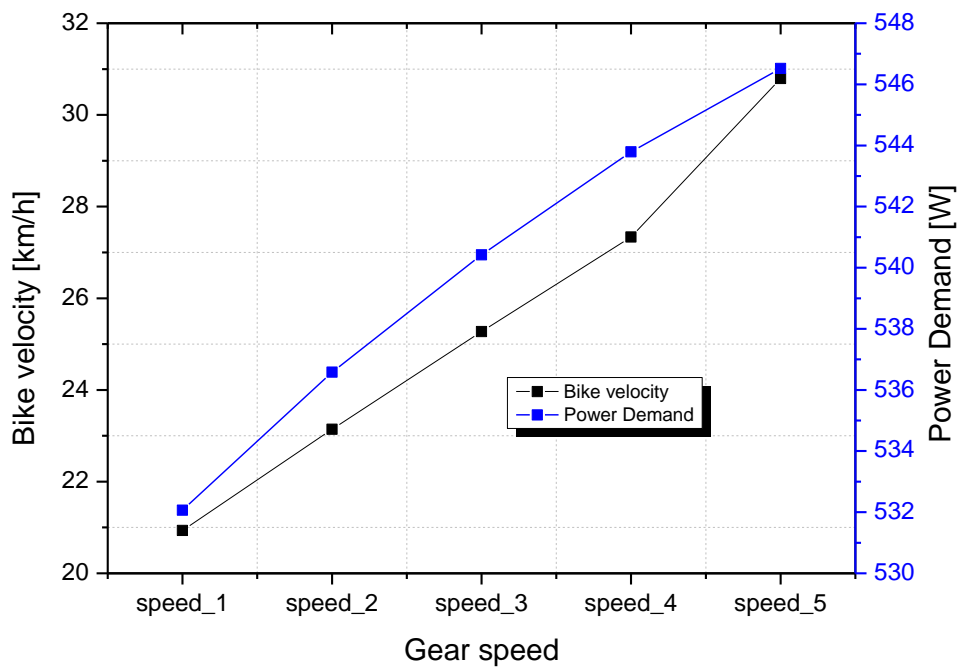
(a)



(b)



©



(d)

**Fig. 6.11** The ANN-GA identified four input factor that yields maximum power demand and velocity, (a) five slope ratio, (b) five wheel radius, (c) five frontal area, (d) five speed level.

A genetic algorithm (GA) optimization method is merged with a trained artificial neural network (ANN) model, with the ANN acting as the fitness function. The input factors for this enhancement include the wheel radius, slope grade, speed level, frontal area, while the outputs are the power demand and voltage. The ANN-GA approach showed that the electric bike could achieve an efficient performance range, with an optimized required power of 546.3 W and a maximum velocity of 30.7 km/h under wheel radius 0.185m, slope grade 0% and wind speed 0 km/h. To validate the powerful performance range and identify the associated input factors, the ANN-GA approach was applied for forecasting and optimizing power demand under five typical wheel radius (0.3, 0.33, 0.36, 0.39 and 0.42m), five typical speed level (from speed level\_1 to speed level\_5), five typical slope grade(0, 0.36, 0.48, 0.65 and 0.85%), five typical frontal area (0.423, 0.723, 1.023, 1.323, 1.623 m<sup>2</sup>). The improved power demand and bicycle velocity by using the ANN-GA approach are illustrated in Fig. 6.11. The relationship between the optimized power demand and slope grade can be observed in Fig. 6.11 (a), where it is evident that the optimum power demand rises as the slope ratio increases from 0% to 0.85%. This observation aligns with the physical principles governing bicycle dynamics. As the slope grade increases, the bicycle's motion slows down, resulting in an increase in the required power. This is due to the fact that an raising in slope grade leads to an raising in both the slope resistance force and the total resistance force experienced by the bicycle. In Fig. 6.11 (b), it can be observed that the highest optimum power demand is 551.3 W, which occurs at a wheel radius of 0.42m. Interestingly, this wheel radius also corresponds to the highest achievable velocity for the electric bicycle within the range of wheel radius tested (0.3-0.42m). As

depicted in Fig. 6.11 (c), the optimum power demand grows with a larger in the frontal area. This observation aligns with the kinetic principles governing the operation of electric bicycles. When the frontal area rises within the range of 0.423-1.623m<sup>2</sup> km/h, the bicycle's velocity decreases. This reduction in velocity is attributed to the higher air resistance force. Consequently, the total resistance force experienced by the bicycle increases, resulting in an increase in the required power. In Fig. 6.11 (d), it may be observed that the optimum power demand increases and the bicycle velocity changes from speed level\_1 to speed level\_5. This observation is in accordance with the physical principles governing the operation of electric bicycles. With an change in speed level, the bicycle velocity becomes larger, resulting in a greater total resistance power. Consequently, a higher power demand is necessary to overcome the increased resistance and maintain the desired velocity. The findings of this study demonstrate that the forecasted results accurately reflect the significant physical motion and dynamic kinetics that impact the optimum power demand of electric bicycle. The suggested ANN-GA method proves to be an effective tool in providing a prompt guideline for determining the optimum power demand and identifying the key input factors associated with it.

## **6.6 Summary**

The MATLAB-Simulink simulation model of electric bicycle is established to create 1000 data point, that is applied in an ANN for training, testing and verifying. The one hidden layer ANN structure with 12 neurons was applied with five input parameters of the slope ratio, transmission ratio, bike velocity, wheel radius, frontal area and the power demand, battery voltage as output parameters. Additionally, the GA is used to find effective performance once the ANN has been trained.

The important results in this section were summarized below:

The power demand showed an uptrend as well as the bicycle velocity uptrend, specifically increasing 531 to 546 W and from 20.9 to 30.7 km/h with speed level changing level1 to level5.

The maximum difference in the power demand between predicted and simulated results was 3.4%.

The maximum velocity decreased from 27.9 to 21.3 km/h; power demand increased 540 – 554 W when the slope grade rose from 0% to 0.85%. Besides that, the highest difference between simulated and predicted results was 5.2%.

The power demand increases from 486 to 553.6 W when the frontal area increases from 0.423 to 1.623 m<sup>2</sup>. The battery voltage decreased 0.3% in the same condition. The highest difference between simulated as predicted results is 4.3%.

The power demand increased from 536.4 to 554.9 W when the wheel radius increased from 0.3 to 0.42 m. The highest difference between forecasted and simulated results is 4.5%

The ANN-GA approach was used to improve the electric bike performance and its accompanying structure and operating parameters, it demonstrated that the EB could reach 30.7 km/h with an optimum power demand of 546.3 W at speed level\_5, frontal area of 0.423 m<sup>2</sup>, wheel radius of 0.42 m, slope grade of 0%. Furthermore, the forecasted results were correlated with simulated results with R<sup>2</sup> value of 0.998. It demonstrated that the ANN-GA approach is an effective approach to solve complex problems such as performance prediction, identification, operating control of electric bicycle.

## 7. CONCLUSION AND CONTRIBUTION

The objective of this thesis is to investigate the effects of pivotal structure parameters such as transmission ratio, wheel size, frontal area, bicycle weight on dynamic characteristics, acceleration and fluctuations and battery voltage during starting period of electric bicycle by combining experimental and simulation approach.

Chapter 1: The research background of the work undertaken is introduced. An overview of the trends and challenges of electric bicycle research on improving bicycle efficiency is produced by correlating the relevant literature and the recent progress of the previous author's research methods. Furthermore, the research objectives are presented at the end of this chapter, followed by the organization of the thesis.

Chapter 2: Based on literature review, most of previous studies have focused on the environmental benefit, innovative motor, torque measurement, control strategies, battery technology. However, the previous studies haven't mention to the crucial structure parameters such as transmission ratio, wheel size, frontal area, bicycle weight and consider addition external factor to have comprehensive assessment results on power, acceleration, maximum velocity of electric bicycle. All these drawbacks and gaps in the existing literature are the motivation for this study to be carried out.

Chapter 3: The experimental system setup of electric bicycle was detailly explained. The experimental outcome for maximum velocity, duration to reach stable velocity, and fluctuation and voltage value in starting period of electric bicycle under each case will be obtained in real road test with detail ambient conditions. This output experimental data will be used in validating the outcome of simulation model to ensure the accuracy of simulation model.

Chapter 4: The zero-dimension model of electric bicycle has been analyzed under mathematical equation and performed in MATLAB-Simulink program. The simulations are conducted under full boundary conditions with each specific parameter to obtain comprehensive results. The results from the simulation closely match the experimental data, as evidenced by the negligible difference in velocity profiles over the 60-second test period. The comparison between simulation and experimental results showed that, highest different velocity of 7.42%, travel distance of 3.38%, voltage value of 1.7%. It demonstrates that the simulation model accurately performed the real-world behavior of the electric bicycle under the specified test conditions.

Chapter 5: The objective of this section is to determine crucial parameters, which affect maximum velocity, acceleration, fluctuation of voltage value in the starting period of electric bicycle. The results were obtained by an experimental and simulation technique. Following the investigation, the influence level of each critical parameter was determined. The importance results in chapter 5 were summarized as below:

- This study investigated the dynamic behavior of electric bicycles under varying conditions and identified critical factors influencing performance and battery voltage fluctuation. The external factors including slope ratio, wind speed have crucial role with acceleration and fluctuation of battery voltage in start period. To enhance the reliability of the results, this research also considered the above factor with detail value in common range. Minimizing the impact of these factors can improve velocity and electric consumption.
- With adjusting of wheel radius. The maximum of bicycle velocity could be improved [9.1-12,7%] with wheel radius changing (0.3-0.42m), However the duration for reaching stable velocity was extended and battery voltage value in stable period was decreased.

- The frontal area has a significant impact on bicycle dynamics. The maximum velocity could be improved [25.6-31.2%] with reducing frontal area (1.623-0.423m<sup>2</sup>). The duration for reaching stable velocity was reduced.
- The transmission ratio has a significant impact on bicycle dynamics. The velocity could be increased [26.3-29.2%], however the battery voltage value in stable period was decreased. Meanwhile, bicycle weight has slightly effects performance and reduce electric consumption.

Chapter 6: The objective of this chapter is to optimize power and dynamic by using crucial parameters as input parameters in ANN model for training, testing and verifying to predict output parameters including power and velocity. After the ANN is exactly trained, it is applied into the GA method to find the optimal output parameters with the best input value. The importance results in chapter 6 were summarized as below:

- The ANN model has 5-12-2 structure including 5 inputs consisting of transmission ratio, frontal area, slope ratio, velocity, wheel radius result with largest correlation coefficient ( $R^2$ ) of 0.998 and minimum MSE of 0.003.
- The transmission ratio significantly impacted on maximum velocity and power of e-bike such as increasing 34% of velocity, and 2.82% of power. Additionally, voltage value in stable period decreased by changing speed level 1 to speed level 5.
- The frontal area can improve e-bike performance. Maximum velocity improved 35%, power improved 15.3% by reducing frontal area.
- Maximum velocity increased 16.3% by increasing wheel radius. However, the power rose 3.6 %. Additionally, voltage value in stable period decreased by increasing wheel radius (0.3 – 0.42 m).
- The maximum difference between predicted and simulated results of power and velocity curve with wheel radius changing, frontal area changing, gear speed level

changing are 4.5%, 4.3%, 3.4%. After ANN-GA was exactly trained, the study found that, the electric bicycle could reach optimized power (546.3W) with velocity was 30.7 km/h at speed level\_5, frontal area of 0.423 m<sup>2</sup>, wheel radius of 0.42 m, slope grade of 0%.

The research contributions: The research has discovered different influence levels of design factors in electric bicycles, and the important levels of influences are arranged as follows: gear ratio, frontal area, wheel size and finally vehicle mass. It provides an information platform to optimize performance through applications such as: Firstly, providing useful information to develop high-performance powertrain systems suitable for motor capacity, secondly optimizing streamlined shapes aim to reduce drag and improve efficiency, provide a suitable size range of wheel to improve acceleration, stability and efficiency, lastly applying lightweight frame and optimize structure design to enhance acceleration, handling and efficiency. Additionally, the study determined the complex correlation between input and output parameters for the optimization process using ANN-GA. Besides that, the prediction model demonstrated high accuracy on predicting optimum parameters with having the minimum MSE of 0.03 and correlation coefficient ( $R^2$ ) of 0.998. By leveraging ANN-GA, the study found the optimal gear ratio to balance power consumption and maximum speed, in addition found the appropriate wheel size and smallest drag coefficient to improve maximum velocity and optimal power of electric bicycle. The above contributions provide a comprehensive insight into the work of electric bicycle performance advancement as well as providing useful information in the electric bicycle performance field for manufacturers and researchers.

## NOMENCLATURES

### Nomenclature

#### Abbreviation

ANN	Artificial neural network
EB	Electric bicycle
GA	Genetic algorithm
LIB	Lithium-ion battery
MAPE	Mean absolute percentage error
PV	Photovoltaic
OCV	Open circuit voltage
MSE	Mean square error
ECU	Electric control unit
LM	Levenberg-Marquardt
SOC	State of charge

## Latin symbols

$A_a$	Frontal area, $m^2$
$B_1$	Coefficient of viscous friction
$C_a$	Coefficient of aerodynamic drag
$C_{rr}$	Colling coefficient
$C_s$	Slope coefficient
$T_{pf}$	Propulsion torque, N
$U_a$	Motor voltage terminal, V
$v_{EB}$	Bicycle velocity, km/h
$V_w$	Wind speed, km/h
$M$	Bicycle and rider mass, Kg
$F_{pf}$	Propulsion force, N
$F_{rf}$	Rolling resistance force, N
$F_{sf}$	Slope resistance force, N
$F_{af}$	Air resistance force, N
$i_a$	Armature current, A
$J$	Inertia torque, N.m
$K_b$	Torque constant, N.m
$L_a$	Armature inductance
$M_{EB}$	Electric bicycle mass
$M_r$	Rider mass
$P_{friction}$	Friction power, W
$P_{slope}$	Slope grade power, W
$P_{total}$	Total power, W
$P_{air}$	Air power
$R^2$	Correlation coefficient

$R_a$	Armature resistance
$R_w$	Wheel radius, m
$T_l$	Load torque, N.m
$w_m$	Motor speed, rpm
$b$	Bias value of neuron
$x_i$	Input value if neuron
$w_i$	Linked weight of neuron
$t$	Time, s
$p$	The number of inputs

**Greek symbols**

$\alpha$	Slope ratio
$\rho$	Air density, kg/m <sup>3</sup>

## REFERENCES

- [1] Chuanxue Song, Yulong Shao, Shixin Song, Silun Peng, Feng Xiao. A Novel Electric Bicycle Battery Monitoring System Based on Android Client. *Journal of Engineering*, 2017, 2017.1: 2579084.
- [2] Heshou Wang, Ka Wai Eric Cheng, Yun Yang. A New Resonator Design for Wireless Battery Charging Systems of Electric Bicycles. *IEEE Journal of Emerging and Selected Topics in Power Electronics*, vol. 10, no. 5, pp. 6009-6019, Oct. 2022
- [3] Mihai Machedon-Pisu, Paul Nicolae Borza. Are Personal Electric Vehicles Sustainable? A Hybrid E-Bike Case Study. *Sustainability* 2020, 12(1), 32; <https://doi.org/10.3390/su12010032>.
- [4] Diego Carracedo, Hamid Mostofi. Electric cargo bikes in urban areas: A new mobility option for private transportation. *Transportation Research Interdisciplinary Perspectives*. Volume 16, December 2022, 100705.
- [5] Raky Julio, Andres Monzon. Long term assessment of a successful e-bike-sharing system. Key drivers and impact on travel behaviour. *Case Studies on Transport Policy* Volume 10, Issue 2, June 2022, Pages 1299-1313.
- [6] Chuanxue Song, Yulong Shao, Shixin Song, Cheng Chang, Fang Zhou, Silun Peng and Feng Xiao. Energy Management of Parallel-Connected Cells in Electric Vehicles Based on Fuzzy Logic Control. *Energies* 2017, 10(3), 404; <https://doi.org/10.3390/en10030404>.
- [7] Heshou Wang, Ka Wai Eric Cheng, Yun Yang. A New Resonator Design for Wireless Battery Charging Systems of Electric Bicycles. *IEEE Journal of Emerging and Selected Topics*

in *Power Electronics*, vol. 10, no. 5, pp. 6009-6019, Oct. 2022, doi: 10.1109/JESTPE.2022.3157729.

[8] Yan Hong, Changyong Jin, Siqi Chen, Chengshan Xu, Huaibin Wang, Hang Wu, Shaokang Huang, Qinzheng Wang, Haoran Li, Yuejiu Zheng, Xuning Feng, Mingguo Ouyang. Experimental study of the suppressing effect of the primary fire and thermal runaway propagation for electric bicycle batteries using flood cooling. *Journal of Cleaner Production* Volume 435, 5 January 2024, 140392.

[9] Józef Gromba. Torque Control of BLDC Motor for Electric Bicycle. 2018 International Symposium on Electrical Machines (SME), Andrychow, Poland, 2018, pp. 1-5, doi: 10.1109/ISEM.2018.8442987.

[10] Ji-Chang Son, Dong-Kuk Lim. Novel Stator Core of the Permanent Magnet Assisted Synchronous Reluctance Motor for Electric Bicycle Traction Motor Using Grain-Oriented Electrical Steel. 2021 24th International Conference on Electrical Machines and Systems (ICEMS), Gyeongju, Korea, Republic of, 2021, pp. 1215-1218, doi:10.23919/ICEMS52562.2021.9634439.

[11] Chih-Lyang Hwang, Hsiu-Ming Wu, Ching-Long Shih. An autonomous dynamic balance of an electrical bicycle in motion using variable structure under-actuated control. *Asian Journal of Control*, 2011, 13.2: 240-254.

[12] I Ketut Adi Atmika, I Dewa Gede Ary Subagia, I Wayan Surata, I Nyoman Sutantra, I Gusti Agung Kade Suriadi. Study of Mechanical Properties of Hemp Fiber Composites for Electric Bicycle Frames. *Materials Science Forum*. Trans Tech Publications Ltd, 2020. p. 167-172.

- [13] Weeberb J. Requia, Moataz Mohamed, Christopher D. Higgins, Altaf Arain, Mark Ferguson. How clean are electric vehicles? Evidence-based review of the effects of electric mobility on air pollutants, greenhouse gas emissions and human health. *Atmospheric Environment*. Volume 185, July 2018, Pages 64-77.
- [14] Andrew A. Campbell, Christopher R. Cherry, Megan S. Ryerson, Xinmiao Yang. Factors influencing the choice of shared bicycles and shared electric bikes in Beijing. *Transportation Research Part C: Emerging Technologies*. Volume 67, June 2016, Pages 399-414.
- [15] Petter Næss, Jin Xue, Harpa Stefansdottir, Rasmus Steffansen, Tim Richardson. Second home mobility, climate impacts and travel modes: Can sustainability obstacles be overcome?. *Journal of Transport Geography*. Volume 79, July 2019, 102468.
- [16] Shuguang Ji, Christopher R. Cherry, Lee D. Han, David A. Jordan. Electric bike sharing: simulation of user demand and system availability. *Journal of Cleaner Production*. Volume 85, 15 December 2014, Pages 250-257.
- [17] John Pucher, Jennifer Dill, Susan Handy. Infrastructure, programs, and policies to increase bicycling: An international review. *Preventive Medicine*. Volume 50, Supplement, January 2010, Pages S106-S125.
- [18] Nguyen Ba Hung, Ocktaeck Lim. The effects of operating conditions and structural parameters on the dynamic, electric consumption and power generation characteristics of an electric assisted bicycle. *Applied Energy* 247 (2019) 285–29.
- [19] Nitipong Somchaiwong, Wirot Ponglangka. Regenerative Power Control for Electric Bicycle. *SICE-ICASE International Joint Conference 2006 Oct. 18-21, 2006 in Bexco, Busan, Korea*.

- [20] P Vishnu Sidharthan and Yashwant Kashyap. Brushless DC Hub Motor Drive Control for Electric Vehicle Applications. 2020 First International Conference on Power, Control and Computing Technologies (ICPC2T), Raipur, India, 2020, pp. 448-453, doi: 10.1109/ICPC2T48082.2020.9071469.
- [21] C. Abagnale, M. Cardone, P. Iodice, R. Marialto, S. Strano, M. Terzo, G. Vorraro. Design and Development of an Innovative E-Bike. Energy Procedia. Volume 101, November 2016, Pages 774-781.
- [22] Nguyen Ba Hung, Ocktaeck Lim. The effects of operating conditions and structural parameters on the dynamic, electric consumption and power generation characteristics of an electric assisted bicycle. Applied Energy. Volume 247, 1 August 2019, Pages 285-296.
- [23] Magno Mendes, Gonçalo Duarte, Patricia Baptista. Introducing specific power to bicycles and motorcycles: Application to electric mobility. Transportation Research Part C: Emerging Technologies. Volume 51, February 2015, Pages 120-135.
- [24] Marco Dozza, Giulio Francesco Bianchi Piccinini, Julia Werneke. Using naturalistic data to assess e-cyclist behavior. Transportation Research Part F: Traffic Psychology and Behaviour. Volume 41, Part B, August 2016, Pages 217-226.
- [25] Seyed Mojib Zahraee, Saeed Rahimpour Golroudbary, Nirajan Shiwakoti, Peter Stasinopoulos. Particle-Gaseous pollutant emissions and cost of global biomass supply chain via maritime transportation: Full-scale synergy model. Applied Energy. Volume 303, 1 December 2021, 117687
- [26] Jarosław Brodny, Magdalena Tutak. Assessing the energy security of European Union countries from two perspectives – A new integrated approach based on MCDM methods. Applied Energy. Volume 347, 1 October 2023, 121443.

- [27] Mohammed M. Tumala, Afees Salisu, Yaaba B. Nmadu. Climate change and fossil fuel prices: A GARCH-MIDAS analysis. *Energy Economics*. Volume 124, August 2023, 106792.
- [28] Dallas Wood, Justin Larson, Jason Jones, Diana Galperin, Michael Shelby, Manuel Gonzalez. World oil price impacts on country-specific fuel markets: Evidence of a muted global rebound effect. *Energy Economics*. Volume 111, July 2022, 106024.
- [29] Bumin Meng, Feifan Yang, Jingang Liu, Yaonan Wang. A Survey of Brake-by-Wire System for Intelligent Connected Electric Vehicles. *IEEE Access*, 2020, 8: 225424-225436.
- [30] Nguyen Ba Hung, Jaewon Sung, Ocktaeck Lim. A simulation and experimental study of operating performance of an electric bicycle integrated with a semi-automatic transmission. *Applied Energy*. Volume 221, 1 July 2018, Pages 319-333.
- [31] Thomas Elliot, Sarah J. McLaren, Ralph Sims. Potential environmental impacts of electric bicycles replacing other transport modes in Wellington, New Zealand. *Sustainable Production and Consumption*  
Volume 16, October 2018, Pages 227-236.
- [32] Min Liu, Kexin Zhang, Yiping Liang, Yuzhe Yang, Zhihui Chen, Wei Liu. Life cycle environmental and economic assessment of electric bicycles with different batteries in China. *Journal of Cleaner Production*  
Volume 385, 20 January 2023, 135715.
- [33] Dominik Bucher, René Buffat, Andreas Froemelt, Martin Raubal. Energy and greenhouse gas emission reduction potentials resulting from different commuter electric bicycle adoption scenarios in Switzerland. *Renewable and Sustainable Energy Reviews*. Volume 114, October 2019, 109298.

[34] Lorenzo Stilo, Diana Segura-Velandia, Heinz Lugo, Paul P. Conway, Andrew A. West. Electric bicycles, next generation low carbon transport systems: A survey. *Transportation Research Interdisciplinary Perspectives*

Volume 10, June 2021, 100347.

[35] Yan Chen, Yongping Zhang, D'Maris Coffman, Zhifu Mi. An environmental benefit analysis of bike sharing in New York City. *Cities*. Volume 121, February 2022, 103475.

[36] Ivan ArangoORCID,Carlos Lopez and Alejandro Ceren. Improving the Autonomy of a Mid-Drive Motor Electric Bicycle Based on System Efficiency Maps and Its Performance. *World Electr. Veh. J.* 2021, 12(2), 59; <https://doi.org/10.3390/wevj12020059>.

[37] Sheng-Peng Zhang, Tae-Oh Tak. Efficiency Evaluation of Electric Bicycle Power Transmission Systems. *Sustainability* 2021, 13(19), 10988; <https://doi.org/10.3390/su131910988>.

[38] Reza Nasiri-Zarandi, Ahmadreza Karami-Shahnani, Mohammad Sedigh Toulabi, Alberto Tassarolo. Design and Experimental Performance Assessment of an Outer Rotor PM-Assisted SynRM for the Electric Bike Propulsion. *IEEE Transactions on Transportation Electrification*, vol. 9, no. 1, pp. 727-736, March 2023, doi: 10.1109/TTE.2022.3202819

[39] S. Farina, R.N. Firdaus, F. Azhar, M. Azri, M. S. Ahmad, R. Suhairi, A. Jidin, T. Sutikno. Design and Analysis of In-Wheel Double Stator Slotted Rotor BLDC Motor for Electric Bicycle Application. *International Journal of Power Electronics and Drive System (IJPEDS)* Vol. 9, No. 1, March 2018, pp. 457~464.

- [40] Felipe Tobar, Iván Castro, Jorge Silva, Marcos Orchard. Improving battery voltage prediction in an electric bicycle using altitude measurements and kernel adaptive filters. *Pattern Recognition Letters*. Volume 105, 1 April 2018, Pages 200-206.
- [41] S. A. Farisi, G. S. Ajie, R. B. Setyawati, K. N. R. Stulasti, Y. R. Azinuddin, D. A. P. B. Sudian, R. A. Nurfi, S. Sulistiyawan, H. K. (Kiwi) Aliwarga, and W. G. Suci. Increasing Electric Bicycle Performance using Lithium Ferro Phosphate Batteries with a Battery Management System. *Energy Storage Technology and Applications 2022*.
- [42] Wayan Nata Septiadi, Muhamad Alim, Made Nara Pradipta Adi. The application of battery thermal management system based on heat pipes and phase change materials in the electric bike. *Journal of Energy Storage*  
Volume 56, Part B, 10 December 2022, 106014.
- [43] Chuanxue Song, Yulong Shao, Shixin Song, Silun Peng, Feng Xiao. A Novel Electric Bicycle Battery Monitoring System Based on Android Client. *Journal of Engineering*, 2017, 2017.1: 2579084.
- [44] Chiharu Misaki, Daisuke Hara, Noboru Katayama and Kiyoshi Dowaki. Improvement of Power Capacity of Electric-Assisted Bicycles Using Fuel Cells with Metal Hydride. *Energies* 2020, 13(23), 6272; <https://doi.org/10.3390/en13236272>.
- [45] Sen-Yung Lee, Cho-Pei Jiang, Cheng-Kang Lee, Wei-Han Huang, and Yung-Chang Cheng. Optimization of design and fatigue simulations for an electric assisted bicycle frame using uniform design and grey relational analysis. *The Journal of Strain Analysis for Engineering Design*, 2023, 58.1: 3-16.

- [46] Norihito Fukushima, Yasutaka Fujimoto. Experimental verification of torque sensorless control for electric power-assisted bicycles on sloped environment. 2018 IEEE 15th International Workshop on Advanced Motion Control (AMC), Tokyo, Japan, 2018, pp. 66-71, doi: 10.1109/AMC.2019.8371064.
- [47] Kai Zhang, Mingdi Fan, Yong Yang, Rong Chen, Zhongkui Zhu, Cristian Garcia, Jose Rodriguez. Tolerant Sequential Model Predictive Direct Torque Control of Permanent Magnet Synchronous Machine Drives. IEEE Transactions on Transportation Electrification, vol. 6, no. 3, pp. 1167-1176, Sept. 2020, doi: 10.1109/TTE.2020.3008828
- [48] Okan Uyar, Mehmet Çunkaş, Hulusi Karaca. Enhanced intelligent control with adaptive system for electrically assisted bicycle. Engineering Science and Technology, an International Journal. Volume 30, June 2022, 101047.
- [49] Tinghua Li, Qinghua Yang, Xiaowei Tu, Bin Ren. An improved torque sensorless speed control method for electric assisted bicycle with consideration of coordinate conversion. IEEE/CAA Journal of Automatica Sinica, vol. 7, no. 6, pp. 1575-1584, November 2020, doi: 10.1109/JAS.2020.1003360.
- [50] C. Abagnale, M. Cardone, P. Iodice, R. Marialto, S. Strano, M. Terzo, G. Vorraro. Design and Development of an Innovative E-Bike. Energy Procedia. Volume 101, November 2016, Pages 774-781.
- [51] Berno J.E. Misgeld, Lukas Bergmann, Bence Szilasi, Steffen Leonhardt, Dietmar Greven. Virtual torque sensor for electrical bicycles. IFAC-PapersOnLine. Volume 53, Issue 2, 2020, Pages 8903-8908.
- [52] Jianmiao Liu, Junyi Li, Yong Chen, Song Lian, Jiaqi Zeng, Maosi Geng, Sijing Zheng, Yinan Dong, Yan He, Pei Huang, Zhijian Zhao, Xiaoyu Yan, Qinru Hu, Lei Wang, Di Yang,

Zheng Zhu, Yilin Sun, Wenlong Shang, Dianhai Wang, Lei Zhang, Simon Hu, Xiqun (Michael) Chen. Multi-scale urban passenger transportation CO2 emission calculation platform for smart mobility management. *Applied Energy*. Volume 331, 1 February 2023, 120407.

[53] Qing Yu, Yingkun Xie, Weifeng Li, Haoran Zhang, Xiaolei Liu, Wen-Long Shang, Jinyu Chen, Dongyuan Yang, Jinyue Yan. GPS data in urban bicycle-sharing: Dynamic electric fence planning with assessment of resource-saving and potential energy consumption increasement. *Applied Energy*. Volume 322, 15 September 2022, 119533.

[54] Peter K. Joseph, D. Elangovan, G. Arunkumar. Linear control of wireless charging for electric bicycles. *Applied Energy* 2019. Volume 255, 1 December 2019, 113898.

[55] Rumeng Yin, Jiang He. Design of a photovoltaic electric bike battery-sharing system in public transit stations. *Applied Energy*. Volume 332, 15 February 2023, 120505.

[56] David Vetturi, Monica Tiboni, Giulio Maternini, Benedetto Barabino, Roberto Ventura. Kinematic performance of micro-mobility vehicles during braking: experimental analysis and comparison between e-kick scooters and bikes. *Transportation Research Procedia*. Volume 69, 2023, Pages 408-415.

[57] Ximing Chang, Jianjun Wu, Huijun Sun, Xuedong Yan. A Smart Predict-then-Optimize method for dynamic green bike relocation in the free-floating system. *Transportation Research Part C: Emerging Technologies*. Volume 153, August 2023, 104220.

[58] Nguyen Ba Hung, Jaewon Sung, Ocktaeck Lim. A simulation and experimental study of operating performance of an electric bicycle integrated with a semi-automatic transmission. *Applied Energy*. Volume 221, 1 July 2018, Pages 319-333.

- [59] Le Trong Hieu, Nguyen Xuan Khoa, Ock Teack Lim. An investigation on the effective performance area of the electric bicycle with variable key input parameters. *Journal of Cleaner Production*. Volume 321, 25 October 2021, 128862.
- [60] Roushan Kumar, Rupendra Kumar Pachauri, Pankaj Badoni, Deepak Bharadwaj, Udayveer Mittal, Abhishek Bisht. Investigation on parallel hybrid electric bicycle along with issuer management system for mountainous region. *Journal of Cleaner Production*. Volume 362, 15 August 2022, 132430.
- [61] Le Trong Hieu, Nguyen Xuan Khoa, Ock Teack Lim. An investigation on the effective performance area of the electric bicycle with variable key input parameters. *Journal of Cleaner Production*. Volume 321, 25 October 2021, 128862.
- [62] Le Trong Hieu, Nguyen Xuan Khoa, Ock Teack Lim. An Investigation on the Effects of Input Parameters on the Dynamic and Electric Consumption of Electric Motorcycles. *Sustainability* 2021, 13(13), 7285; <https://doi.org/10.3390/su13137285>.
- [63] Rishi Roy, Ashwani K. Gupta. Data-driven prediction of flame temperature and pollutant emission in distributed combustion. *Applied Energy*. Volume 310, 15 March 2022, 118502.
- [64] S.V. Channapattana, Abhay A. Pawar, Prashant G. Kamble. Optimisation of operating parameters of DI-CI engine fueled with second generation Bio-fuel and development of ANN based prediction model. *Applied Energy*. Volume 187, 1 February 2017, Pages 84-95.
- [65] Jingfan Hu, Wandong Zheng, Sirui Zhang, Hao Li, Zijian Liu, Guo Zhang, Xu Yang. Thermal load prediction and operation optimization of office building with a zone-level artificial neural network and rule-based control. *Applied Energy*. Volume 300, 15 October 2021, 117429.

[66] Heng Chen, Fengmei Lu, Bifang He. Topographic property of backpropagation artificial neural network: From human functional connectivity network to artificial neural network. *Neurocomputing* 2020. Volume 418. 200-210.

[67] Pengjie Tian, Xuejun Liu, Kaiyao Luo, Hongkun Li, Yun Wang. Deep learning from three-dimensional multiphysics simulation in operational optimization and control of polymer electrolyte membrane fuel cell for maximum power. *Applied Energy* 2021. Volume 288. 116632.

[68] Liu X, Fotouhi A. Formula-E race strategy development using artificial neural networks and Monte Carlo tree search. *Neural Computing and Applications* 2020. 32. 15191–15207.

[69] Shivakumar, Srinivasa Pai P, Shrinivasa Rao BR. Artificial Neural Network based prediction of performance and emission characteristics of a variable compression ratio CI engine using WCO as a biodiesel at different injection timings. *Applied Energy* 2011. Volume 88. 2344-2354.

[70] CARR, Jenna. An introduction to genetic algorithms. Senior Project, 2014, 1.40: 7.

## PUBLICATIONS AND CONFERENCES

### A. List of Publications

1. **Le Trong Hieu**, Nguyen Xuan Khoa , Ock Teack Lim, “An investigation on the effective performance area of the electric bicycle with variable key input parameters”, *Journal of Cleaner Production, Elsevier*, Volume 321, 25 October 2021, 128862. <https://doi.org/10.1016/j.jclepro.2021.128862>.
2. **Le Trong Hieu**, Ocktaeck Lim, “A deep learning approach for optimize dynamic and required power in electric assisted bicycle under a structure and operating parameters”, *Applied Energy, Elsevier*, Volume 347, 1 October 2023, 121457. <https://doi.org/10.1016/j.apenergy.2023.121457>.
3. **Le Trong Hieu**, Ocktaeck Lim, “Deep learning application in fuel cell electric bicycle to optimize bicycle performance and energy consumption under the effect of key input parameters”, *Applied Energy Elsevier*, Volume 369, 1 September 2024, 123588
4. **Le Trong Hieu**, Ocktaeck Lim, “An Investigation on the Effects of Input Parameters on the Dynamic and Electric Consumption of Electric Motorcycles”, *Sustainability-MDPI*, 2021, 13(13), 7285. <https://doi.org/10.3390/su13137285>.
5. **Le Trong Hieu**, Ocktaeck Lim, “ Effects of the Structure and Operating Parameters on the Performance of an Electric Scooter”, *Sustainability-MDPI*, 2023, 15(11), 8976. <https://doi.org/10.3390/su15118976>.
6. **Le Trong Hieu**, Ocktaeck Lim, “A deep learning approach to optimize the performance and power demand of electric scooters under the effect of operating and structure parameters.”, *Energies 2024, 17(2), 427*; <https://doi.org/10.3390/en17020427>.
7. **Le Trong Hieu**, Ocktaeck Lim, “ A deep learning technique for optimizing consumed power and performance of fuel cell electric bicycle under operating and structure parameters”, *Applied Energy, Elsevier*, under review. (submitted day 2023/12/09).

## **B. List of Conferences**

### **International Conferences**

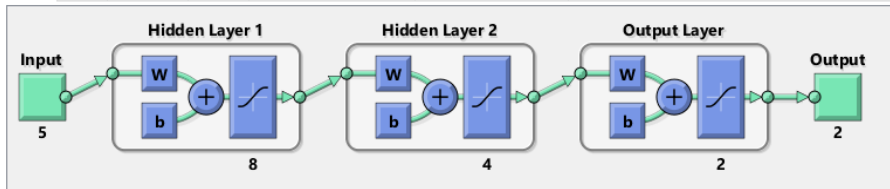
1. **Le Trong Hieu** and Ocktaeck Lim, SpliTech2020 – 5th International Conference on Smart and Sustainable Technologies. Bol and Split, Croatia, September 23 – 26, 2020
2. **Le Trong Hieu** and Ocktaeck Lim, International Conference on Applied Energy 2020, November 29, 2020, Bangkok, Thailand.
3. **Le Trong Hieu** and Ocktaeck Lim, International Conference on Applied Energy 2021, November 29, 2021, Bangkok, Thailand.
4. **Le Trong Hieu** and Ocktaeck Lim. International Conference on Applied Energy 2022, August 8, 2022. Bochum, Germany.
5. **Le Trong Hieu** and Ocktaeck Lim. International Conference on Applied Energy 2023, December 3, 2023. Doha, Qatar.

### **Domestic Conferences**

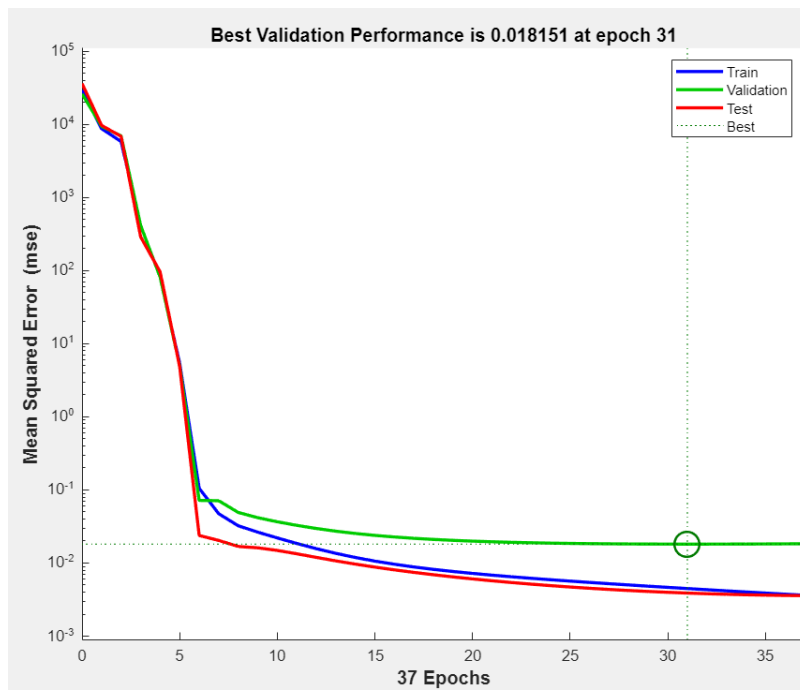
1. **Le Trong Hieu**, Ocktaeck Lim, KSAE, Annual Autumn Conference and Exhibition. Samcheok. 2020.
2. **Le Trong Hieu**, Ocktaeck Lim, KSAE, Annual Spring Conference and Exhibition. Shinhwaworld Jeju, Jeju Island. 2021
3. **Le Trong Hieu**, Ocktaeck Lim, KSAE, Annual Spring Conference and Exhibition. Bexco, Busan. 2022.
4. **Le Trong Hieu**, Ocktaeck Lim, KSAE, Annual Autumn Conference and Exhibition. Shinhwaworld Jeju, Jeju Island. 2022

## APPENDIX

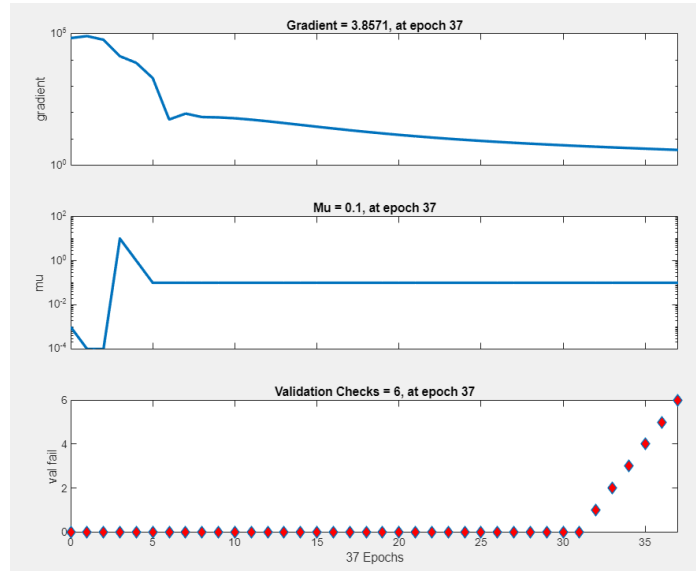
1. The architecture of ANN with inputs, hidden layers, and output.



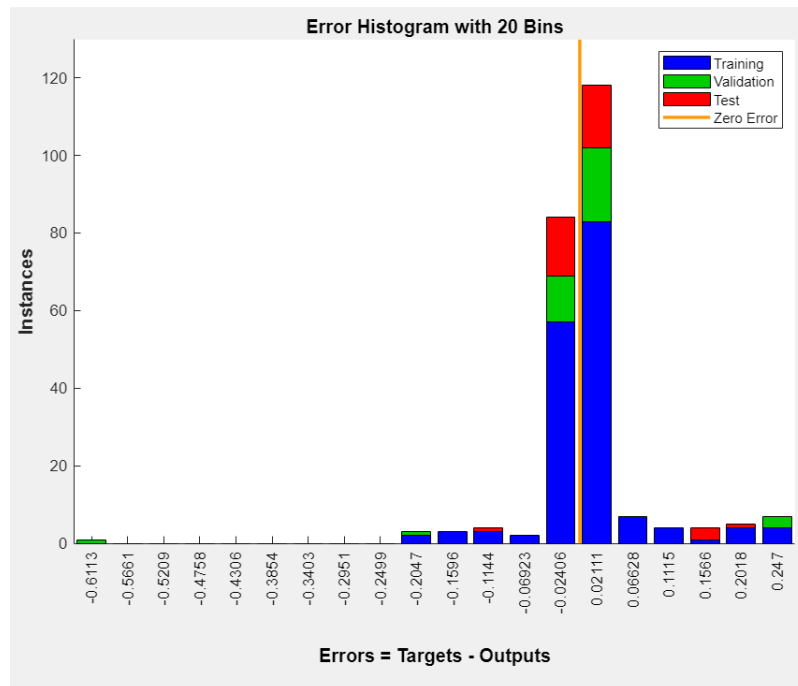
2. ANN performance plot showing best validation in terms of mean square error



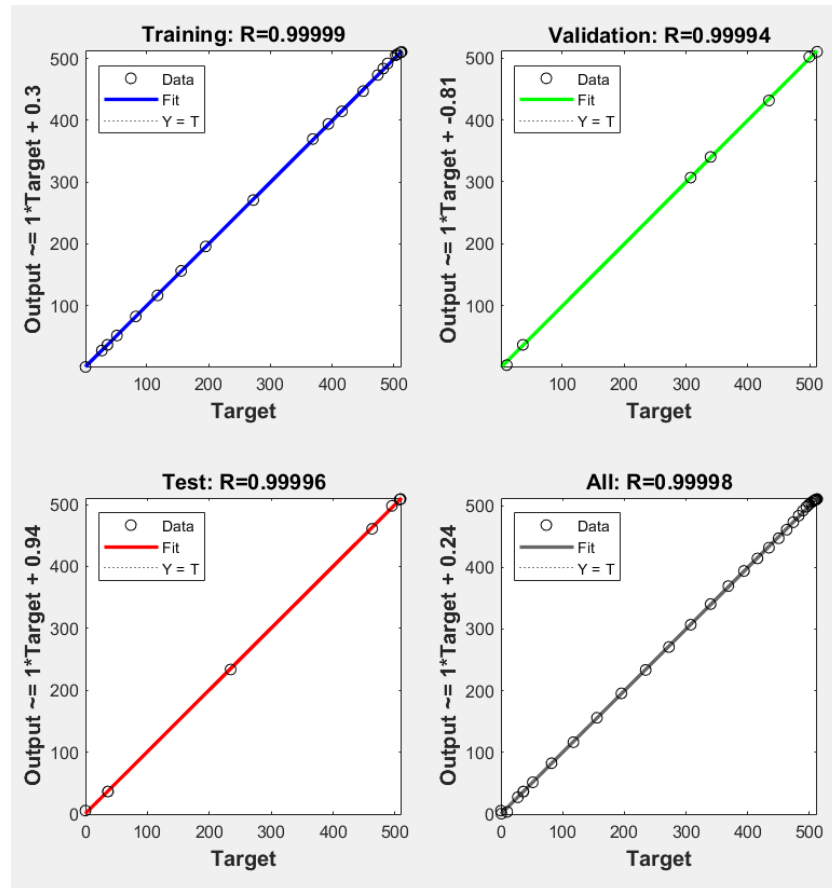
3. The training state plot comprises gradient, scalar  $\mu$ , and validation check



4. The histogram showing the difference between the actual and the target output



5. The Regression plot showing regression relation between the actual output and the targets



## 6. Properties of GA algorithm in MATLAB

Solver	gamultiobj- Multiobjective optimization using Genetic Algorithm
Number of input variables	3
Quantity of datasets	125
Lower limit range $[R_w A_a \gamma]$	[0.3 0.423 2.18]
Upper limit range $[R_w A_a \gamma]$	[0.42, 1.623, 3.43]
Pareto front population	0.35
Current iteration	155

Optimization Tool

File Help

**Problem Setup and Results**

Solver: gamultiobj - Multiobjective optimization using Genetic Algorithm

Problem: @harman

Fitness function: @harman

Number of variables: 3

Constraints:

Linear inequalities: A: [0.3 0.423 2.18] b: [0.42, 1.623, 3.43]

Linear equalities: Aeq: [] beq: []

Bounds: Lower: [0.3 0.423 2.18] Upper: [0.42, 1.623, 3.43]

Run solver and view results

Use random states from previous run

Start Pause Stop

Current iteration: 155 Clear Results

Optimization terminated: average change in the spread of Pareto solutions less than options.TolFun.

Optimization running.

Optimization terminated: average change in the spread of Pareto solutions less than options.TolFun.

**Pareto front - function values and decision variables**

Index	f1	f2	x1	x2	x3
1	1.299373	-249.811	0.304	1.615	2.244
2	-1.86578	857.66	0.416	1.611	2.25
3	450.625	48.356	0.334	1.591	2.264
4	-1.253278	643.534	0.394	1.613	2.25
5	969.998	-136.629	0.312	1.39	2.245
6	-1.658215	789.035	0.409	1.603	2.252
7	-287.122	306.151	0.36	1.61	2.248
8	-684.243	451.827	0.408	1.088	2.88
9	778.986	-66.604	0.322	1.609	2.26
10	-1.409378	698.147	0.4	1.605	2.249
11	-32.629	217.35	0.351	1.601	2.258

**Options**

Initial range:  Specify:  Use default: [0.1]

Selection: Selection function: Tournament

Tournament size:  Use default: 2  Specify:

Reproduction: Crossover fraction:  Use default: 0.8  Specify:

Mutation: Mutation function: Constraint dependent

Crossover: Crossover function: Intermediate

Ratio:  Use default: 1.0  Specify: 1.0

Migration: Direction: Forward

Fraction:  Use default: 0.2  Specify:

Interval:  Use default: 20  Specify: